ABSTRACT

A PHASE STUDY AND THERMODYNAMIC INVESTIGATION OF THE EUROPIUM-OXYGEN-BROMINE SYSTEM

BY

John Maurice Haschke

Eight binary and ternary europium phases have been observed in the europium-oxygen-bromine system. The phases: trieuropium tetraoxide (Eu₃O₄), europium monoxide (EuO), europium dibromide (EuBr₂), europium tribromide (EuBr₃), trieuropium tetraoxide monobromide (Eu₃O₄Br), europium monoxide monobromide (EuOBr), and trieuropium monoxide tetrabromide (Eu₃OBr₄), have been prepared from the sesquioxide and were analyzed by chemical and X-ray crystallographic procedures. Guinier X-ray powder diffraction data, which were collected for all phases, have been indexed. Single crystal diffraction data were collected for the dibromide and tetraoxide monobromide. Lattice parameters were also determined for europium dibromide monohydrate (EuBr₂·H₂O) and europium tribromide hexahydrate (EuBr₃·6H₂O).

The following vaporization reactions were characterized by a combination of X-ray diffraction, weight loss, effusate collection, and high temperature mass spectrometric techniques:

$$3 \text{ Eu}_3O_4(s) \longrightarrow 4\text{Eu}_2O_3(s, \text{monoclinic}) + \text{Eu}(g).$$
 (1)

$$4EuO(s) \longrightarrow Eu_3O_4(s) + Eu(g).$$
 (2)

$$3Eu_3O_4Br(s) \longrightarrow 4Eu_2O_3(s, monoclinic) + EuBr_2(g) + Br(g).$$
(3)

$$\operatorname{EuBr}_{2}(\ell) \longrightarrow \operatorname{EuBr}_{2}(g).$$
 (4)

$$4EuOBr(s) \longrightarrow Eu_3O_4Br(s) + EuBr_2(g) + Br(g).$$
 (5)

Equilibrium vapor pressure measurements for reactions (1-4) have been made by target collection Knudsen effusion techniques. Microgram quantities of the condensed effusates were analyzed by an X-ray fluorescence procedure, which involved the establishment of linear external calibration curves.

The following second law enthalpies and entropies of vaporization were obtained for the median measurement temperatures: Eu₃O₄(s), $\Delta H_{1810}^0 = 86 \cdot_2 \pm 1 \cdot_4 \text{ kcal/gfw}$, $\Delta S_{1810}^0 = 28 \cdot_2 \cdot_2 \pm 0 \cdot_8 \cdot_2 \text{ eu}$; EuO(s), $\Delta H_{1546}^0 = 75 \cdot_9 \cdot_1 \pm 0 \cdot_9 \cdot_4 \text{ kcal/gfw}$, $\Delta S_{1546}^0 = 28 \cdot_6 \cdot_6 \pm 0 \cdot_6 \cdot_1 \text{ eu}$; Eu₃O₄Br(s), $\Delta H_{1399}^0 = 129 \cdot_0 \pm 1 \cdot_1 \text{ kcal/gfw}$, $\Delta S_{1399}^0 = 50 \cdot_8 \cdot_1 \pm 0 \cdot_8 \cdot_1 \text{ eu}$; and EuBr₂(ℓ), $\Delta H_{1377}^0 = 58 \cdot_7 \cdot_2 \pm 0 \cdot_7 \cdot_6 \text{ kcal/gfw}$, $\Delta S_{1377}^0 = 23 \cdot_0 \cdot_3 \pm 0 \cdot_5 \cdot_6 \text{ eu}$. At its boiling point (2530 ± 35°K), EuBr₂(ℓ) has a second law enthalpy and entropy of $\Delta H_V^0 = 52 \cdot_0 \pm 3 \cdot_0 \text{ kcal/gfw}$ and $\Delta S_V^0 = 20 \cdot_6 \pm 1 \cdot_9 \text{ eu}$. A general scheme for approximation of heat capacities of the solid phases has been derived, and the ensuing estimated values have been combined with approximated entropies in the calculation of free energy functions.

At 2980K, the following second and third law enthalpies and second law entropies of vaporization were obtained: Eu₃O₄(s), ΔH_{298}^{0} (2nd) = 93.5 ± 2.5 kcal/gfw, ΔH_{298}^{0} (3rd) = 92.28 ± 0.56 kcal/gfw, $\Delta S_{298}^{0} = 39.4 \pm 1.7 eu$; EuO(s), ΔH_{298}^{0} (2nd) = $80.3 \pm 1.7 eu$ $2._0 \text{ kcal/gfw}, \Delta H_{298}^0 \text{ (3rd)} = 80.0_0 \pm 0.4_2 \text{ kcal/gfw}, \Delta S_{298}^0 =$ 33.9 \pm 1.3 eu; EuBr₂(s), $\triangle H_{298}^{0}$ (2nd) = 71.4 \pm 2.7 kcal/gfw, ΔH_{298}^{0} (3rd) = 69.5₄ ± 0.4₀ kcal/gfw, ΔS_{298}^{0} = 36.₈ ± 2.₈ eu; and $Eu_3O_4Br(s)$, $\triangle H_{298}^0$ (2nd) = 137.6 ± 2.0 kcal/gfw, $\triangle H_{298}^0$ $(3rd) = 139.4_7 \pm 0.9_2 \text{ kcal/gfw}, \Delta S_{298}^0 = 64._7 \pm 2._9 \text{ eu}.$ The enthalpies and free energies of formation and the standard entropies calculated from second law results are: Eu304(s), $\Delta H_{f\ 298}^{0} = -542._{4} \pm 3._{6} \text{ kcal/gfw}, \Delta G_{f\ 298}^{0} = -510._{4} \pm 3._{6}$ kcal/gfw, $S_{298}^{0} = 48.6 \pm 2.6$ eu; EuO(s), $\Delta H_{f_{298}}^{0} = -145.2$ $4._1 \text{ kcal/gfw}, \triangle G_{f\ 298}^0 = -136._6 \pm 4._1 \text{ kcal/gfw}, S_{298}^0 = 15._0 \pm$ $3._0$ eu; $EuBr_2(s)$, $\triangle H_{f\ 298}^0 = -178._0 \pm 3._0$ kcal/gfw, $\triangle G_{f\ 298}^0 =$ $-173._{2} \pm 3._{0}$ kcal/gfw, $S_{298}^{0} = 39._{5} \pm 3._{0}$ eu; and Eu₃O₄Br(s), $\Delta H_{f\ 298}^{0} = -597._{7} \pm 5._{1} \text{ kcal/gfw}, \Delta G_{f\ 298}^{0} = -565._{0} \pm 5._{1}$ kcal/gfw, $S_{298}^{0} = 64.5 \pm 3.1$ eu. Thermodynamic data have been estimated for the vaporization of EuOBr(s) according to reaction (5) and the following thermochemical values obtained for the phase: $\Delta H_{f\ 298}^{0} = -203_{\cdot 3} \pm 6_{\cdot 5} \text{ kcal/gfw}$, $\Delta G_{f\ 298}^{0} = -193._{4} \pm 6._{5} \text{ kcal/gfw.}$ The thermochemical data obtained for europium oxides and oxide bromides have been employed in calculations which indicate that the lower oxides of ytterbium and of other lanthanides (LnO and Ln3O4) are unstable at temperatures greater than 2980K.

A PHASE STUDY AND THERMODYNAMIC INVESTIGATION OF THE EUROPIUM-OXYGEN-BROMINE SYSTEM

Ву

John Maurice Haschke

A THESIS

Submitted to
Michigan State University
in partial fulfillment of the requirements
for the degree of

DOCTOR OF PHILOSOPHY

Department of Chemistry

1969

9.17.69

ACKNOWLEDGMENTS

The author wishes to express his sincere appreciation to Dr. Harry A. Eick for the encouragement, the suggestions, and the assistance which he has generously given during this investigation.

A deep expression of gratitude is also extended to the author's wife, Bernadette, and to his parents for their assistance and encouragement in the attainment of this educational goal.

The aid of past and present members of the High Temperature Group is appreciated, and the assistance of Dr. Philip Pilato and Mr. Donald Werner in mass spectrometric analysis is gratefully acknowledged.

A special expression of appreciation is extended to Dr. W. W. Wendlandt for the insight and guidance which he has offered.

The financial support of the Atomic Energy Commission under Contract AT (11-1)-716 and the National Science Foundation is gratefully acknowledged.

TABLE OF CONTENTS

I	Page
I. INTRODUCTION	1
II. PREVIOUS INVESTIGATIONS OF THE EUROPIUM-OXYGEN-BROMINE SYSTEM	4
A. The Oxides of Europium	4 4 5
B. The Bromide and Hydrated Bromides of Europium. 1. Preparative and Structural Investigations a. Europium Bromides	6 6 6 7
2. Thermodynamic Investigations of Europium Bromides	7
C. The Oxides of Bromine	8
 D. The Oxide Bromides of Europium 1. Preparative and Structural Investigations 2. Thermodynamic Investigations 	8 8 9
III. THEORETICAL CONSIDERATIONS PERTINENT TO THIS INVESTIGATION	10
A. Phase Relationships	10
Bromine System	10 11 11 11 12
B. Vapor Pressure Measurement by the Knudsen Effusion Technique	12 12 13 15

		Page
	a. Non-Ideal Cell	15 15
	 (2) Non-Ideal Collection Geometry . (3) Thermal Expansion of the Orifice 	16 16
	b. The Non-Ideal Gas	17 17
	(1) Sampling and the "Orifice Effect"	17
	(2) The Vaporization Coefficient (3) Diffusion	18 18
	d. Additional Limitations to Target Collection Effusion Measurements	19
С.	X-Ray Fluorescence	20
	 The Basic Phenomenon The Bragg Equation 	20 21
D.	Temperature Correction	21
Ε.	Thermodynamic Calculations	23
	1. Second Law Calculations	23
	a. Derivation of Relationshipsb. Assumptions of the Second Law	23
	Treatment	24
	Temperature	25
	d. Calculation of the Second Law Entropy 2. Third Law Calculations	26 27
	a. Derivation of Relationships	27
	b. The Value of Third Law Calculations.	28
	3. Energetics of Formation	29
	 Approximation of Thermodynamic Functions a. Approximation of High Temperature Heat 	30
	Capacities	30
	(1) Solids	30
	(2) Simple Polyatomic Gases	31
	b. Approximation of Standard Entropies	32
	c. Estimation of Enthalpy and Entropy	34
	Functions	34 34
	a. Least Squares and Standard Error	34 34
	b. Combination of Errors	34

		Page
IV. E	EXPERIMENTAL EQUIPMENT AND MATERIALS	36
Α.	Target Collection Apparatus	36
в.	X-Ray Fluorescence Equipment	36
	1. Spectrometer	36
	2. Specimen Mount	37
	3. Effusate Geometry	37
c.		37
	1. Powder Diffraction Equipment	37
	2. Single Crystal Diffraction Equipment .	38
D.	Temperature Measuring Equipment	38
E.	High Temperature Mass Spectrometer	38
F.	Micrograph	38
G.	Miscellaneous Measuring Equipment	39
н.	Heating Equipment	39
ı.	Vacuum Systems	40
J.	Inert Atmosphere Glove Box	40
К.	Effusion Cell Design	40
	1. Target Collection Cells	40
	2. Mass Spectrometer Cells	41
L.	Chemicals and Materials	41
V. E	XPERIMENTAL PROCEDURES	43
7	Dranarative Machaigues	43
Α.	Preparative Techniques	43 43
	2. Europium Monoxide	43 44
	3. Europium Dibromide	44
	4. Europium Monoxide Monobromide	45
	5. Trieuropium Tetraoxide Monobromide	45 46
	6. Europium Tribromide	46
	7. Hydrated Bromide Phases	47
	a. Europium Tribromide Hexahydrate	47
	b. Europium Dibromide Monohydrate	47

		Page
В.	Additional Preparative and Phase Studies 1. Attempts to Prepare Europium Tribromide 2. Attempts to Prepare Additional Oxide	48 48
	Bromide Phases	49
	bromide and Sesquioxide	49
	b. Oxidation of Europium Dibromide	49
	c. Direct Combination of Europium Mon-	
	oxide and Dibromide	49
c.	Analytical Techniques	50
	1. Europium Analysis	50
	2. Bromine Analysis	50
	3. Oxygen Analysis	50
D.	Density Measurement	50
Ε.	X-Ray Diffraction Procedures	51
	1. Powder Diffraction Techniques	51
	2. Single Crystal Techniques	51
F.	Characterization of Vaporization Reactions .	52
	1. Weight Loss Measurements	52
	2. Mass Spectrometric Investigations	5 3
	3. Effusate Collection Experiments	53
	4. X-Ray Investigations	54
G.	X-Ray Fluorescence Procedures	54
	1. Optimization of Spectrometer Parameters	54
	2. Counting Procedures	55
	3. Preparation of Standard Solutions	56
	4. Preparation of Calibration Curves	56
н.	Target Collection Technique	57
	1. General Collection Procedures	57
	2. Measurement of Orifice Areas	59
	3. Specific Experimental Procedures and Conditions	59
т	Sticking Coofficient Experiments	60

P	a ge
VI. RESULTS	62
 A. Results of Preparative Techniques 1. The Europium-Oxygen-Bromine System 2. Results of Additional Preparative and 	62 62
Phase Investigations	62 65
of the Binary and Ternary Phases	65
B. Analytical Results	66 66 69
C. Results of X-Ray Fluorescence Calibration .	70
D. Vaporization Results	71
Tetraoxide	71 71
Dibromide	72 70
Tetraoxide Monobromide	72 76
6. Pressure-Composition Diagrams	76
E. The Results of Sticking Coefficient Measurement	s79
F. Vapor Pressure Equations	80
G. Thermodynamic Values Employed in Data Reduction	85
1. Heat Capacity, Enthalpy and Entropy Functions	85
 a. Literature Values	85 85 86
Phases	87 87 87
3. Free Energy Functions	88
4. Additional Thermochemical Values	89

	Page
H. Thermodynamic Results	89
1. Treatment of Trieuropium Tetraoxide Data	89
2. Treatment of Europium Monoxide Data	90
3. Treatment of Europium Dibromide Data .	91
4. Treatment of Trieuropium Tetraoxide	00
Monobromide Data	93
Europium Monoxide Monobromide	95
6. Compilation of Thermodynamic Results	97
•	
VII. DISCUSSION	100
A. The Phase Diagram	100
1. Phases in the Europium-Oxygen-Bromine System	100
System	
and the Literature	101
a. On the Crystal Structure of Europium	
Dibromide	101
b. On the Preparation of Europium Tri-	
bromide and Triiodide	102
c. On the Composition of the Hexagonal	104
Oxide Bromide	104 105
a. Elucidation of the Vaporization	103
Process	105
b. Disproportionation of the Oxide	
Bromides	107
B. The X-Ray Fluorescence Technique	109
C. The Target Collection Knudsen Effusion	
Technique	112
1. The Attainment of Knudsen Conditions	112
2. Temperature Gradients	113
3. Crucible Materials	114
D. Evaluation of Thermodynamic Approximations .	115
 Heat Capacity Approximations Entropy Approximations 	115 117
	11/
E. Evaluation of Vaporization and Thermo-	440
dynamic Results	118
 Trieuropium Tetraoxide Data Europium Monoxide Data 	118 120
Z. Europium Monoxide Data	123
4. Trieuropium Tetraoxide Monobromide and	120
Europium Monoxide Monobromide Data	123

																								Page
	F	•	On	the	Ex	is	te	nc	е	of	L	ow	er	0	хi	de	s	of	Y	tt	er	bi	um	124
VIII.	•	SU	IGGE	STIC	ons	F	OR	F	UT	UR.	E	IN	VE	ST	IG.	ΑT	IO	NS		•	•	•	•	131
	RF	EFE	REN	ICES	•	•	•	•	•	•	•	•	•	•	•	•	•		•	•	•	•	•	132
	ΑI	PE	NDI	CES											•									139

LIST OF APPENDICES

APPENDIX			Pag	је
I. Observed $\sin^2\theta(\lambda = 1.54051 \text{ Å})$ and Inter-				
planar d-Values	•	•	. 13	19
A. Tetragonal Europium Dibromide				19
B. Orthorhombic Europium Dibromide Monohyd				19
C. Orthorhombic Europium Tribromide				ŀO
D. Monoclinic Europium Tribromide Hexahydra	at	е	. 14	0
II. X-Ray Fluorescence	•	•	. 14	1
A. Linear Calibration Curves for X-Ray				
Fluorescence			. 14	1
B. The Vapor Pressure of Gold	•	•	. 14	1
C. Equilibrium Pressures and Third Law Entl	na.	1 –		
pies for Gold	•	•	. 14	3
III. Equilbrium Pressures and Third Law Enthalp	ρi	es	. 14	4
A. Trieuropium Tetraoxide Vaporization .	•		. 14	4
B. Europium Monoxide Vaporization	•		. 14	4
C. Europium Dibromide Vaporization	•		. 14	5
D. Trieuropium Tetraoxide Monobromide Vapor	ri	za	tion14	.5
IV. Thermodynamic Values for Data Reduction	•	•	. 14	6
A. Approximated Heat Capacity, Enthalpy, an	nd			
Entropy Values	•	•	. 14	_
B. Enthalpy, Entropy, and Free Energy Function	ιi	on	s 14	:6
C. Free Energy Function Changes for the				
Vaporization Reactions	•	•	. 14	
D. Thermodynamic Functions from the Literat	cu:	re	14	:8
V. Data for Thermodynamic Calculations	•		. 14	9

LIST OF TABLES

TABLE	1	Page
ı.	Analytical results	67
II.	Powder diffraction results	68
III.	Second law results at median measurement temperature	98
IV.	Thermodynamic results at $298^{0}{ m K}$	99
٧.	Thermodynamic results for liquid europium dibromide at the boiling point	99
VI.	Comparison of estimated and experimental S_{298}^{0}	118
VII.	Correlation of the divalent radii and enthalpies of formation of metal monoxides	122
VIII.	Free energy changes calculated for the reduction of europium and ytterbium oxide bromides with lithium hydride	129
IX.	Free energy changes for the reaction of europium and ytterbium with their sesquioxides at various temperatures	129

LIST OF FIGURES

FIGURE		Page
1.	A schematic of the X-ray fluorescence spectrometer	22
2a.	Asymmetric Knudsen cell design	42
2b.	Symmetric Knudsen cell design	42
3.	The europium-oxygen-bromine phase diagram	63
4.	The europium-oxygen pressure-composition phase diagram	77
5.	The europium-bromine pressure-composition phase diagram	78
6.	The europium sesquioxide-europium tribromide pseudobinary pressure-composition phase diagram	78
7.	The pressure of $Eu(g)$ in equilibrium with $Eu_3O_4(s)$ and $Eu_2O_3(s)$	81
8.	The pressure of $Eu(g)$ in equilibrium with $EuO(s)$ and $Eu_3O_4(s)$	82
9.	The pressure of $\operatorname{EuBr}_2(g)$ in equilibrium with $\operatorname{EuBr}_2(\ell)$	83
10.	The pressure of $EuBr_2(g)$ in equilibrium with $Eu_3O_4Br(s)$, $Eu_2O_3(s)$, and $Br(g)$	84

CHAPTER I

INTRODUCTION

In a day when the inorganic chemist is concerned with a variety of complex molecular species, it is often surprising to discover that the present knowledge of the simple binary compounds of the alkaline earths and lanthanides with the nonmetal elements of groups IVA - VIIA is incomplete and often inaccurate. Many of the investigations of these binary systems were conducted prior to 1940, and as a result of either impure materials or less accurate methods of data collection and treatment than are presently available, the results are often in error. Therefore, the present investigation was initiated to characterize the phase diagrams, the crystal structures, and the thermodynamic properties of some binary and ternary phases.

Since metal carbides, pnictides, chalcogenides, and halides tend to be refractory, high temperature techniques are generally employed in preparative procedures and may be used to provide information about the vaporization reactions, vapor pressures, and, hence, the thermodynamic data of the phases. In high temperature studies, additional knowledge may be obtained about the stabilities of gaseous species,

the properties of high temperature container materials in the presence of reactive compound, and the phase diagrams of the investigated systems.

Because of the magnetic nature of europium phases, many more physical than chemical properties of its compounds have been measured. Chemically, europium is probably the most unusual of the lanthanides because it appears to exhibit not only the true divalent character of alkaline earths, but also the trivalent character of other lanthanides. The former behavior allows for comparison of chemical properties with those of the alkaline earths, ytterbium, samarium, and possibly thulium, while the latter often enables prediction of properties for analogous materials of neighboring lanthanides and permits establishment of trends within the lanthanide series. The potential for variation of both the ratio of di- and trivalent europium and the ratio of the two anions makes the europium-oxygen-bromine system particularly intriguing.

The general plan for this investigation was to characterize as fully as possible the europium-oxygen-bromine phase diagram and the properties of its phases by X-ray diffraction and high temperature Knudsen effusion techniques. If possible, the ensuing thermodynamic results were to be employed in an attempt to resolve certain problems in lanthanide chemistry. A secondary goal was the development of X-ray fluorescence spectroscopy for quantitative analyses in

target collection effusion measurements and the evaluation of this technique by collection of vapor pressure data for a previously measured system.

CHAPTER II

PREVIOUS INVESTIGATIONS OF THE EUROPIUM-OXYGEN-BROMINE SYSTEM

A. The Oxides of Europium

1. Preparative and Structural Investigations

The phase diagram of the europium-oxygen system is probably the most studied and best characterized portion of the entire europium-oxygen-bromine ternary. The sesquioxide, Eu₂O₃, exists in both the monoclinic B- and cubic C-forms. However, the lattice constants reported by Gschneidner in his review of the structural chemistry of these phases differ from those more recently reported 2,3. The first reported lower oxide of europium, the monoxide, described by Eick et al.4, was prepared by reduction of the sesquioxide with elemental lanthanum and reported to possess a NaCl-type structure. The monoxide subsequently has been prepared by reduction of the sesquioxide with either graphite5 or europium metal, 6,7 and by reduction of europium monoxide monochloride, EuOCl, with lithium hydride 3. A second lower oxide, trieuropium tetraoxide, was first prepared by reduction of the sesquioxide with graphite⁸ and subsequently by reduction of Eu₂O₃ with EuO ⁹. An orthorhombic calcium

and this assignment has since been confirmed by both powder² and single-crystal¹⁰ measurements. More recently, Baernighausen has reported the preparation of the tetra-oxide by reduction of a mixture of either EuOCl and Eu₂O₃,³ or of trieuropium tetraoxide monobromide, Eu₃O₄Br, with lithium hydride ¹¹.

2. Thermodynamic Investigations

Only fragmentary thermodynamic data have been determined on the otherwise well-characterized europium-oxygen binary phases. The enthalpies of formation of both B- and C-forms of the sesquioxide have been measured by bomb calorimetry, 12 while that of the C-form has also been determined by solution calorimetry 13. The high temperature heat capacities of both its B- and C-forms, and the enthalpy and temperature of transition have been reported 14. Only one vaporization study has been performed--that by Panish¹⁵ who measured mass-spectrometrically the pressures of the species in equilibrium with the congruently vaporizing sesquioxide at 20000K. Less is known about europium monoxide. Its enthalpy of formation has been measured by solution calorimetry, 7 and its low temperature heat capacity investigated over a limited temperature range 16. No thermochemical measurements of trieuropium tetraoxide are available. However, Westrum¹⁷ has estimated some of the thermodynamic values for the monoxide and sesquioxide phases.

B. The Bromides and Hydrated Bromides of Europium

1. Preparative and Structural Investigations

a. Europium Bromides

The preparative procedures for and the properties of anhydrous lanthanide bromides are given in several reports. Taylor and Carter 18 have described a preparative procedure for europium tribromide -- the careful heating of a hydrated tribromide-ammonium bromide matrix in vacuum. They report the results of chemical analysis, the color of the phase, and the color of its aqueous solution. Europium tribromide has also been reported as an intermediate product in the thermogravimetric studies of the hydrated tribromide 19. Controlled vacuum dehydration of the hexahydrates has yielded impure tribromides of the heavy lanthanides (Gd-Lu), 20 but no corresponding data are reported for the europium phase. However, application of radius ratio rules to the ions indicates that EuBr₃ should crystallize in the orthorhombic $PuBr_3$ -type structure, 20 while $GdBr_3$ should form the observed hexagonal FeCl₃-type structure. Europium dibromide is also poorly characterized. In 1939, Klemm and Doell²¹ reported preparation of a chocolate-colored phase by heating the hydrated tribromide under a stream of hydrogen bromide. When this phase was subsequently reduced under hydrogen, a colorless phase resulted. Magnetic measurements on the chocolate-colored phase indicated 90% divalent europium.

additional investigations of the dibromides, Doell and Klemm²² obtained an X-ray powder diffraction pattern which was similar to that obtained for strontium and samarium dibromides and indicated that the three phases were isostructural, but they were unable to index it. In the same year, the single-crystal data of Kammermans²³ indicated an orthorhombic structure for SrBr₂. These two results have been interpreted to mean²⁴ that the europium phase has the structure described by Kammermans. However, SrBr₂ recently has been shown to possess tetragonal symmetry²⁵; Kammermans determined the structure of SrBr₂·H₂O. In addition to the preparative procedures reviewed by Taylor,²⁶ Cotton and Wilkinson²⁴ report that europium dibromide may also be prepared by thermal decomposition of the tribromide.

b. Hydrated Europium Bromides

Although europium tribromide hexahydrate is occasionally mentioned as a starting material for other investigations, 18,21 conformation of the hexahydrate composition 19 is the only information reported for hydrated europium bromide phases.

2. Thermodynamic Investigations of Europium Bromides

As Nikova and Polyachenok²⁷ noted in their recent review, no experimental thermodynamic data have been reported for either lanthanide dibromides or tribromides. However, estimated values for heat capacities and thermodynamics of fusion, vaporization, formation, and dissociation have been

compiled by Brewer, 28 Brewer et al., 29 Feber, 30 and Wicks and Block 31.

C. The Oxides of Bromine

The following oxides have been reported for bromine:

Br₂O, BrO, BrO₂, BrO_{2.5}, BrO_{2.67}, and BrO₃³²⁻³⁵, but none appears to be stable at room temperature unless under an atmosphere of ozone. Since the presence of binary bromine-oxygen compounds is not expected at high temperatures, these phases will not be considered further in this investigation.

D. The Oxide Bromides of Europium

1. Preparative and Structural Investigations

of the limited work expended on lanthanide oxide bromide phases, investigations of the europium system have been most numerous. Baernighausen et al. have prepared the monoxide monobromide, EuOBr, both by bromination of the sesquioxide at 700° under a bromine-laden inert gas stream, and by heating the tribromide hexahydrate at 350° for 1-2 d in air. For this phase, their X-ray powder diffraction data indicated the tetragonal PbFCl-type structure characteristic of other lanthanide oxide bromides 37. The second preparative technique is consistent with the thermogravimetric study of Mayer and Zoltov¹⁹ who found EuOBr to be the only oxide bromide of europium. However, this result disagrees with additional experiments of Baernighausen³⁶ who

obtained previously unreported trieuropium tetraoxide monobromide, Eu₃O₄Br, by heating an equimolar mixture of EuOBr and Eu₂O₃ in a nitrogen atmosphere at 950°. Analogous samarium and ytterbium phases were prepared by heating the monoxide monobromides in air at 680° and 440°, respectively. More recently, the preparation of Nd₃O₄Br has been reported³⁸. The X-ray powder diffraction data for these phases have been indexed on orthorhombic symmetry, but neither the space group nor the structure type has been reported.

2. Thermodynamic Investigations

Although thermodynamic measurements have been made on selected monoxide monochlorides by two different static equilibrium techniques, 39-43 no measurement has been made on any lanthanide oxide bromide phase.

CHAPTER III

THEORETICAL CONSIDERATIONS PERTINENT TO THIS INVESTIGATION

A. Phase Relationships

1. Possible Phases in the Europium-Oxygen-Bromine System

A general formulation for all stoichiometric phases in the europium-oxygen-bromine ternary system where all possible Eu(II)-Eu(III) and all possible oxygen-bromine ratios may occur is Eu $_{\ell}^{O}[(3\ell^{-m})/2]-[n/2]^{Br}n$. The coefficients ℓ , m, and n may assume integral values in accordance with the restriction that $\ell \geq 1$, $0 \leq m \leq \ell$, and $0 \leq n \leq (3\ell^{-m})$. The metal oxygen and metal-halide binary systems are defined by n=0 and $n=(3\ell^{-m})$, respectively. Numerous values are degenerate as a result of successive multiplication of their simplest formulas; however, no possible stoichiometric phase is excluded. Although one would not anticipate the existence of an exceedingly large number of phases, the ternary system does possess potential for preparative investigations.

2. Vaporization and the Phase Rule

a. Vaporization Modes

The vaporization behavior of a single phase may be either congruent or incongruent. Congruent vaporization occurs when the composition of the vapor is always the same as that of the condensed phase. The vaporization of a condensed phase to give a second condensed phase and a vapor of different composition is an incongruent process.

b. The Phase Rule

One of the most useful relationships in vaporization studies is Gibb's phase rule:

$$F = C - P + 2. (III-1)$$

The number of degrees of freedom, F, is expressed in terms of the number of components, C, and the number of phases, P. When a vaporizing system is fixed at its equilibrium pressure, the system is invarient, i.e. F = 0.

Application of the phase rule to vaporization processes falls into two classes according to the congruency or incongruency of the behavior. For congruent processes, P=2 (condensed phase and vapor), and F=C. Even though C=2 in a binary system, only the temperature need be fixed since the one necessary additional restriction—that the composition of the vapor and condensed phase be the same (i.e. fixed)—is implied in the congruency definition. For incongruent processes, P=3 (2 condensed phases and vapor),

and F = C-1. In a binary system (C = 2), a definition of temperature fixes the pressure, but in a ternary system (C = 3), the temperature plus the composition of either the second condensed phase or of the vapor phase (one fixes the other) must be defined. One point which must be mentioned is that the phase rule only fixes the composition of the vapor phase, and in no way defines the vapor species.

c. The Pressure-Composition Diagram

The qualitative results of vaporization studies for two-component systems may be presented easily by a pressure-composition diagram drawn for a constant temperature. Such a diagram conveniently defines all stoichiometric and non-stoichiometric phases, whether incongruently or congruently vaporizing, and the compositions of their vapors. Examples of pressure-composition diagrams are given by Gilles 44.

B. <u>Vapor Pressure Measurement by the Knudsen Effusion</u> <u>Technique</u>

1. General Introduction

Vapor pressures in the range 10^{-9} to 10^{-3} atm may be measured by either Langmuir (free) vaporization or Knudsen effusion techniques ⁴⁵. The latter method, which is based on the rate of effusion of the vapor through an orifice, may assume one of several forms: vacuum microbalance, torsion effusion, target collection, mass spectrometric measurement, or various combinations of these.

2. Theoretical Considerations of the Target Collection Method

If an isotropic vapor in thermal, chemical, and mechanical equilibrium with a condensed phase is confined in a volume, its motion may be described by the kinetic theory of gases. In the theoretical treatment first described by Knudsen⁴⁶,⁴⁷ and more recently by Ackermann⁴⁸ and Ward⁴⁹, the number of molecules striking the container per unit time, Z, is related to the number of molecules per unit volume, n, and the average molecular velocity, \bar{v} , by equation (III-2).

$$Z = n\overline{v}/4 \text{ molecules cm}^{-2} \text{sec}^{-1}$$
. (III-2)

If a small, circular, ideal (infinitesmally thin) orifice is placed in the container wall, such that vapor is allowed to effuse into a perfect void in such small quantities that equilibrium in the container is not destroyed, the number of molecules passing through an orifice of area S_0 is simply $S_0\left(n\bar{v}/4\right)$.

The fraction of the effusing molecules striking a circular collector plate of radius r, the center of which is located at a perpendicular distance d from the orifice, may be calculated from the cosine distribution law. The flux of molecules leaving the orifice and arriving at an area increment dN on the collection plate is given by:

$$dN = \pi^{-1} N_0 \cos \theta d\omega,$$
 (III-3)

where N_0 is the total molecular flux at the orifice and θ is the angle between the perpendicular and the axis of $d\omega$, the solid angle increment of the effusate intersected by area dN. Qualitatively, $\pi^{-1}\cos\theta \ d\omega$ is the fraction of the total flux moving in a specific direction. Substitution in terms of the variables r, d, S_0 , and Z into the cosine function and integration over the hemisphere of space above the orifice gives relationship (III-4).

$$N = Z S_0(r^2/d^2 + r^2)$$
 molecules sec⁻¹. (III-4)

If the pressure in the container is $\leq 10^{-3}$ atm, the gas may be assumed ideal, and n=p/kT. Multiplication of equation (III-4) by a time interval, t, combination with relationship (III-2), substitution of $\bar{v}=\left(8kT/\pi\right)^{1/2}$ from kinetic theory, and inclusion of the ideal gas assumption gives equation (III-5) for the equilibrium vapor pressure.

$$P = [W/S_0t] [2\pi RT/M]^{1/2} [(d^2 + r^2)/r^2].$$
 (III-5)

If W grams of effusate of molecular weight M is collected in t minutes by a circular collector of radius r cm located at a perpendicular distance d cm above an orifice of area S_0 cm², and if R is defined in ergs deg⁻¹mole⁻¹, P is obtained in units of dynes cm⁻² and may be converted easily to atmospheres. The terms in equation (III-5) may be combined to give the following:

$$P = [3.760 \times 10^{-4} \text{ W/s}_0 \text{t}] [T/M]^{1/2} [(d^2 + r^2)/r^2] \text{ atm.} (III-6)$$

Measurement of the parameters in equation (III-6) constitute vapor pressure determination by the target collection

Knudsen effusion technique.

3. Limitations of the Knudsen Method

a. Non-Ideal Cells

(1) The Non-Ideal Orifice

One basic assumption in the derivation of the Knudsen equation is that the orifice is ideal (infitesmally thin). However, since attainment of such orifices is impossible, the channeling effect (resistance of a tube to a passing vapor) of an orifice as a function of its geometry must be considered. As Clausing first demonstrated 50, the effusion probability (so-called Clausing factor), Wo, can be calculated as a function of the length L and the radius R of the orifice channel by $W_0 = 8R/3L^{51}$. Clausing corrections are often only applicable to total effusion (weight loss) measurements, in which $W_{\mathbf{0}}$ appears in the right-hand denominator of equation (III-5) and the term for the fraction of effusate collected (a function of r and d) is unity. Correction factors for channel orifices as a function of both L/R and θ , the angle defining the fraction of effusate collected, have recently been tabulated 52,53, so that corrections may also be made for target collection experiments in which cylindrical orifices are employed. The effusion probabilities of conical orifice geometries have also been treated by Iczkowski et al.54.

(2) Non-Ideal Collection Geometry

Ward⁴⁹ has recently examined the validity and limits of the cosine distribution law for real "knife-edged" (conical) orifices by both collection experiments and Monte Carlo calculations. Both sets of results confirm that the orifice and Knudsen cell geometries have little effect on the cosine distribution for small angles of θ , i.e. in the forward direction, while severe deviations may be observed for large angles of θ . Irregularities in the cell walls or the sample surface may give rise to corresponding deviations in the cosine distribution by a "pinhole camera effect". Ward concludes that total effusion measurements (weight loss) will probably be in error, but, if the collection geometry is chosen properly, target collection results will be less ambiguous than those of weight loss experiments.

(3) Thermal Expansion of the Orifice

The change in orifice area as a function of the linear expansion coefficient of the crucible material, a function of temperature, must be considered. However, the results of Kent⁵⁵ indicate that changes in orifice diameters between room temperature (measurement temperature) and 2500° is of the order of 0.1% for most materials. Such corrections are negligible and are not considered further in this investigation.

b. Non-Ideal Gas

In the derivation of the Knudsen equation, the ideal gas assumption is invoked. So-called "viscous flow", and not the "free molecular flow" prescribed by Knudsen conditions, results if the vapor is too concentrated. Dushman⁵⁶ states that the ratio of mean free path of the vapor to the radius of the orifice should be equal to or greater than unity. The experiments of Mayer⁵⁷ indicate that the cosine law is obeyed at pressures up to 5×10^{-3} atm with orifices of 10^{-4} - 10^{-5} cm².

c. Non-Equilibrium Conditions

(1) Sampling and the "Orifice Effect"

The derivation of the Knudsen equation assumes that the vapor is in physical equilibrium in the cell, but the presence of even the smallest orifice upsets this condition. An expression derived by Carlson et al. 58 may be employed to correct the observed pressure to the equilibrium value, a function of the observed pressure, the orifice area, and the sample area. Experimentally, large deviations from vapor saturation result in the so-called "orifice effect". If equilibrium is severely displaced by the presence of an orifice, a large change in orifice area will be accompanied by an inverse change in the measured pressure for any given set of conditions.

(2) The Vaporization Coefficient

The vaporization coefficient, $\alpha_{_{\mathbf{v}}}$, is defined as the ratio of the rate of evaporation into a void to the rate at which a saturated (equilibrium,) vapor impinges on the sample, or simply the ratio of the Langmuir pressure to the Knudsen pressure. Values of α_{τ_r} may vary from 0 to 1. The condensation coefficient, α_{c} , may also be defined, but ambiguity often arises. As Margrave has noted 45 , $\alpha_{\tau\tau}$ and α_{c} are generally assumed equal. Regardless of the definition, the net effect is the same; namely, a system with a non-unity vaporization coefficient is only able to attain a steady state and not a true equilibrium pressure. Ackermann et al. 59 have analyzed the problem of a nonunity vaporization coefficient by a nonequilibrium thermodynamic treatment and indicate that difficulties may arise from a temperature gradient at the surface, or from surface contamination or strain. Experimental results 60 agree with these postulates in that α_{ij} for the formation of tetrameric arsenic gas from the solid is 4.6×10^{-4} . The difficulty apparently lies in the energetics or strain of the mechanism by which the tetramer forms on the surface. Rosenblatt⁶¹ notes that α_{ij} is usually unity if the sample is finely divided so that the effective vaporization area is large.

(3) <u>Diffusion</u>

Additional difficulties arise in incongruently vaporizing systems where a solid product tends to grow on the surface of

the reactant such that contact of the vapor phase with the reactant is hindered. The calculation of Ackermann et al.⁵⁹ indicates that most vapor species escape from the outermost atomic layer. Diffusion of species through the solid coating would appear to be the only mechanism for their reaching the surface. Several experimental procedures which may be employed to detect the effects of diffusion in Knudsen experiments are: (a) comparison of the measured pressures at a given temperature as a function of time, (b) comparison of data collected for samples of different particle size (different surface area), and (c) comparison of pressures measured at successively increasing and decreasing temperatures. If no systematic trends are observed in these comparisons, diffusion effects are probably negligible.

d. Additional Limitations to Target Collection Effusion Measurements

Many of the problems often encountered in collection experiments are obvious, but should be mentioned.

- (1) All effusate impinging on the collection plate must adhere. Experiments may be designed to measure the sticking coefficient, which may vary with target temperature.
- (2) Evaporation of effusate from the walls of the vacuum system must not occur. This problem could be very significant for conducting effusates when induction heating is employed.

- (3) Residual pressures must be low enough to preclude scattering of the effusate between orifice and collector, or appreciable effusion of residual gas into the Knudsen cell.
- (4) Temperature gradients within the effusion cell must be avoided.
- (5) Changes in the thermodynamic acitivity of a sample by contamination from reaction with either the atmosphere or the crucible material must be avoided.

C. X-Ray Fluorescence

1. The Basic Phenomenon

When an atom has sufficient energy as a result of radioactive decay or excitation by an electron beam, gamma ray, or X-ray, the atom may de-excite by ejection of an electron from an inner atomic shell. If atomic structure is treated by the Bohr model, the filling of an electron vacancy by decay of a second electron from a higher level results in emission of a photon of fixed energy. Since the inner atomic structure is only slightly affected by chemical bonding, quantitative and qualitative analysis may be accomplished without concern for the chemical environment of the sample. Thorough treatments of the origin of primary and secondary (fluorescent) X-rays are available 62,63.

2. The Bragg Equation

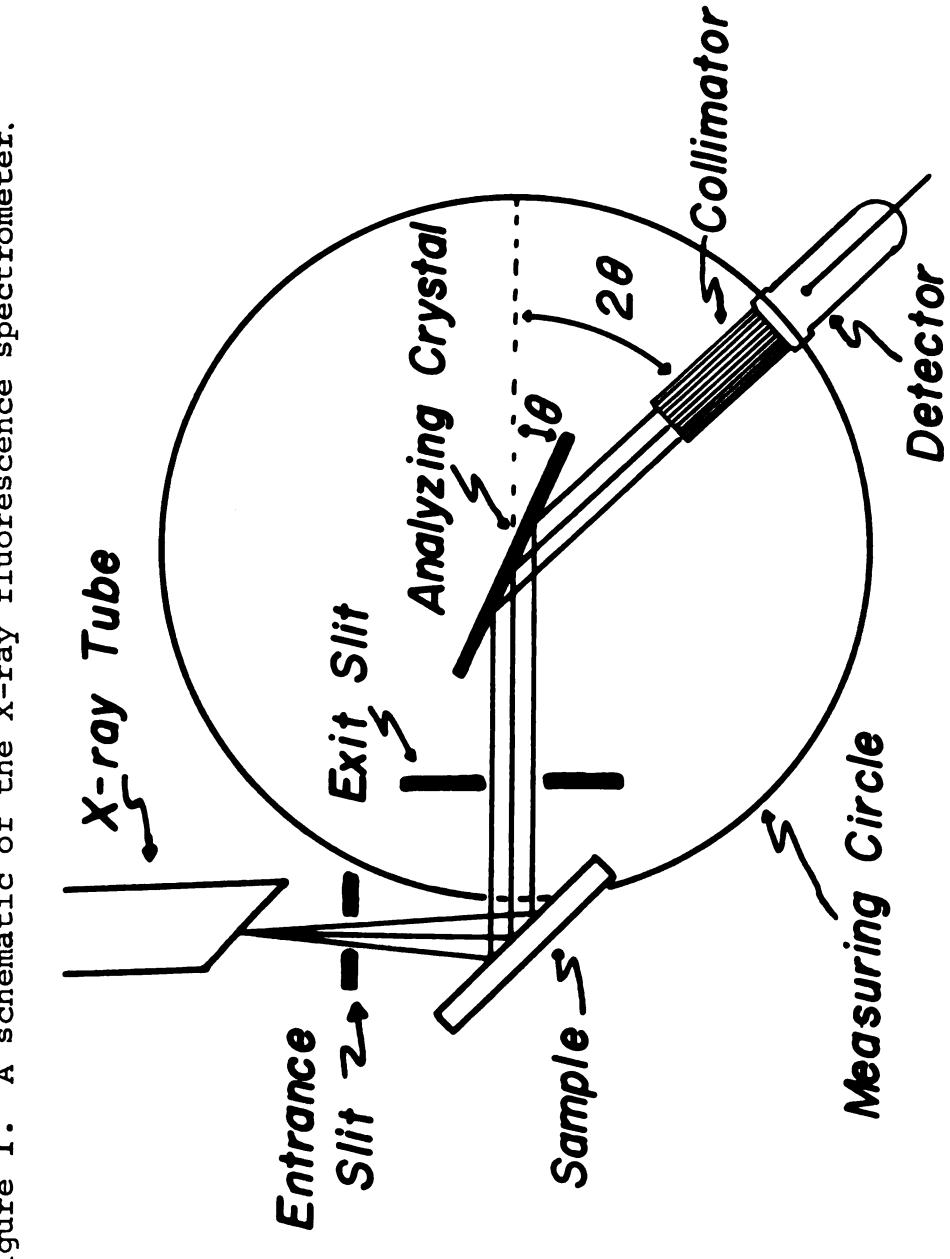
Analysis of the energies of fluorescent X-rays may be accomplished by the principle of X-ray diffraction given by the Bragg equation: $n\lambda = 2d \sin \theta$. In the normal diffraction experiment, a fixed X-ray energy, λ , is diffracted at different angles, θ , by various crystallographic planes of separation d. Analysis of photon energies may be accomplished by fixing d with a given analyzing crystal so that the various energies are diffracted at different θ values. A schematic representation of the spectrometer is given in Figure 1.

D. Temperature Correction

Measurement of temperature by optical pyrometry presents difficulties in that the transmission loss from optical windows and prisms results in a low observed temperature. As Margrave has indicated 64 , consideration of Wein's radiation law leads to a relationship between the reciprocal of the true temperature, T, and that of the observed temperature, T_0 , as follows:

$$(1/T - 1/T_0) = F,$$
 (III-7)

where F is a constant. Values of F for a given optical path may be obtained by measuring the temperature of a reference source directly and via the optical path.



A schematic of the X-ray fluorescence spectrometer. Figure 1.

E. Thermodynamic Calculations

1. Second Law Calculations

a. Derivation of Relationships

The free energy change in a reaction at a given temperature T is related to the changes in enthalpy and entropy of reaction and to the equilibrium constant by equations (III-8) and (III-9), respectively.

$$\triangle G_{T}^{0} = \triangle H_{T}^{0} - T \triangle S_{T}^{0} . \qquad (III-8)$$

$$\triangle G_{\mathbf{T}}^{0} = -R^{\mathsf{T}} \log K_{\mathbf{T}}. \qquad (III-9)$$

The product of 2.3026 and the gas constant, R, is designated by R'. Combination of these equations gives the following linear relationship:

$$\log K_{T} = -(\Delta H_{T}^{0}/R'T) + \Delta S_{T}^{0}/R'. \qquad (III-10)$$

Treatment of experimental log K <u>versus</u> 1/T data by a linear least squares regression (<u>cf. III</u>, 5, 1) gives an equation of the form $\log K_T = (m/T) + b$. By equating coefficients, values for the enthalpy and entropy of reaction are obtained as follows:

$$\triangle H_{\mathbf{T}}^{\mathbf{0}} = - R^{\dagger} m, \qquad (III-11)$$

$$\triangle S_{T}^{0} = R'b.$$
 (III-12)

b. Assumptions of the Second Law Treatment

Several assumptions are made in the second law treatment of equilibrium vapor pressure data. First, the equilibrium constant for a general reaction, in which ν_i and ν_j are the stoichiometric coefficients and a_i and a_j are the thermodynamic activities of the products and reactants, respectively, is given by equation (III-13).

$$K = \prod_{i} (a_{i})^{\nu_{i}} / \prod_{j} (a_{j})^{\nu_{j}} . \qquad (III-13)$$

The activities of all solid phases are assumed to be unity, while those of all gaseous species are replaced by their fugacities. For an ideal gas, the fugacity is equated with its partial pressure. For high temperature effusion measurements, the vapor is sufficiently dilute so that it may be assumed ideal (cf. III, B, 3, b). However, the assumption that the activities of the solid phases are unity rests on more tenuous ground, and is most difficult to validate experimentally. Even if the mutual solubilities of condensed phases, the solubility of contaminant or container materials in the equilibrium phases, or slight variations from stoichiometry could be accurately determined at the reaction temperature, their effect on the various activities is yet another problem. Though very unrepresentative, examination of the equilibrium phases at room temperature by X-ray diffraction can give indications of contamination or stoichiometric changes by variation in lattice parameter. A second

assumption is that the log K versus 1/T equation is linear. Because Δ Cp for the reaction over the temperature range of the measurements is generally non-zero, the data should exhibit slight curvature. The Σ -plot treatment, which employs heat capacity equations⁶⁵ or tabulated thermochemical data⁶⁶, allows correction of this difficulty.

c. Data Reduction to the Reference Temperature

If the enthalpy change for a reaction is measured at some median temperature, T, it may be expressed in terms of the enthalpy change at a reference temperature (2980K is selected here) and the change in heat capacity for the reaction as follows:

$$\Delta H_{T}^{0} = \Delta H_{298}^{0} + \int_{298}^{T} \Delta Cp \ dT.$$
 (III-14)

Similarly for the entropy change of the reaction, it follows that:

$$\Delta S_{T}^{0} = \Delta S_{298}^{0} + \int_{298}^{T} \Delta Cp/T dT.$$
 (III-15)

For a general reaction where v_i and v_j are coefficients of the products and reactants, respectively, Δ Cp is given by equation (III-16).

$$\triangle Cp = \sum_{i} v_{i} Cp_{i} - \sum_{j} v_{j} Cp_{j}. \qquad (III-16)$$

However, since enthalpy and entropy functions are most often

tabulated, equations (III-14) and (III-15) are generally more useful in their following integrated and rearranged forms.

$$\Delta \mathbf{H_{298}^{0}} \; = \; \Delta \mathbf{H_{T}^{0}} \; - \; [\sum_{\mathbf{i}} \; \mathbf{v_{i}} (\mathbf{H_{T}^{0}} \; - \; \mathbf{H_{298}^{0}})_{\mathbf{i}} \; - \; \sum_{\mathbf{j}} \; \mathbf{v_{j}} (\mathbf{H_{T}^{0}} \; - \; \mathbf{H_{298}^{0}})_{\mathbf{j}}] \; . \\ (\mathbf{III-17})$$

$$\Delta \mathbf{s_{298}^{0}} = \Delta \mathbf{s_{T}^{0}} - \left[\sum_{i} v_{i} (\mathbf{s_{T}^{0}} - \mathbf{s_{298}^{0}})_{i} - \sum_{j} v_{j} (\mathbf{s_{T}^{0}} - \mathbf{s_{298}^{0}})_{j} \right] \cdot (\mathbf{III-18})$$

If heat capacity data are not available, they may often be approximated as described in a following section (\underline{cf} . III, E, 4).

d. Calculation of the Second Law Entropy

The standard entropy at the reference temperature of any one of the reactants or products may be obtained from the measured entropy change for the reaction, provided the standard entropies of all other reactants and products are known. The entropy change may again be expressed in terms of the general coefficients, v_i for products and v_j for reactants, as follows:

$$\Delta S_{298}^{0} = \sum_{i} v_{i} S_{298i}^{0} - \sum_{j} v_{j} S_{298j}^{0} . \qquad (III-19)$$

Since vaporization reactions are a special case in that there is only one reactant, the summation on j may be dropped, and the standard entropy of a vaporizing phase j is obtained as follows:

$$s_{298j}^{0} = (1/v_{j})(\sum_{i} v_{i} s_{298i}^{0} - \Delta s_{298}^{0}).$$
 (III-20)

2. Third Law Calculations

a. <u>Derivation of Relationships</u>

In addition to its usefulness as a quantity which may be interpolated easily, the free energy function may be employed to reduce thermodynamic data to the reference temperature⁶⁵. The free energy function, hereafter abbreviated as fef, is defined as follows:

fef
$$\equiv (G_T^0 - H_{298}^0)/T$$
. (III-21)

Substitution of basic thermodynamic relationships leads to another expression.

fef =
$$(H_T^0 - H_{298}^0)/T - S_T^0 = (H_T^0 - H_{298}^0)/T - (S_T^0 - S_{298}^0)-S_{298}^0$$
.

When free energy functions are not tabulated they may be readily calculated from tabulated data and equation (III-22). The necessary enthalpy and entropy functions and standard entropy may also be approximated (cf. III, E, 4).

If fef values for the products and reactants with coefficients ν_i and ν_j , respectively, are known, Δ fef for the reaction may be calculated as follows:

$$\Delta fef = \sum_{i} v_{i} fef_{i} - \sum_{j} v_{j} fef_{j}$$
. (III-23)

Like fef, values of \triangle fef may be accurately interpolated by graphing \triangle fef versus T. From equation (III-21), \triangle fef may also be expressed by the following relationship:

$$\triangle fef = (\triangle G_{T}^{0} - \triangle H_{298}^{0})/T. \qquad (III-24)$$

Substitution from equation (III-9) for the free energy change and rearrangement of the relationship leads to an equation for the enthalpy change at the reference temperature.

$$\Delta H_{298}^{0} = -(\Delta fef + R' \log K_{T})T.$$
 (III-25)

Since a value for log K is obtained at each measurement temperature, the Δfef value for that temperature may be employed to calculate a ΔH_{298}^0 for each data point.

b. The Value of Third Law Calculations

Because each experimental point yields an enthalpy value at the reference temperature, the individual values may be examined for consistency and trend, either with temperature or chronological sequence. A temperature trend may arise from a systematic error in pressure or temperature measurement or in the free energy function change for the reaction. Large discrepancies between second and third law results may be interpreted as a gross error in measurement, or an incorrect definition of the vaporization process. Large deviations of the vaporization coefficient from unity also result in second—third law disagreement. A second utility of the comparison lies in the evaluation of approximated thermodynamic values such as high temperature heat capacities and absolute entropies of solids. Since second and third law methods employ the same approximated Cp data

through different paths, agreement of the results is at least indicative of internal consistency in the estimated values, if not of the accuracy.

3. Energetics of Formation

The results of a vaporization reaction may be employed to obtain entalpies, entropies, and free energies of formation of one reactant or product if the values are known for all other reactants and products. For a general reaction, an equation in terms of a general variable Q^0 ($Q^0 = G^0$, H^0 , S^0) may be written for any temperature (usually 298^0K) as follows:

$$\Delta Q_{98}^{9} = (\sum_{i} v_{i} \Delta Q_{f298i}^{0} - \sum_{j} v_{j} \Delta Q_{f298j}^{0}).$$
 (III-26)

Since ΔQ_{298}^0 is obtained experimentally for the vaporization reaction, any of the other quantities may be calculated. For a vaporization reaction, the summation on j may again be dropped and the value of ΔQ_{f298}^0 for a vaporizing phase j becomes:

$$\Delta Q_{f_{298}}^{0} = (1/v_{j})(\sum_{i} v_{i} \Delta Q_{f_{298i}}^{0} - \Delta Q_{298}^{0}).$$
 (III-27)

Since the entropies of the elements in their standard states are generally available at the reference temperature, and since S_{298}^0 for a given compound may also be evaluated from second law results (cf. III, E, 1, d) or estimated (cf. III, E, 4, b), ΔS_{f298}^0 for that compound may be evaluated from relationship (III-28).

$$\Delta s_{f298i}^{0} = s_{298i}^{0} - \sum_{j} v_{j} s_{298j}^{0}. \qquad (III-28)$$

In this case, v_j designates the coefficients of the reacting elements j in the formation reaction for compound i.

4. Approximation of Thermodynamic Functions

a. The Approximation of High Temperature Heat Capacities

(1) Solids

The lack of heat capacity data for many of the compounds studied in this investigation has necessitated approximation of the values. Attempts to employ measured enthalpy functions $(H_T^0 - H_{298}^0)$ of stoichiometrically identical phases by exchanging the $(H_T^0 - H_{298}^0)$ value of one element with that of the desired element has proven unsatisfactory, even though the approach has been used successfully for some systems 67,68 . However, if high temperature heat capacity data as a function of temperature are available for any phase, A_uB_v , in a binary system, a heat capacity equation may be obtained for any other binary phase A_xB_y by use of the following formula:

$$CpA_xB_v = [x/u][CpA_uB_v] + [(uy - vx)/2][3R].$$
 (III-29)

The second term arises through application of Kopp's rule⁶⁵ which states that at high temperatures, the contribution to the heat capacity by each atom in a solid is 3R. The same type of equation is also applicable to ternary systems of

one metal and two cations. For a compound $A_x B_y C_z$, the heat capacity of any binary phase $A_u B_v$ may be employed as follows:

$$CpA_xB_vC_z = [x/u][CpA_uB_v] + [(uy - vx)/2 + (z)][3R].$$
 (III-30)

Experimental data may come from either the A-B or the A-C binary system. Care should be taken in use of equations (III-29) and (III-30) to the extent that; (a) element A represents the component with highest molecular weight, i.e. the largest contributor to the heat capacity, (b) the phases considered have comparable degrees of ionic character, and (c) the approximations not be extended below 298°K where anomolous heat capacity functions are common.

2. Simple Polyatomic Gases

In the absence of spectroscopic and structural data for a gaseous molecule, a normal statistical thermodynamic treatment is impossible, and other approximations must be made. Vibrational frequencies or force constants and ground state electronic levels might be estimated, but the likelihood of success is small. Data for gaseous metal dibromides, the only polyatomic species encountered in this investigation, are scant, but values are available for linear (D_{ODh}) TiBr₂ and HgBr₂, and bent (C_{2V}) PbBr₂ $(Br-Pb-Br \ angle = 95^{\circ})$ and $ZrBr_2$ $(Br-Zr-Br \ angle = 120^{\circ})$. The heat capacities of the linear molecules differ by only 0.06 eu (0.025%) at $298^{\circ}K$ and converge at higher temperatures,

even though a large mass difference exists between Ti and Hg. A similar deviation is observed for the bent case (0.875%), while the two sets of values (linear versus bent) differ by 1.5 eu (> 10%). Based on these data, the high temperature heat capacity of a gaseous dihalide seems to be most dependent upon molecular symmetry, with negligible effects from molecular weight, or even the magnitude of molecular bend. Therefore, satisfactory approximations of heat capacities and $(H_T^0 - H_{298}^0)$ or $(S_T^0 - S_{298}^0)$ functions may be made by identification of the molecular geometry.

be unimportant in approximations. However, if the free energy functions of the previously mentioned gases⁶⁹, or those estimated for a large number of metal dibromides⁷⁰ are examined according to molecular weight, a definite trend with mass is observed. Why is there an apparent discrepancy? The answer lies in the low temperature heat capacities of the gases. Marked differences occur below 200°K, and these effects appear in two thermodynamic functions—the standard entropy and, hence, the free energy function. Though high temperature heat capacity functions and second law calculations are essentially unaffected by mass differences of gaseous molecules, free energy functions and third law calculation are dependent on mass effects.

b. Approximation of Standard Entropies of Solids

From the measured entropies of numerous solids, Latimer 71

has tabulated the average lattice contribution per atom to the total entropy at $298^{\circ}K$. Single values are listed for cations, while those given for anions take cognizance of the ionic charge normally assigned both to the cation and its anion. From equation (III-31), the entropy of a solid of n components, $(A_{i})_{xi}$ (where $1 \leq i \leq n$), is calculated from the sum of the lattice contributions, S_{i}^{0} , for each component multiplied by its coefficient, xi, in the molecular formula.

$$S_{298}^{0}(A_{i})_{xi} = \sum_{i} xi S_{i}^{0}$$
 (III-31)

Grønvold and Westrum⁷² have reevaluated Latimer's scheme, and Westrum¹⁷ has made specific application to the lanthanide oxides. These more recent contribution values are recommended when approximations are necessary for binary oxide phases.

In addition to the entropy obtained by equation (III-31), the total entropy may also include magnetic contributions. Westrum¹⁷ gives the estimated magnetic contribution per atom for various lanthanide ions. When the magnetic properties must be considered, equation (III-31) is modified to include an additional set of terms based on the magnetic contribution, M_i, such that:

$$S_{298(A_i)_{xi}}^0 = \sum_{i} x_i S_i^0 + \sum_{i} x_i M_i.$$
 (III-32)

These estimated values should be comparable with the second law entropy (\underline{cf} . III, E, 1, d).

c. The Estimation of Enthalpy and Entropy Functions

If heat capacity functions are available or have been approximated as described in parts a and b of this section, the functions $(H_{T}^{0} - H_{298}^{0})$ and $(S_{T}^{0} - S_{298}^{0})$ are obtained by integration of the following equations.

$$(H_T^0 - H_{298}^0) = \int_{298}^T Cp dT.$$
 (III-33)

$$(s_T^0 - s_{298}^0) = \int_{298}^T Cp/T dT.$$
 (III-34)

5. Statistical Methods

a. Least Squares and Standard Error

A least squares regression with associated standard error analysis has been employed for evaluation of all linear data, while a least squares method has been employed for tabular values 73 . All deviations are reported as $\pm \sigma$.

b. Combination of Errors

In thermochemical cycles, the summation of values, each having an associated error, becomes necessary. A common solution to this problem of error estimation appears to be: (a) ignore the problem, (b) give the error of only the present measurement, or (c) average the errors. None of these is a representative estimator. However, this problem has been treated by Feller 4 as follows. If X_i $(1 \le i \le n)$ is a set of variables with standard deviations σ_i , the

deviation in their sum, Y, is $\sigma_{\mathbf{y}}$, where,

$$\sigma_{\mathbf{y}} = \left(\sum_{i=1}^{n} \sigma_{i}^{2}\right)^{1/2}. \qquad (iii-35)$$

If X_i is not an internally independent set, a second term must be included to describe the covariance. However, the data encountered in thermochemical cycles are generally independent.

CHAPTER IV

EXPERIMENTAL EQUIPMENT AND MATERIALS

A. Target Collection Apparatus

The target collection apparatus used in these measurements has been described previously by Kent⁵⁵. However, the quartz effusate shutter was replaced by one of 0.16 cm copper sheet, and the collimator was not employed for the definition of θ , the subtended effusate collection angle (cf. IV, B, 3). Residual pressures were maintained at 10^{-5} - 10^{-6} torr during data collection.

B. X-Ray Fluorescence Equipment

1. Spectrometer

The instrumentation employed in analysis of the collected effusate was the Siemens Model 4b nonfocussing spectrometer equipped with a LiF analyzing crystal, tungsten tube, water-cooled scintillation detector (0.1 mm beryllium window) and Siemens Kompensograph scaling unit. At various times, three different generators (Siemens Kristalloflex IV, Norelco, and Norelco XRG-5000), two different analysing crystals (normal and high intensity) and two different X-ray tubes (AGOW and AGW60) were used.

2. Specimen Mount

The sample mount in the spectrometer was modified to accommodate the 2.6 cm diameter copper targets, which were machined with a 0.19 cm high rim and an internal diameter of 2.0 cm. The original spectrometer geometry was maintained in the modified mount and in a second holder equipped with an eight rpm electric motor for continuous specimen rotation.

3. Effusate Geometry

The fraction of effusate sampled was defined by controlling the amount of target surface exposed to the primary X-ray beam, not by the usual method of limiting the amount of target surface exposed to the effusate. A 45° beveled aluminum insert placed inside the rim of the targets reproducibily defined the area (2.00 cm²) exposed to the primary X-rays.

C. X-Ray Diffraction Equipment

1. Powder Diffraction Equipment

An 80 mm radius Haegg-type focussing X-ray diffraction camera⁷⁵ was utilized for crystallographic analyses of powdered samples. Diffraction data were occasionally obtained with 114.7 mm Debye-Scherrer cameras.

2. Single Crystal Diffraction Equipment

An equi-inclination Weissenberg camera (Charles Supper Co., Watertown, Mass.) was used in the investigation of single crystals.

D. Temperature Measuring Equipment

Temperature measurements in vaporization experiments were made with a National Bureau of Standards-calibrated Leeds and Northrup disappearing filament pyrometer (serial number 1572579). The NBS calibration data allowed for correction of the measured temperature⁵⁵. Additional temperature measurements during preparative reactions were made either with a platinum-platinum-10% rhodium thermocouple and a Honeywell potentiometer, or with a chromel-alumel thermocouple and a Sym-Ply-Trol meter.

E. High Temperature Mass Spectrometer

Mass spectrometric investigation of effusate species was effected with the Model 12, Bendix Time of Flight instrument described previously 67.

F. Micrograph

A Bausch and Lomb Dynazoom micrograph, equipped with a Polaroid 4 X 5 Land camera attachment, was used to obtain photographs of orifices for orifice area determination.

G. Miscellaneous Measuring Equipment

The measurement of various distance, area, volume, and time parameters critical to the vaporization experiments were made with the following equipment. A cathetometer (Gaertner Scientific Co.) was employed in the measurement of orifice-target rim distances. The diameter of the insert defining the collection geometry and the distances from target rim to target face were measured with precision calipers or micrometers. A compensating polar planimeter (Keuffel and Esser Co.) and a micrometer slide with 0.01 mm divisions (American Optical Co.) were used for the measurement of orifice areas. Time intervals of vaporization were measured with a Lab-Chron (Labline, Inc.) 60 cycle timer. An ultra precision micrometer buret (Kontes Glass Co.) with a 0.25 ml capacity, 0.00001 ml division, and 0.04% accuracy was employed for volumetric measurements in X-ray fluorescence standardization.

H. Heating Equipment

A 20-kva Thermonic high-frequency induction generator was employed for heating effusion cells and selected preparative reactants. Additional heating equipment used in preparative experiments were a Marshall Products Co. platinum-40% rhodium wound tube furnace and ordinary laboratory tube furnaces.

I. Vacuum Systems

In addition to the previously mentioned target collection apparatus, the following three vacuum systems were used in this investigation: (a) the water-cooled Pyrex and Vycor system described by Kent⁵⁵, (b) the fast pumping system equipped with a current concentrator⁶⁷, and (c) a second glass system constructed of Pyrex for lower temperature reactions. This latter system consisted of a 2 cm o.d. reaction tube which was mounted vertically into the Marshall furnace. The reaction tube was connected via ground glass joints to a manifold with outlets to a cryogenic trap for condensation of volatile reaction products and to a tube which led to a larger cryogenic trap, a mercury diffusion pump, and a forepump.

J. <u>Inert Atmosphere Glove Box</u>

The glove box with a recirculated, argon atmosphere and with oxygen (BASAF catalyst) and water (alumina and phosphorus pentoxide) removal systems described by Stezowski⁷⁵ was employed during manipulation of air sensitive samples.

K. Effusion Cell Design

1. Target Collection Cells

Two types of effusion cells were used in the target collection measurements: one asymmetric with a black body hole drilled in its bottom, and the other symmetric with an

	:
	i
	1
	-
1	ı
	1

optical cavity identical to the sample cavity. Cells of the asymmetric design, which were machined from molybdenum, are sketched in Figure 2a, while those of symmetric design, which were of both molybdenum and graphite, are illustrated in Figure 2b.

2. Mass Spectrometer Cells

The effusion crucibles employed in mass spectrometric measurements were of the design described by Pilato⁶⁷.

L. Chemicals and Materials

Chemicals and materials used were: (a) europium sesquioxide, (99.9% lanthanide content) spectrographic analysis; 0.05% La₂O₃, 0.01% Nd₂O₃, other lanthanides below detectable limits, 0.02% Zn; American Potash and Chemical Corp., West Chicago, Ill., (b) europium metal; 99.9%, Michigan Chemical Corp., St. Louis, Mi., (c) bromine, technical grade; Dow Chemical Co., Midland, Mi., (d) hydrobromic acid; 48%, reagent grade; Matheson Coleman and Bell, East Rutherford, N.J., (e) ammonium bromide; 99.8%, reagent grade; Matheson Coleman and Bell, East Rutherford, N.J., (f) lithium hydride; unspecified purity; Metal Hydrides Inc., Beverley, Mass., (g) bromoform; purified; Allied Chemical Corp., Morristown, N.J., (h) potassium bromide; spectrographic grade; Matheson Coleman and Bell, East Rutherford, N.J., (i) molybdenum stock; Kulite Tungsten Corp., Ridgefield, N.J., (j) graphite stock; spectrographic grade; Becker Brothers Carbon Co., Cicero, Ill., and (k) quartz; Englehardt Industries Inc., Hillside, N.J.

	; ;
	j
	!
	1
	(

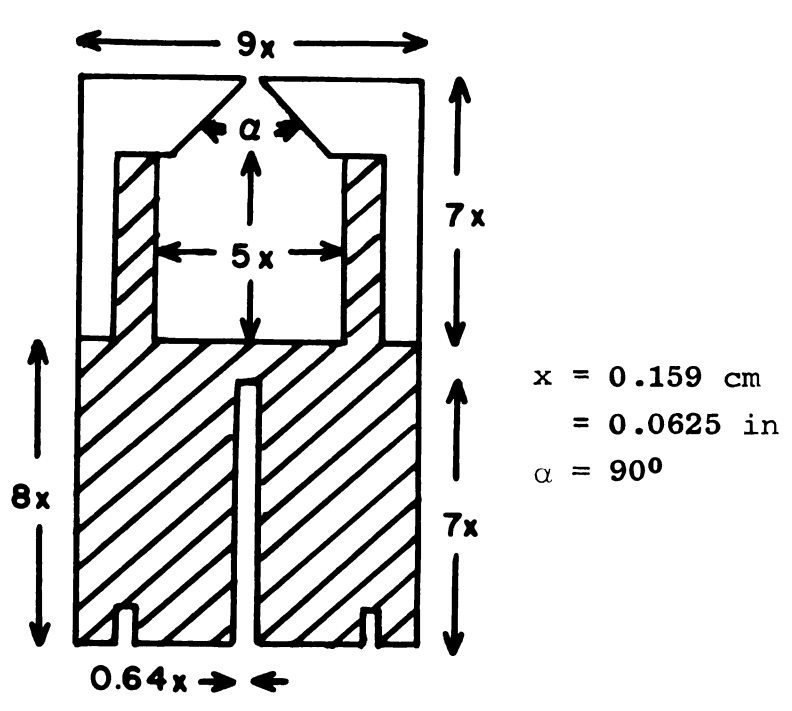
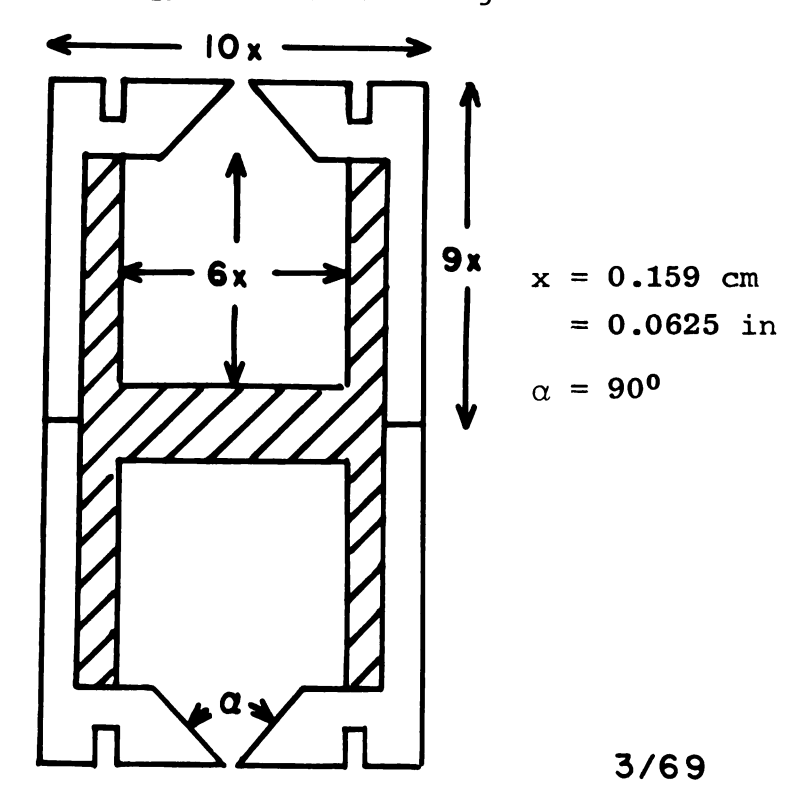


Figure 2a. Asymmetric Knudsen cell design.

Figure 2b. Symmetric Knudsen cell design.



CHAPTER V

EXPERIMENTAL PROCEDURES

A. Preparative Techniques

1. Trieuropium Tetraoxide

Trieuropium tetraoxide was prepared by an adaptation of the method reported by Baernighausen3. Europium monoxide monochloride was prepared by dissolving the sesquioxide in 6 M HCl, evaporating the solution to obtain the hydrated trichloride, and igniting in air at 5000 for several hours3. This EuOCl, which was identified by its X-ray diffraction pattern, was combined in a 1:1:2 stoichiometric ratio with Eu₂O₃ and LiH. The blended reactants were placed in an outgassed tungsten crucible in the glove box and were subsequently heated by induction in the water-cooled Vycor vacuum system in which the residual pressure was $10^{-6}-10^{-7}$ torr. The temperature was increased slowly to 9000 so that the pressure never exceeded 10^{-3} torr. Heating was continued for approximately 5 hr, by which time the pressure had decreased to 10^{-6} torr, an indication that the loss of H_2 , LiCl, and excess LiH, and consequently the reaction, was complete. The product often contained a few small particles of a white phase which could be separated physically from the

reddish black Eu₃O₄. The powder X-ray diffraction pattern of this white phase did not correspond to that of any known lithium-europium-oxygen, or lithium-or europium-oxygen phase. These white particles were combined with additional EuOCl and LiH on the assumption that their molecular weight corresponded to that of Eu₂O₃, and were mixed with the Eu₃O₄ phase before the entire sample was reheated to a maximum of about 1200°.

2. Europium Monoxide

Like the tetraoxide, europium monoxide was prepared by lithium hydride reduction of the monoxide monochloride. The EuOCl and LiH were combined in a 1:2 stoichiometric ratio, placed in a nickel crucible, and heated in vacuum by induction. The temperature was increased slowly to 900° as described previously for Eu₃O₄. After the reaction was complete, the sample was removed, crushed, and reheated at 1000° for 2 hr to remove occluded LiCl.

3. Europium Dibromide

Europium dibromide was prepared by dehydration of a tribromide hexahydrate-ammonium bromide matrix as described by Taylor and Carter¹⁸ for the preparation of the tribromide. Each gram of europium sesquioxide was combined with 15 ml of 48% HBr and 3.5 g of NH₄Br, dissolved with heating and stirring, and finally concentrated at 100° with aeration. The resultant, solid product was placed in the reaction tube

of the Pyrex vacuum system and heated with the Marshall furnace to 200° for 12--15 hr. The final product was obtained by increasing the temperature slowly over an 8 hr period to a maximum of 350° and then decreasing it slowly (3--4 hr) to room temperature. The vacuum system, which contained two liquid nitrogen traps and a mercury diffusion pump, attained residual pressures of $10^{-4}\text{--}10^{-5}$ torr when no sample was present; however, pressure measurements were not made during the heating cycle because of the corrosive nature of the ammonia and bromine vapors.

Single crystal samples of the dibromide were prepared by a vapor transport technique. A sample of the product obtained by the matrix dehydration procedure described above was placed in a 1 cm o.d. quartz tube which had been sealed on one end and connected to the fast pumping vacuum system. This tube was inclined at a 45° angle, and the closed end containing the dibromide was heated at approximately 1000° with a Meeker burner for 36-48 hr.

4. Europium Monoxide Monobromide

Since attempts to prepare europium monoxide monobromide by extended heating of the hydrated tribromide in air at 400° produced impure, amorphous products, samples were prepared by direct bromination of the sesquioxide. A continuous helium flow, which was swept through a reservoir containing liquid bromine, carried the halogen vapor through a tube furnace system constructed of quartz and over a sample of

 $\mathrm{Eu_2O_3}$ confined in a quartz boat. After the oxide had been heated at 400° under a purge of helium, the bromine reservoir was switched into the system. The sample was then heated at $750-800^{\circ}$ for 8 hr under the helium-bromine vapor, cooled to room temperature, and subsequently removed to the glove box.

5. Trieuropium Tetraoxide Monobromide

Samples of trieuropium tetraoxide monobromide were prepared by two techniques—combination of EuOBr and Eu₂O₃ and bromination of the sesquioxide. Mixtures of EuOBr prepared by direct bromination of Eu₂O₃ were blended with the sesquioxide in a 1:1 stoichiometric ratio and placed in 7-10 mm o.d. quartz ampoules which previously had been outgassed in air at 1000°. After the ampoules had been prepared, they were removed from the glove box, evacuated, sealed, and heated in a tube furnace at 900-1050° for 12 hr. Samples of Eu₃O₄Br were also prepared by use of the bromination procedure described for the preparation of EuOBr, with the following exceptions: (a) the system was not initially purged with helium; (b) a very low flow rate of the carrier gas was used to maintain a relatively high partial pressure of oxygen in the vapor.

6. Europium Tribromide

Europium tribromide was prepared by direct reaction of europium dibromide and bromine. Heavy-walled quartz ampoules

(7 cm o.d., 3 cm i.d.) were outgassed as described previously and charged with 0.3-0.7 g samples of EuBr₂. The ampoules were stoppered and removed from the glove box before an excess (1-2 ml) of liquid bromine was added. After the bromine had been frozen in the closed end of the ampoule by immersion in liquid nitrogen, the ampoule was evacuated and sealed. Various ampoules were heated at 60°, 110°, 225°, and 275° (1, 12, 53, and 69 atm of bromine pressure, respectively) in a tube furnace for 12-18 hr. After reaction, the solid products were separated from the excess bromine by cryogenically trapping the halogen vapor.

7. Hydrated Bromide Phases

a. <u>Europium Tribromide Hexahydrate</u>

Europium tribromide hexahydrate was prepared by dehydration of a tribromide solution which was formed by dissolving europium sesquioxide in 48% HBr. The solid, which resulted from evaporation of this solution, was subsequently contained in a porcelain crucible and heated at 125° in a muffle furnace for 30 hr.

b. Europium Dibromide Monohydrate

Although europium dibromide monohydrate was not prepared in pure form, it was observed as an intermediate phase when europium dibromide hydrolyzed in situ in the Guinier camera. Successive X-ray diffraction patterns were obtained to indicate its formation and disappearance.

B. Additional Preparative Reactions and Phase Studies

1. Attempts to Prepare Europium Tribromide

Several attempts were made to prepare the tribromide. In addition to numerous trials to dehydrate a tribromide hexahydrate-ammonium bromide matrix in a manner similar to that described previously, bromination with bromoform and direct combination of the elements were attempted. A sample of europium oxide bromide of unknown oxygen or bromine composition was placed in a quartz boat in a flow system similar to that used for direct bromination procedures. For 4 hr, bromoform vapor was swept by a helium flow from a reservoir containing the liquid at its boiling point into the tube furnace containing the sample at 6250. In the direct combination experiment, a sample of europium metal was placed in an outgassed quartz ampoule. The sample was removed from the glove box, and excess bromine was added and frozen in the closed end of the ampoule, which was then evacuated and The ampoule (30 cm in length) was placed in a tube furnace so that the end containing the metal sample was in the heat zone, while the other end extended outside the furnace and served as a pressure control. The temperature of the metal was slowly increased to $800-900^{\circ}$ and maintained at that value for 12 hr. .

2. Attempts to Prepare Additional Oxide Bromide Phases

a. <u>Direct Combination of Europium Tribromide and</u> Sesquioxide

In an attempt to prepare europium(III)-oxide-bromide phases which are more bromine rich than EuOBr, a 4:1 molar ratio of EuBr₃ and Eu₂O₃ was sealed in an evacuated quartz ampoule (<u>cf</u>. IV, A, 5), heated at 425° for 12 hr, and cooled slowly.

b. The Oxidation of Europium Dibromide

Another attempt to prepare bromide rich ternary phases involved oxidation of europium dibromide. A sample of EuBr₂ was placed in a quartz boat in a tube furnace while oxygen was passed through the system. The oxygen was dried with a dry ice-ethylene glycol trap and a magnesium perchlorate drying tower. Back-flow of air was prevented by a paraffin oil bubbler and a second magnesium perchlorate drying tube. The sample was heated successively for 12 hr at 200°, 250°, and 300°, and heating was discontinued after a change was observed in the sample.

c. Direct Combination of Europium Monoxide and Dibromide

Attempts to prepare divalent oxide bromides were effected as follows. Mixtures of EuO and EuBr₂ in the stoichiometric ratios 1:3, 1:2, 2:3, and 1:1 were prepared and heated in evacuated quartz ampoules at 650-700° for 5 hours.

Several of the stoichiometries were annealed for 2-5 d at 400° .

C. Analytical Techniques

1. Europium Analysis

Metal analysis was effected by conversion of samples to the sesquioxide. Samples were weighed directly into constant-weight crucibles and ignited to the sesquioxide at 1000° in a muffle furnace. Air sensitive samples were weighed in the glove box.

2. Bromide Analysis

Analysis of bromine was accomplished by a gravimetric silver bromide technique. Weighed samples were dissolved in HNO₃ or water as necessary and a standard gravimetric silver halide analysis effected⁷⁶. However, the bromine percentage of monoxide monobromide samples was obtained from the weight gain observed in bromination reactions of the sesquioxide.

3. Oxygen Analysis

Direct analysis for oxygen was not attempted.

D. Density Measurement

The density of europium dibromide was determined by the buoyancy technique. The mass of a crystalline fragment

(approximately 0.1 g), which was hung by a fine nylon fiber, was measured both while the crystal was suspended in the argon atmosphere of the glove box and while it was submerged in dibromomethane at a carefully measured temperature.

E. X-Ray Diffraction Procedures

1. Powder Diffraction Techniques

The techniques of sample preparation and film measurement were essentially identical to those described previously for the Guinier camera by Stezowski⁷⁵. All bromide and oxide bromide samples, except those in which hydrolysis was being investigated, were prepared in the glove box and coated with paraffin oil to prevent decomposition. Both annealed potassium chloride $(a_0 = 6.29300 \pm 0.00009 \,^{\circ}_{A})^{77}$ and platinum $(a_0 = 3.9237 \pm 0.0003 \,^{\circ}_{A})^{78}$ were employed as internal standards. The diffraction data were reduced with the least squares regression program of Lindqvist and Wengelin⁷⁹.

2. Single Crystal Techniques

Oscillation and equi-inclination Weissenberg photographs were obtained by the usual procedures⁶²,⁸⁰. However, because of their hydroscopic nature, crystals were preserved under paraffin oil during both selection and manipulation. Since coatings of Canada balsam and Duco cement were found unsatisfactory for protection of the dibromide, crystals were wedged tightly in 0.2 mm Pyrex Debye-Scherrer

capillaries which were then sealed with a microburner to form capsules (5-6 mm in length). The encapsuled crystals were mounted and examined optically. The air stable trieuropium tetraoxide monobromide crystals were mounted with Canada balsam.

F. Characterization of Vaporization Reactions

1. Weight Loss Measurements

Weight loss data were collected to help characterize the vaporization process and to indicate interaction between sample and crucible. The general procedure involved outgassing a crucible to constant weight, charging it with a known weight of pure sample, and measuring the weight loss which occurred upon complete vaporization, <u>i.e.</u> on disappearance of the initial sample. By measuring the rate of vaporization of a sample (weight loss through an orifice in a given time) at different temperatures, data were simultaneously collected for preliminary vapor pressure estimates needed for the initial target collection experiments.

A sample of Eu₃O₄ was heated by induction to constant weight at 1400-1500° in a molybdenum cell. Similarly a sample of EuO was vaporized in one-hour increments until X-ray diffraction patterns indicated only the presence of Eu₃O₄. Several attempts were made to find a suitable container for vaporization of Eu₃O₄Br. Molybdenum and tungsten cells, both with and without quartz liners, and thoria lined graphite cells were employed. However, the final weight

loss measurements were made with a quartz lined graphite effusion cell in which a sample of ${\rm Eu_3O_4Br}$ was heated to constant weight at $1000-1200^{\circ}$.

2. Mass Spectrometric Investigations

The quilibrium vapors were also analyzed mass spectrometrically employing effusion cells of the materials described in the weight loss experiments. The crucibles were heated by electron bombardment and electron ionizing beams of 10-70 eV were employed. The following temperature ranges were examined for the various compounds: Eu₃O₄, 1400-1700°; EuO, 1100-1450°; and Eu₃O₄Br, 900-1350°; and the relative intensities of all effusate species were measured. The appearance potentials of europium (Eu⁺) and europium bromide (EuBr⁺) were obtained by the linear extrapolation technique using mercury as a reference.

3. Effusate Collection Experiments

Large quantities of the condensable effusates from trieuropium tetraoxide monobromide and europium monoxide monobromide were collected in a quartz cup (1.5 cm o.d., 2 cm high), which was inverted over the orifice of a large quartz-lined crucible (internal diameter = internal height = 2.5 cm). The condensates from Eu₃O₄Br and EuOBr samples, which were heated by induction in the Vycor vacuum system at 950-1150° and 950-1050°, respectively, and the solid residues were transferred to a vacuum desiccator and removed to the glove box, where X-ray diffraction samples were prepared.

4. X-Ray Investigations

The solid residues from the various target collection experiments were examined crystallographically by powder X-ray diffraction techniques. The diffraction data were examined not only for the presence of the equilibrium phases, but also for changes in spacing or relative intensity and for the presence of any additional phases. Samples were obtained from both the bulk residues and the residue-crucible interfaces.

G. X-Ray Fluorescence Procedures

1. Optimization of Spectrometer Parameters

The operating parameters of the spectrometer were adjusted to obtain maximum sensitivity with pulse height discrimination. The spectra of the analyzed elements⁸¹ were recorded and compared with those of the selected target material to check for possible background interferences, i.e. spectra of target material, of contaminents in the target, or of scattered tungsten radiation. The operating maxima for the most interference-free emission were selected by one of two procedures. The first method employed a large sample of the element of interest. The various parameters affecting sensitivity (kilovoltage and milliamperage of the tube, and attenuation, pulse height, and channel width of the discriminator) were adjusted for greatest recorded intensity at the spectral maximum. The second technique

was the procedure for maximization of sensitivity in microanalysis described by Neff⁸². In this technique, 5-10 μ g samples of the elements were employed, and both background and standard counting rates. $(r_b$ and $r_s)$ were measured as a function of the previously mentioned parameters. Conditions for maximum detectability were selected by minimization of the function $(r_b)^{1/2}/(r_s-r_b)$ for each parameter.

2. Counting Procedures

Because a given diffraction angle could not be reproduced accurately with the available instrumentation, a scanning procedure was selected. The 2θ region of \pm 0.25^{o} bracketing the spectral maximum was scanned at a rate of 0.1250/min (equivalent to a 4 min preset time) for both background and sample counting. In an identical way, a control target was counted either before or after each ordinary target, such that variations in conditions or sensitivity which occurred between initial and final counting could be determined. The observed counts/4 min was taken as the average of four successive measurements. When the static sample holder was employed, these counting rates were obtained at four orthogonal target positions. Prior to each set of measurements, the angular position of the spectral maximum was determined such that scanning always covered a reproducible 0.500 region. This counting procedure was employed for both the preparation of calibration curves and for the analysis of condensed effusates.

		,
		·
		,

3. Preparation of Standard Solutions

Standard solutions of europium and bromine were prepared from europium sesquioxide and spectroscopic grade potassium bromide. For europium analysis, samples of calcined Eu₂O₃ (0.02-0.09 g) were weighed with a semi-micro balance, dissolved in a minimal quantity of 6 M HCl, and diluted volumetrically to prepare solutions of 40-100 μ g Eu/ml. For simultaneous europium and bromine analyses, weighed samples of calcined Eu₂O₃ and dried (110°) KBr were combined to prepare standard solutions of 40-100 μ g Eu/ml and 75-200 μ g Br/ml.

4. Preparation of Calibration Curves

Data for linear external calibration curves were obtained by measuring the counting rate from characteristic radiation of standard targets. These standards were prepared by adding known volumes of standard solution to the copper targets which had previously been subjected to background counting. The targets employed were identical in material and design to those used in the collection experiments. Volumetric additions were made both by weighing and by use of the ultra precision microburet. In the first procedure, the mass of added solution at a measured temperature was determined with a semi-micro balance. Between the initial and final weighings, approximate quantities of solution (0.025-0.150 ml) were added with a 10 ml buret. During

the weighing procedure, the targets were enclosed in weighing bottles for the minimization of evaporation effects. In the second method, precise volumes of standard were added directly to the targets with the microburet. The standards were then dried over phosphorus pentoxide and subjected to the final counting procedure. The corrected observed counting rate for a given quantity of an element was obtained by subtracting the initial background rate from the corrected final rate, which was the product of the observed final counts and the ratio of initial to final counts of the control target. The linear calibration data (counts/4 min versus µg of element) were treated by a least squares regression, and the slope was employed as the sensitivity factor for analysis.

H. Target Collection Technique

1. General Collection Procedures

The following procedures were common to all vaporization experiments. The glass portions of the collection apparatus were washed with dilute hydrochloric acid to remove deposits from previous vaporization studies, scrubbed thoroughly with detergent solution, rinsed with distilled water, and allowed to dry in air. The metal target magazine, the copper shutter, and the copper targets were washed with dilute hydrochloric acid, burnished with steel wool, rinsed, and dried with Kimwipes. After their background counts had

been determined, the targets were placed in the magazine, the effusion cell was positioned, and the apparatus assembled and evacuated. After the collection apparatus had attained a 10^{-5} torr residual pressure, liquid nitrogen was added to the magazine dewar, and the orifice to target rim separation was measured with the cathetometer. The effective orificetarget distance was obtained by adding the orifice-rim distance to that from target rim to target face (determined with a micrometer). The effusion cell was heated by induction to the desired temperature and the attainment of thermal equilibrium was determined by repeated temperature measurement with an optical pyrometer. At the beginning of an experiment, temperature measurements also were made through the wall of the vacuum system, and the induction coil adjusted such that both halves of the cell were at the same temperature. After a constant temperature had been attained in the black body cavity, the shutter was opened for the desired time interval (measured with a laboratory timer). Temperature measurements were made repeatedly during the exposure period. After exposure, the target was ejected, and the procedure repeated at a different temperature. Exposure times varied from 2 min to 2 hr per target. Data points were collected at both successively increasing and decreasing temperatures. At the conclusion of some experiments, the target magazine was replaced by an optical window, and the temperatures of the sample and black body cavities were measured over the temperature range. The transmission correction of the optical windows was determined as outlined previously (cf. III, D).

2. Measurement of Orifice Areas

The areas of effusion cell orifices were measured both before and after vaporization experiments. Sharp photographs of the orifices were obtained with the bench micrograph by placing the inverted cell lid on the sample stage and employing an external light source above the lid. The areas of the photographed orifices were measured with the compensating polar planimeter. Since a 100x magnification was employed, the true orifice area was 10⁻⁴ times the measured value. To verify the accuracy of this procedure, the areas of several circular orifices were also determined by photographing the orifice over the 0.01 mm division micrometer slide, and thereby measuring the orifice diameters directly. The two procedures yielded identical results within the precision of the measurements.

3. Specific Experimental Procedures and Conditions

In addition to the general procedures described in a previous section (cf. V, H, 1), specific techniques and conditions were employed for each system investigated. All measurements involving trieuropium tetraoxide were made with asymmetric molybdenum cells which were charged with 0.4-0.5 g of Eu₃O₄ and 0.05-0.10 g Eu₂O₃. Measurements were made in the temperature range $1330-1745^0$ with orifices of areas 6.7×10^{-4} , 21.1×10^{-4} , and 59.9×10^{-4} cm². For europium monoxide, both symmetric and asymmetric molybdenum

cells (orifice areas 8.0×10^{-4} , 42.5×10^{-4} , and $60.5 \times$ 10^{-4} cm²) were charged with 0.3-0.4 g EuO and 0.05-0.10 g of Eu₃O₄. Collection measurements were made from 1060-14890. For europium dibromide, symmetric graphite cells (orifice areas 8.6×10^{-4} and 59.0×10^{-4} cm²) were employed over the temperature range 912-12950. A crucible was charged with a 0.1-0.2 g single crystal sample of the dibromide in the glove box, and the orifice was closed with a drop of paraffin oil before the cell was removed to the collection apparatus, where the oil was pumped off under These same graphite cells, when fitted with quartz liners, were employed in the vaporization of trieuropium tetraoxide monobromide. Initial samples of 0.25-0.35 g of Eu₃O₄Br and 0.05-0.10 g Eu₂O₃ were employed, and measurements were made over the temperature range $925-1327^{\circ}$. On the basis of the initial and final sample weight, vaporization measurements were conducted to approximately 50% of sample depletion for Eu₃O₄, EuO, and EuBr₂, and up to 95% for Eu304Br.

I. Sticking Coefficient Experiments

Although the sticking behavior of a gaseous lanthanide metal on a cold metal surface had been examined previously⁶⁸, no such experiments have been reported for gaseous halides. To determine the sticking coefficient (probability) of the dibromide on copper targets, the following apparatus was constructed. A disk (2.38 cm diameter) of 0.2 mm copper

sheet in which a centered 6.4 mm diameter hole had been blanked was fitted into a target and its X-ray fluorescence background determined. The disk was then placed in the target magazine in front of a copper target so that the disk rested 2 mm from the target face with its counted side facing the target. If a significant quantity of effusate struck the target, but did not stick, it would presumably be scattered and would adhere in measureable quantities on the back of the disk. This experimental design was employed for collection of effusate from Eu₂O₄Br at a temperature (11930) well above the median value of the measurements. The exposure time was adjusted so that the quantity of effusate collected on the target was approximately equal to that normally obtained in the collection measurements. Both the target face and the back side of the disk were analyzed for europium.

CHAPTER VI

RESULTS

A. Results of Preparative Techniques

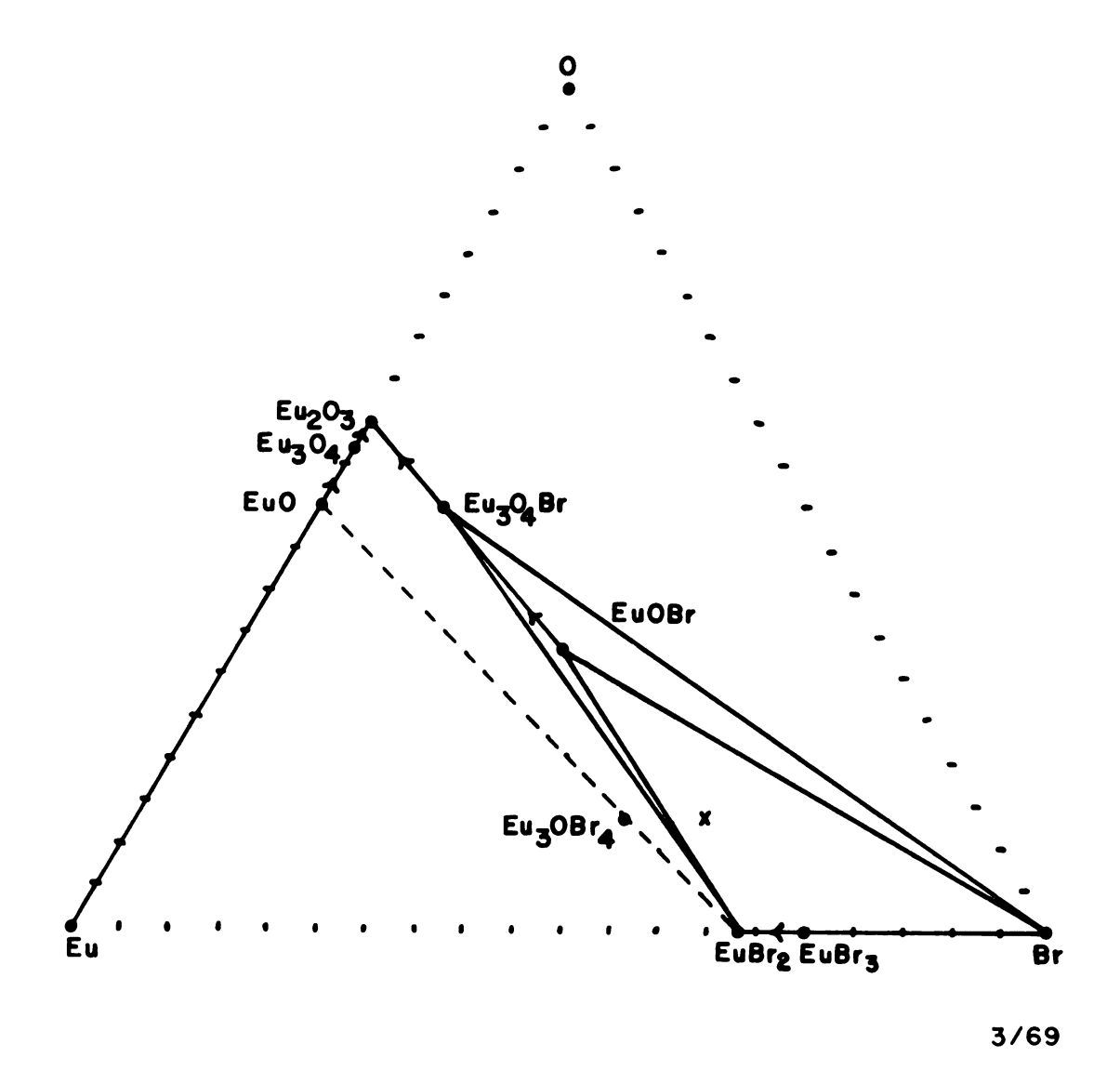
1. The Europium-Oxygen-Bromine System

The eight binary and ternary phases observed in the course of this investigation: europium sesquioxide, trieuropium tetraoxide, europium monoxide, europium tribromide, europium dibromide, trieuropium tetraoxide monobromide, europium monoxide monobromide, and trieuropium monoxide tetrabromide, are indicated in the ternary phase diagram of the system (cf. Figure 3). Seven of the phases were obtained from the sesquioxide via the preparative procedures described previously. The tie lines indicated in the diagram are related to the vaporization behavior of the phases and will be considered in a later section (cf. VI, D, 6).

Results of Additional Preparative and Phase Investigations

The attempts to prepare europium tribromide by techniques other than bromination of the dibromide were unsuccessful. The direct combination of europium and bromine

Figure 3. The europium-oxygen-bromine phase diagram.



yielded pure dibromide, while the reaction of bromoform with the oxide halide produced a mixture of the monoxide monobromide and the dibromide. No evidence for the tribromide was found in either product.

Although attempted preparations of additional trivalent europium phases were unsuccessful, a previously unreported europium(II) oxide bromide phase was obtained. Combination of the tribromide and sesquioxide in a Eu₂OBr₄ stoichiometry (marked by a cross in Figure 3) produced a mixture of EuBra and EuOBr. At the maximum temperature of this reaction, the concentration of free bromine vapor in the ampoule was very high, but as the vessel cooled, the bromine reacted completely with the solid phase. The direct oxidation of EuBr₂ failed to produce any new di- or mixed-valent oxide bromides; only EuOBr was observed. The reaction of the various stoichiometric ratios of EuO and EuBr₂ (all of which necessarily fall along the dashed line in Figure 3) produced a hexagonal phase. However, powder X-ray diffraction data indicated that EuBr₂ was present in the products from EuO: EuBr₂ ratios < 1:2, while a third phase of unknown symmetry, X, was observed for ratios > 1:2. After the latter ratios were annealed, two distinct portions (dark green and light brown) were observed. The dark green color was characteristic of the 1:2 composition, which exhibited only X-ray diffraction lines assignable to the hexagonal phase. Europium analysis of the green-colored portion from the 2:3 composition was consistent with the stoichiometry Eu3OBr4 (EuO:EuBr₂ = 1:2). The identity of phase X was not determined.

3. The Hydrated Bromine Phases

Europium tribromide hexahydrate and europium dibromide monohydrate were also characterized. The tribromide hexahydrate forms white, deliquescent crystals and exhibits the monoclinic symmetry characteristic of other lanthanide trihalide hexahydrates^{20,83}. Two successive phases were observed upon slow hydrolysis of the dibromide. The first of these exhibited the orthorhombic symmetry (cf. VI, B, 2) incorrectly reported for strontium dibromide. By analogy to the X-ray diffraction data reported for BaBr₂·H₂O⁸⁴, this phase was identified as europium dibromide monohydrate. The second phase, which resulted from continued hydrolysis of the monohydrate, was the tribromide hexahydrate, which probably formed together with amorphous hydrous oxide and hydrogen.

4. Observed Physical and Chemical Properties of the Binary and Ternary Phases

Various physical and chemical properties were exhibited by the oxide, bromide, and oxide bromide phases. Trieuropium tetraoxide, a reddish black phase, was stable in air, water, and dilute acetic acid, but reacted at a moderate rate with dilute hydrochloric or nitric acid. Europium monoxide, a brownish-black phase, was stable in air, but reacted rapidly with water to produce hydrous oxide and hydrogen. Europium dibromide formed in clear or white crystals while the tribromide formed as a rust-red phase. Both bromides were

extremely hydroscopic and reacted violently with water. Trieuropium tetraoxide monobromide, europium monoxide monobromide, and trieuropium monoxide tetrabromide exhibited ivory, white, and greenish-black colors, respectively. While Eu₃O₄Br was stable in air, EuOBr reacted slowly and Eu₃OBr₄ reacted rapidly with moisture. The behavior of europium monoxide in the presence of a magnetic field indicated that the phase is ferromagnetic.

B. Analytical Results

1. Results of Chemical Analysis

The results of chemical analyses presented in Table I confirm the existence of the previously mentioned stoichiometric phases. Except for the values of europium dibromide and tribromide, the data presented were from analyses of the phases employed in the vaporization experiments. For EuBr₂, products of ammonium bromide matrix dehydration were analyzed. The error represents the standard deviation of the analyses.

2. X-Ray Powder Diffraction Results

The X-ray powder diffraction data are tabulated in Table II. Except for EuBr₂, which was also studied by single crystal tehcniques, the structure types and space groups were obtained by consideration of crystal symmetry, lattice constants, Molecular formula, and observed extinctions, and by analogy to data reported for both alkaline earth and other lanthanide phases. The lattice constants obtained in this investigation agree within standard error with the values reported previously for $\mathrm{Eu_3O_4^{2}}^{,3}$, $\mathrm{EuO^{2-4}}$, $\mathrm{Eu_3O_4Br^{36}}$, and $\mathrm{EuOBr^{36}}$. The interplanar d-spacings

Table I: Analytical results.

Compound	wt% Eur	opium	wt% Bromine		
Compound	% Observed	% Calculated	% Observed	% Calculated	
Eu ₃ O ₄	87.6 ₂ ± 0.3 ₅	87.67			
EuO	90.3 ₈ ± 0.3 ₄	90.47			
EuBr ₂	48.7 ₆ ± 0.1 ₃	48.74	51.2 ₉ ± 0.3 ₅	51.26	
EuBr ₃	38.76 ± 0.06	38.80	$61.3_3 \pm 0.1_3$	61.20	
Eu ₃ O ₄ Br	75.9 ₆ ± 0.1 ₀	76.00	13.3 ₈ ± 0.1 ₅	13.32	
EuOBr	61.3 ₇ ± 0.1 ₅	61.31	$32.7_3 \pm 0.3_0$	32.63	
Eu ₃ OBr ₄	57.42*	57.60			

^{*}one analysis

Table II. Powder diffraction results.

Phase	Symmetry	La			e Co r de		tants)	Structure Type	Space Group
Eu ₃ O ₄	orthorhombic	a	=	10	.089	±	0.009	CaFe ₂ O ₄	Pnam
		b	=	12	.056	±	0.009		
		С	=	3	.503	±	0.004		
EuO	cubic	a ₀	=	5	.144	±	0.002	NaCl	Fm3m
EuBr ₂	tetragonal	a	=	11	.574	±	0.006	SrBr ₂	P4 /n
		С	=	7	.098	±	0.005		
EuBr ₃	orthorhombic	a	=	9	.115	±	0.013	PuBr ₃	Amam
		b	=	12	.662	±	0.017		
		С	=	4	.013	±	0.005		
Eu ₃ O ₄ Br	orthorhombic	a	=	11	.978	±	0.004		
		b	=	11	.858	±	0.003		
	•	С	=	4	.121	±	0.002		
EuOBr	tetragonal	a	=	3	.926	±	0.003	PbFCl	P4/nmm
		С	=	8	.019	±	0.008		
Eu ₃ OBr ₄	hexagonal	a	=	9	.825	±	0.004		
		C	=	7	.510	±	0.003		
EuBr ₃ ·6H ₂ O	monoclinic	a	=	10	.025	÷	0.008	$\text{NdCl}_3 \cdot 6\text{H}_2\text{O}$	P2 /n
		b	=	6	.757	±	0.005		
		С	=	8	.164	±	0.007		
		β	=	93	.48	±	0.06		
EuBr ₂ ·H ₂ O	orthorhombic	a	=	9	.196	±	0.011	BaCl ₂ ·H ₂ O	Pmcn
		b	=	11	.459	±	0.017		
		С	=	4	.291	+	0.005		

and relative intensites of the diffraction lines of previously unreported phases are listed in Appendices I A - I D.

3. Single Crystal and Density Results

The vapor transport technique produced dibromide crystals which were spherically or hemispherically shaped. Under polarized light, these crystals exhibited optical properties consistent with tetragonal symmetry, i.e. two mutually perpendicular optically active axes, which were subsequently identified by Weissenberg single crystal techniques as the two-fold axes of the tetragonal structure. The flat side of the hemispherically shaped crystals was thereby determined to be coincident with (1 0 0). Oscillation photographs obtained about the optically inactive axis gave a lattice spacing (7.1 Å) consistent with the c parameter of the indexed powder data. The equi-inclination Weissenberg photographs (0-3 layers) indicated four-fold symmetry about this axis of rotation. From the indexed h00 reflections, a lattice parameter (11.7 Å), which is also consistent with the powder results, was obtained. Systematic extinctions (h + k = 2n + 1) were observed only in the hk0 reflections. Even though extinctions in $00 \, \ell$ could not be determined from the Weissenberg data, the powder indexing indicates that none is present. Only two space groups; P4/n and P4/nmm (Nos. 85 and 129 respectively), are possible 85. However, the results of Sass et al. for strontium dibromide²⁵ suggest that No. 85 is the correct space group.

The measured density for europium dibromide of $5.51~\rm g/cm^3$, in combination with X-ray volume of the unit cell (950.85 $^{\circ}$ 3), gives Z = 10.1 molecules/unit cell. An X-ray density of $5.44~\rm g/cm^3$ is calculated for Z = 10.

Direct reaction of europium monoxide monobromide and europium sesquioxide produced single crystals of the tetra-oxide monobromide phase. Two crystalline forms--rectangular plates and long needles--were observed. The platelets, which were of suitable size for single crystal studies, exhibited one optically active axis colinear with the long axis of the rectangle. Oscillation and Weissenberg data taken about this axis indicate that it is coincident with the body diagonal of the orthorhombic cell. However, the crystal could not be alligned on another axis.

C. Results of X-Ray Fluorescence Calibration

The external calibration curves for the Eu L β_1 and Br K α_1 transitions were linear over the concentration ranges of calibration (0-10 μg for Eu and 0-20 μg for Br). The least squares slope and intercept values of the curves employed in the various measurements are presented in Appendix II A. The same Eu and Br calibration curves were employed for the analysis of EuBr₂ and Eu₃O₄Br condensates.

Calibration results for gold are also presented in Appendix II A. These data were collected (cf. Appendix II B) in experiments coordinated by the National Bureau of Standards for the purpose of establishing primary vapor pressure standards.

D. Vaporization Results

1. The Vaporization Mode of Trieuropium Tetraoxide

In the temperature range of the investigation, trieuropium tetraoxide was found to vaporize incongruently according to equation (VI-1).

$$3Eu_3O_4(s) \longrightarrow 4Eu_2O_3$$
 (s, monoclinic) + $Eu(g)$. (VI-1)

This reaction was confirmed by powder X-ray diffraction data which indicated that only $\operatorname{Eu_3O_4}$ and $\operatorname{B-Eu_2O_3}$ were present during the vaporization measurements. No variation in the diffraction patterns was observed as a function of bulk composition, and no evidence for crucible interaction was detected. Weight-loss measurements yielded 99.2% of the theoretical change for reaction (VI-1). Mass spectrometric studies also confirmed the reaction, since only masses attributable to europium (151 and 153) were observed over most of the temperature range. At the maximum temperature (1700°) a faint spectrum of gaseous europium monoxide was observed. The relative intensity of $\operatorname{Eu}(g)$ to $\operatorname{EuO}(g)$ was determined to be ≤ 200 at 1700° . The appearance potential of Eu^+ (5.9 eV) is in agreement with the reported value (5.67 eV)⁸⁶.

2. The Vaporization Mode of Europium Monoxide

For the temperature range of the measurements, the following reaction describes the vaporization mode of europium

		1

monoxide.

$$4EuO(s) \longrightarrow Eu_3O_4(s) + Eu(g).$$
 (VI-2)

The X-ray powder diffraction data of vaporization residues were assignable only to EuO and Eu_3O_4 . Both weight loss measurements (99.1% of theoretical) and mass spectrometric results (only primary Eu(g)) confirmed the incongruent vaporization described by equation (VI-2).

3. The Vaporization Mode of Europium Dibromide

For europium dibromide, congruent vaporization occurs according to reaction (VI-3).

$$EuBr_2(\ell) \longrightarrow EuBr_2(g).$$
 (VI-3)

X-ray diffraction patterns of the condensed phase were invariant even after 50% sample depletion. Simultaneous fluorescence analyses for Eu and Br indicated that the collected equilibrium vapor contained a Eu:Br ratio of 1:2, while mass spectrometric analysis of dibromide vapor showed the presence of only monomeric europium dibromide.

4. The Vaporization Mode of Trieuropium Tetraoxide Monobromide

In the temperature range investigated, trieuropium tetraoxide monobromide vaporized incongruently according to reaction (VI-4).

$$3Eu_3O_4Br(s) \longrightarrow 4Eu_2O_3(s, monoclinic) + EuBr_2(g) + Br(g).(VI-4)$$

A combination of weight loss and X-ray data indicated that molybdenum, tungsten (with and without quartz liners), and thoria-lined graphite reacted with either the solid or vapor phase, or both. Weight losses of 120% of theoretical were observed for Mo and W cells, and the solid residues were contaminated with oxides of the cell material. Weight losses of 110% and 105% were observed for quartz-lined metal and thoria-lined graphite cells, respectively. In the latter case, the solid products were contaminated with ThO2. However, quartz-lined graphite cells were found to be satisfactory, as 99.4% of theoretical weight loss for equation (VI-4) was observed. Powder X-ray diffraction analysis of the solid vaporization products indicated the presence of only Eu₃O₄Br and Eu₂O₃. Although the sesquioxide was principally in monoclinic form, traces of the cubic phase were observed. Mass spectrometric analysis of the effusate indicated the presence of Br (masses 79,81), EuBr (masses 230, 232, 234), Eu⁺ (masses 151, 153), EuBr₂⁺ (masses 309, 311, 313, 315) and $Br_2 + (masses 158, 160, 162)$ in the relative intensities of 1000:100:50:15:5, respectively. The relative intensities of the europium containing species are consistent with the fragmentation pattern observed for EuCl₂ vapor $(EuCl^+ : Eu^+ : EuCl_2^+ = 100 : 46 : 12)^{87}$. The appearance potential measured for EuBr + (10.4 eV) is consistent with that observed for EuCl + (10.3 eV)87. In addition, X-ray and chemical analyses of the effusate obtained in the total collection experiments confirmed that europium dibromide was a vapor species.

The results of the various techniques indicate both a Eu:Br ratio of 1:3 and the presence of molecular $\operatorname{EuBr}_2(g)$ in the equilibrium vapor, but the data do not indicate whether the equilibrium bromine species is the monatomic or the diatomic gas, i.e. should equation (VI-4) have $1/2 \operatorname{Br}_2(g)$ or $\operatorname{Br}(g)$ as the vaporization product. However, this difficulty may be resolved by consideration of the dissociation equation (VI-5).

$$1/2 \operatorname{Br}_{2}(g) \longrightarrow \operatorname{Br}(g).$$
 (VI-5)

If α is defined as the fraction of dissociation, the partial pressures of the two species (P_{Br2} and P_{Br}) may be expressed in terms of the total bromine pressure P₊ as follows:

$$P_{Br_2} = [(1 - \alpha)/(1 + \alpha)]P_{t}.$$
 (VI-6)

$$P_{Br} = [2\alpha/(1 + \alpha)]P_{t}.$$
 (VI-7)

Substitution of these partial pressure into the expression for the equilibrium constant of the dissociation reaction gives equation (VI-8).

$$K(VI-5) = 2\alpha[P_t/(1 - \alpha^2)]^{1/2}.$$
 (VI-8)

While values for K(VI-5) are readily available⁶⁹, the magnitude of P_t must be estimated from experimental data. The bromine pressure may be obtained from the europium dibromide equilibrium by employing the Knudsen equation (III-6) for these vapor species as follows.

		·

$$P_{\text{EuBr}_{2}} = (3.76 \times 10^{-4}/\text{S}_{0} t) (TM_{\text{EuBr}_{2}})^{1/2} (W/M)_{\text{EuBr}_{2}}. (VI-9)$$

$$P_{\text{Br}} = (3.760 \times 10^{-4}/\text{S}_{0} t) (TM_{\text{Br}})^{1/2} (W/M)_{\text{Br}}. (VI-10)$$

If monatomic bromine is produced, the stoichiometry of reaction (VI-4) requires that the ratio of moles of $EuBr_2$, $(W/M)_{EuBr_2}$, to moles or Br, $(W/M)_{Br}$ be unity. Consideration of this requirement and of equations (VI-9) and (VI-10), yields P_{Br} in terms of P_{EuBr_2} .

$$P_{Br} = P_{EuBr_2} (M_{Br}/M_{EuBr_2})^{1/2} = 0.50626 P_{EuBr_2}.$$
 (VI-11)

By similar arguments, the analogous expression for the production of one-half mole of $Br_2(g)$ in equation (VI-4) is:

 $P_{Br_2} = 0.50P_{EuBr_2} (M_{Br_2}/M_{EuBr_2})^{1/2} = 0.35798 P_{EuBr_2}.(VI-12)$ Therefore, from equations (VI-11) and (VI-12) the total bromine pressure is always of the order of magnitude of the europium dibromide pressure, and experimental values for P_{EuBre} (<u>cf</u>. VI, F) may be substituted for P_t in relationship (VI-8). At $1600^{\circ}K$, (K(VI-5) = 0.496 and $P_{EuBr_2} =$ 6×10^{-4} atm), α equals 0.995. At the low measurement temperatures (1200 0 K), K(VI-5) is 0.042, P_{EuBra} equals 8×10^{-7} atm, and α is calculated to be 0.999. On the basis of these results, equation (VI-4) adequately describes the incongruent vaporization of Eu₃O₄Br. Apparently, the Br₂(g) observed in the mass spectrum originated from reaction of the monomeric vapor in the mass spectrometer. should also be noted that the observed relative intensity of Br(g) is more indicative of the bromine pressure in the source region of the mass spectrometer than in the Knudsen

cell.

5. The Vaporization Mode of Europium Monoxide Monobromide

The results of the collection experiment indicated that europium monoxide monobromide vaporizes incongruently according to equation (VI-13).

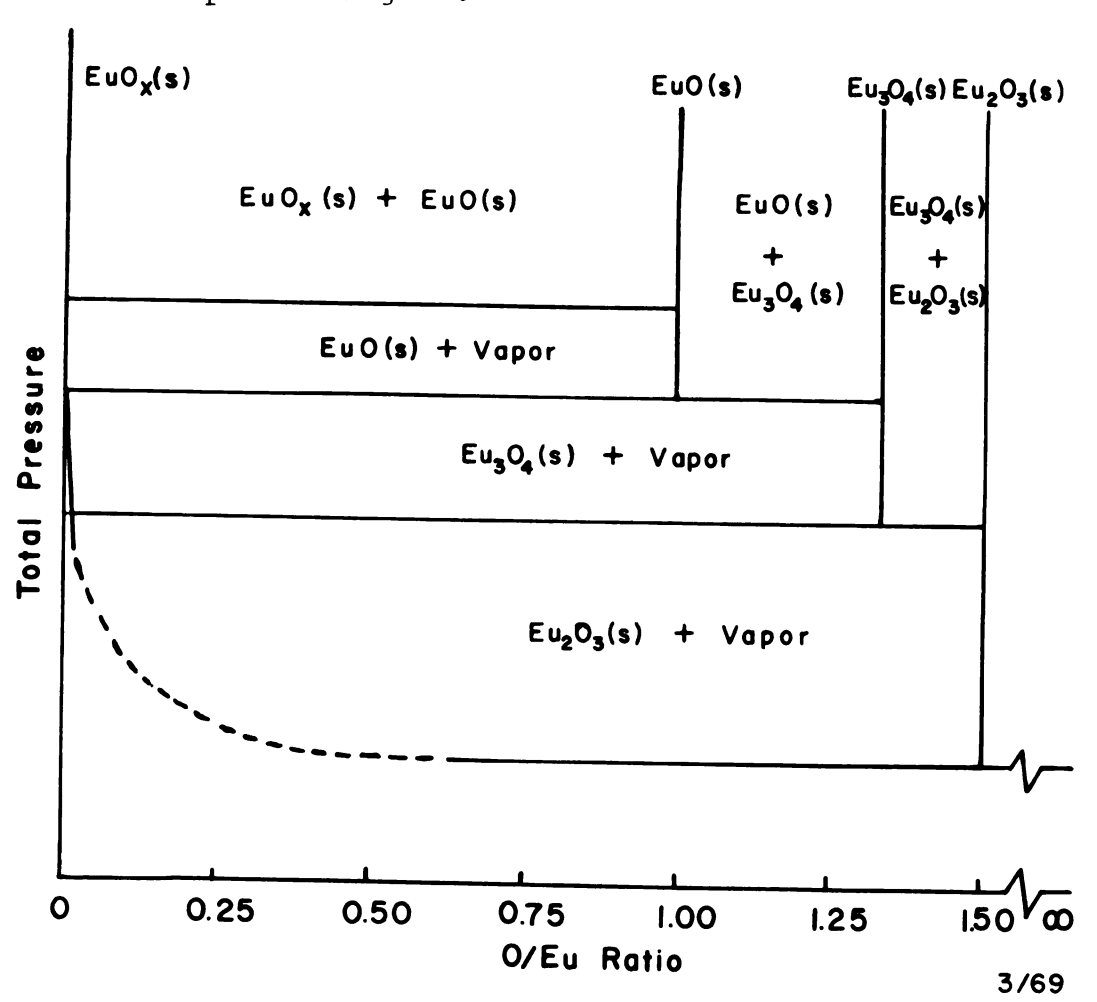
$$4\text{EuOBr}(s) \longrightarrow \text{Eu}_3\text{O}_4\text{Br}(s) + \text{EuBr}_2(g) + \text{Br}(g). (VI-13)$$

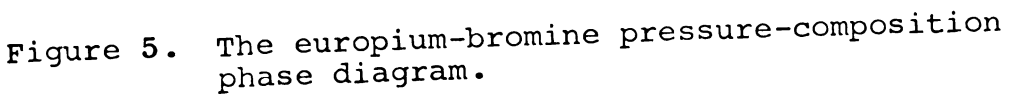
X-ray analysis indicated that the solid residue consisted of EuOBr and Eu_3O_4 Br and that the condensed effusate was the dibromide. By analogy to Eu_3O_4 Br (<u>cf</u>. VI, D, 4), monatomic bromine is assumed to be the second equilibrium vapor species.

6. Pressure-Composition Diagrams

In accordance with a previous discussion (cf. III, A, 2, c), the results of vaporization studies may be presented qualitatively by a pressure-composition phase diagram. The results of the vaporization investigations are given in Figures 4-6. For the europium-oxygen system, Figure 4 indicates that EuO(s) loses metal vapor to form Eu₃O₄(s), which in turn loses gaseous europium to produce congruently vaporizing Eu₂O₃(s)¹⁵. Likewise, in Figure 5, europium tribromide is seen to lose bromine vapor to form the congruently vaporizing dibromide. The existence of the EuBr₃-EuBr₂ equilibrium is evidenced by the preparative results; i.e. EuBr₂ forms at high temperature and low bromine pressure, while EuBr₃ may be prepared only at relatively low

Figure 4. The europium-oxygen pressure-composition phase diagram.





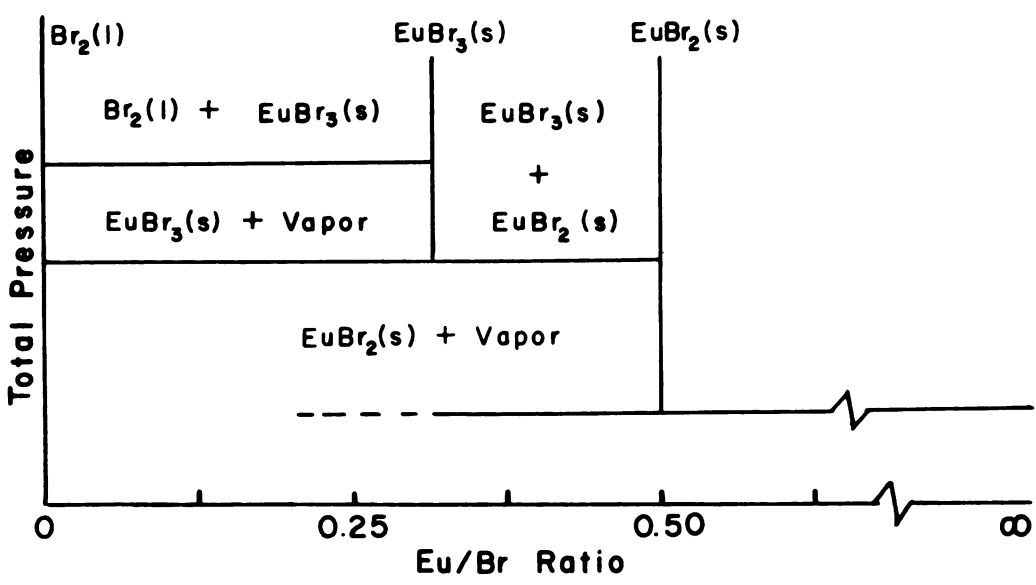
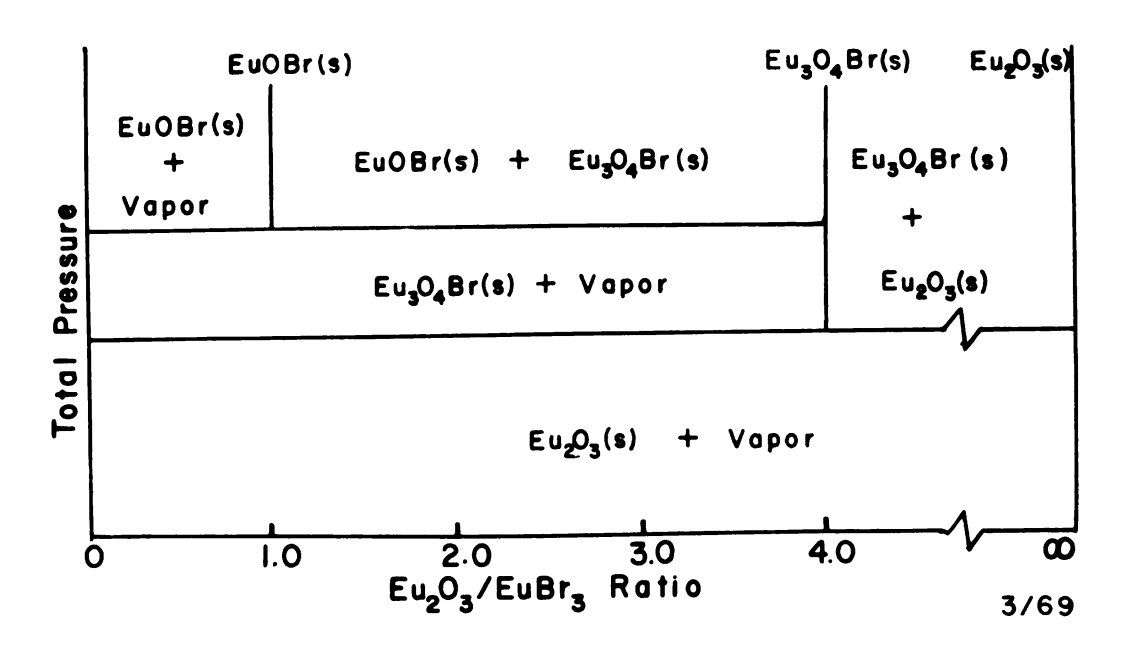


Figure 6. The europium sesquioxide-europium tribromide pseudobinary pressure-composition phase diagram.



temperatures and high bromine pressures. Although phases are not indicated between the di- and tribromide compositions (cf. Figure 5), they are to be anticipated by analogy to the samarium-fluorine system 75 Figure 6 is a pseudobinary section of the ternary diagram (cf. VI, A, 1, Figure 3) along the composition line intersecting all stoichiometric phases of trivalent europium. The diagram is treated as a two-component system of Eu₂O₃ and EuBr₃, and the results are seen to be directly analogous to those of the europium-oxygen binary in that Eu₂O₃ is the terminal, congruently vaporizing phase resulting from a series of incongruent vaporizations. Although it is not indicated in the diagram, the vapor phase contains $EuBr_2(g)$, the vapor species of the other congruently vaporizing phase. entire vaporization scheme is indicated by the tie lines in Figure 3. The vaporization products of any condensed phase other than congruently vaporizing Eu₂O₃ and EuBr₂ are indicated by following the tie lines originating at the vaporizing composition. The condensed vaporization product is obtained by following the direction of the arrow to the next composition, while the gaseous vaporization product(s) is/are found at the terminuses of all other lines originating at the vaporizing composition.

E. Results of Sticking Coefficient Measurements

Results of the bouncing experiment indicate that the sticking coefficient of gaseous EuBr₂ on liquid-nitrogen-cooled copper targets is nominally unity. The quantity of

effusate collected on the target, the lack of any detectable concentration of europium on the back of the disk, and the estimated lower detectable limit of analysis indicate that the sticking coefficient ≥ 0.95 . The measured data have therefore not been corrected.

F. Vapor Pressure Equations

The temperature and corresponding equilibrium vapor pressure values determined for reactions (VI-1)-(VI-4), are presented in Appendices III A-D, and the least squares equations are presented in Figures 7-10. Since the temperature dependence of only the europium dibromide pressure was determined for equation (VI-4) (Eu₃O₄Br vaporization), the least squares equation in Figure 10 does not directly yield second law results for the reaction. The pressure equation (42 independent measurements) for gaseous europium in equilibrium with the tetraoxide and sesquioxide is:

$$\log P_{Eu}(VI-1) = -(1.8832 \pm 0.0320 \times 10^{4}/T) + 6.161 \pm 0.180, (VI-14)$$

for $1604 < T < 2016^0K$. The equation (34 measurements) for the pressure of gaseous europium in equilibrium with the monoxide and the tetraoxide in the temperature range $1334 < T < 1758^0K$ follows:

log
$$P_{Eu}(VI-2) = -(1.6589 \pm 0.0205 \times 10^{4}/T) + 6.263 \pm 0.134.$$
(VI-15)

The pressure of gaseous europium dibromide (36 data points) in equilibrium with the liquid dibromide for $1185 < T < 1568^0 K$

Figure 7. The pressure of Eu(g) in equilibrium with $Eu_3O_4(s)$ and $Eu_2O_3(s)$.

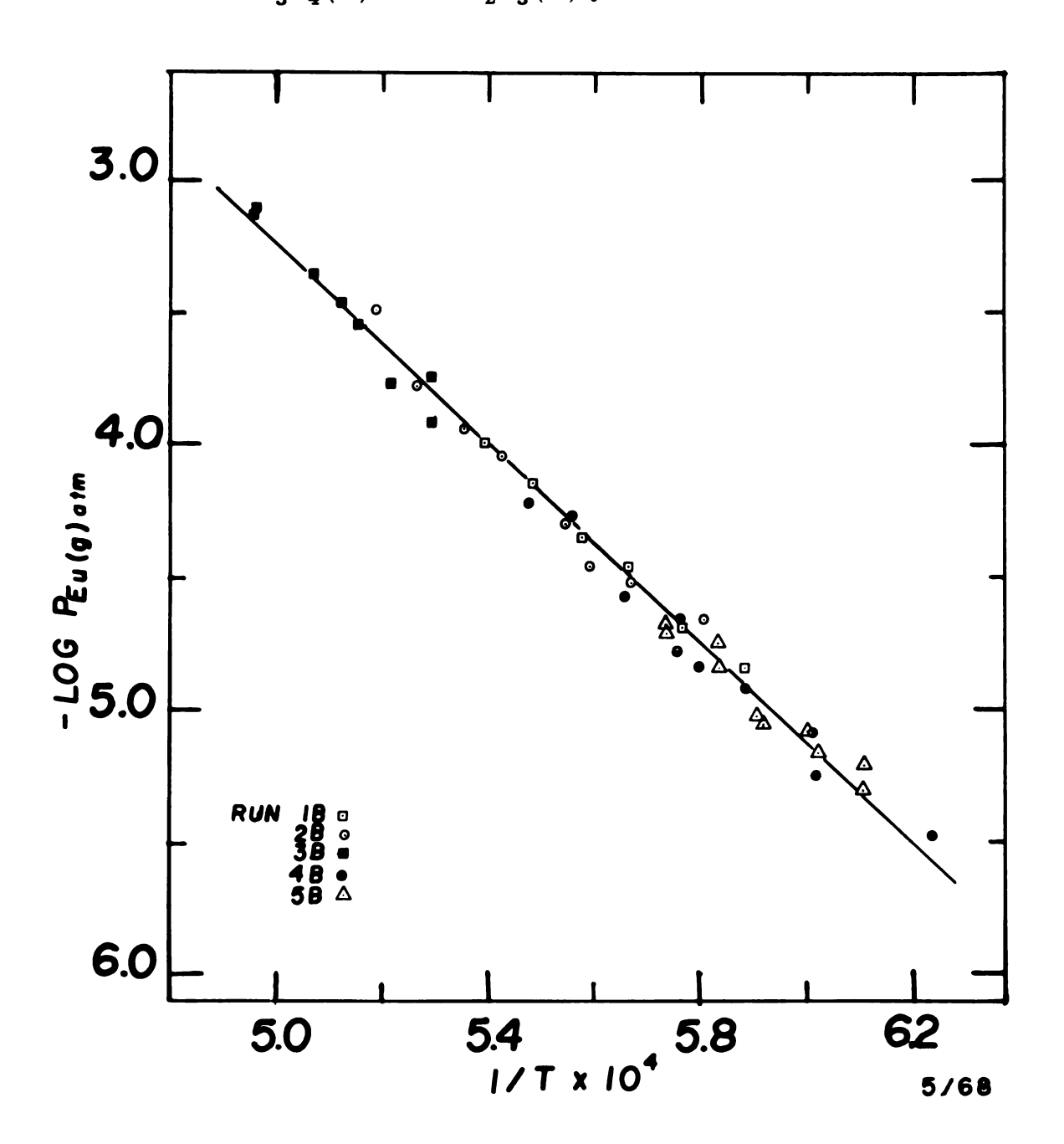


Figure 8. The pressure of Eu(g) in equilibrium with EuO(s) and $Eu_3O_4(s)$.

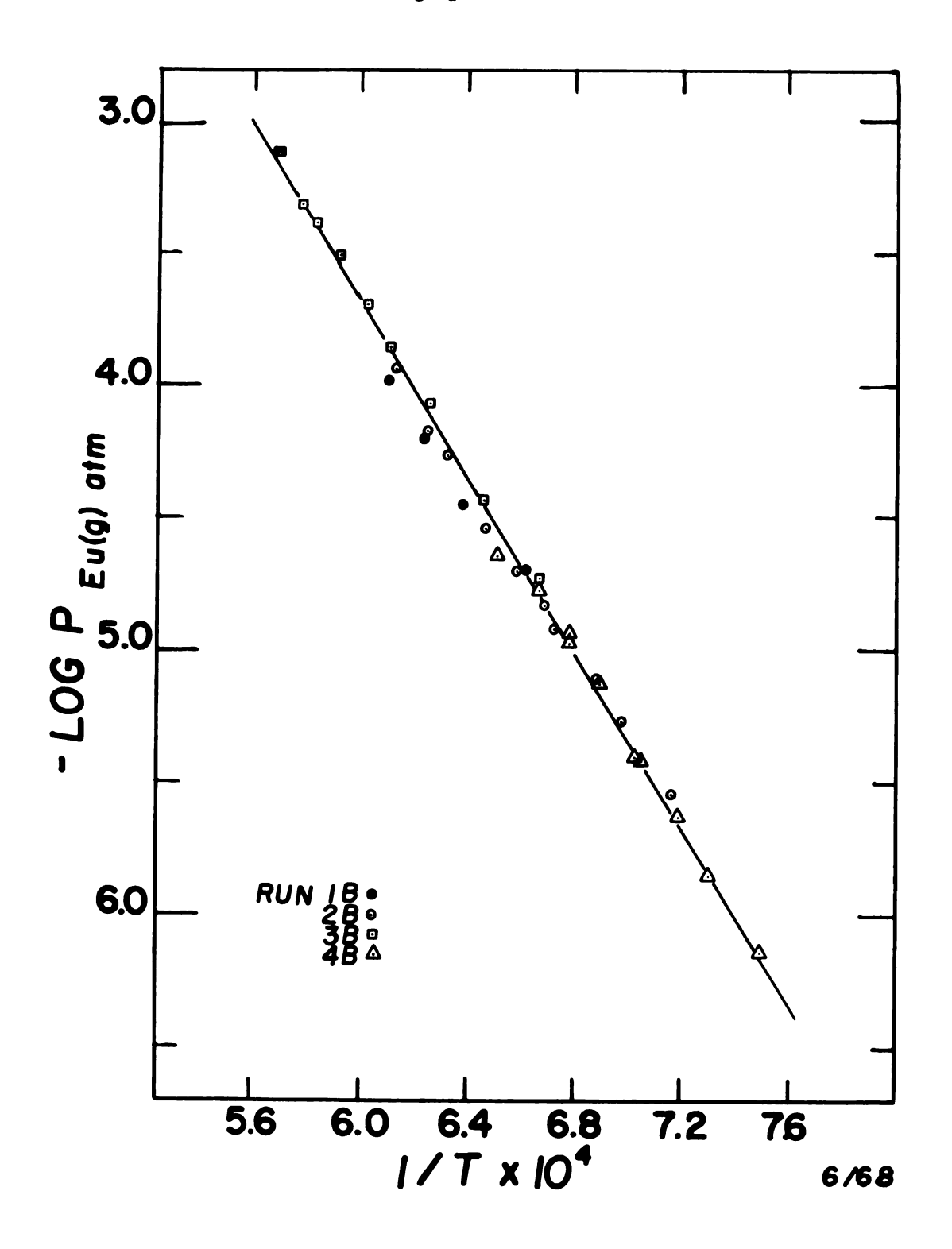


Figure 9. The pressure of $\mathrm{EuBr_2}(\mathsf{g})$ in equilibrium with $\mathrm{EuBr_2}(\ell)$.

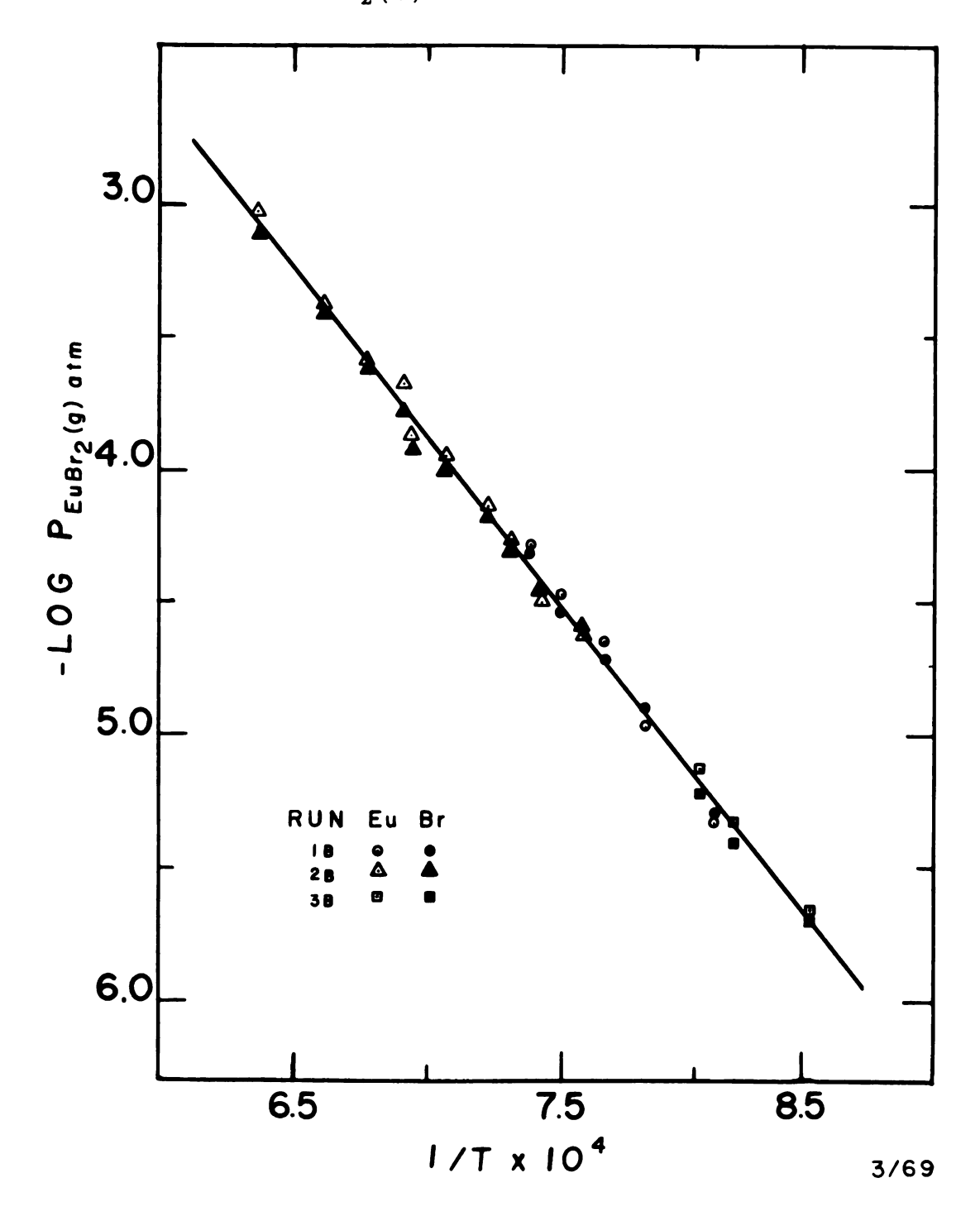
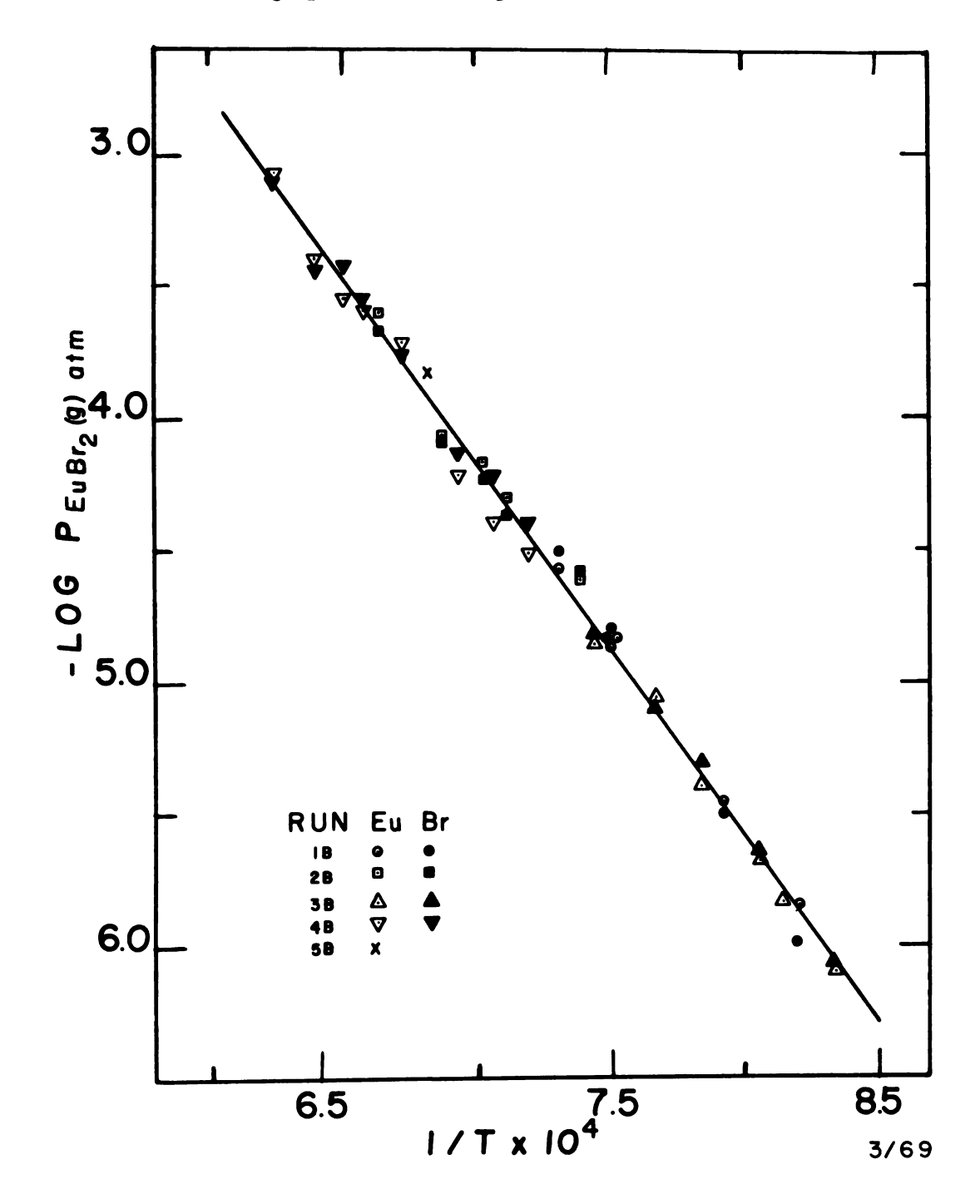


Figure 10. The pressure of $EuBr_2(g)$ in equilibrium with $Eu_3O_4Br(s)$, $Eu_2O_3(s)$ and Br(g).



is given by

log
$$P_{EuBr_2}(VI-3) = -(1.2733 \pm 0.0166 \times 10^4/T) + 5.032 \pm 0.123.$$
(VI-16)

The pressure of europium dibromide (48 measurements) in equilibrium with trieuropium tetraoxide monobromide, europium sesquioxide, and gaseous monatomic bromine in the temperature range $1198 < T < 1600^{\circ}K$ is:

log
$$P_{EuBr_2}(VI-4) = -(1.4098 \pm 0.0172 \times 10^4/T) + 5.699 \pm 0.125.$$

$$(VI-17)$$

G. Thermodynamic Values Employed in Data Reduction

1. Heat Capcaity, Enthalpy, and Entropy Functions

a. Literature Values

Measured values were available for ${\rm Eu_2O_3(s)^{14}}$, ${\rm Eu(g)^{88}}$, and ${\rm Br(g)^{69}}$, while estimated functions were employed for ${\rm EuBr_2(s,\ell)^{29},^{31}}$. Values for $({\rm H_T^0-H_{298}^0})$ and $({\rm S_T^0-S_{298}^0})$ for the dibromide were obtained by graphical interpolation of the tabulated estimates.

b. Approximate Values for Solid Phases

For the remainder of the condensed phases encountered in this investigation, the heat capacity, enthalpy, and entropy functions were approximated. The heat capacity data for monoclinic $\mathrm{Eu_2O_3(s)^{14}}$ and equations (III-29), (III-30), (III-33), and (III-34) were employed to obtain $\mathrm{C_p}$, ($\mathrm{H_T^0} - \mathrm{H_{298}^0}$), and ($\mathrm{S_T^0} - \mathrm{S_{298}^0}$) equations for $\mathrm{Eu_3O_4(s)}$,

EuO(s), Eu₃O₄Br(s), and EuOBr(s) in the following forms:

$$C_p = a + b \times 10^{-3} T$$
, (VI-18)

$$(H_{T}^{0} - H_{298}^{0}) = aT + (b/2) \times 10^{-3} T^{2} - C, \quad (VI-19)$$

$$(S_T - S_{298}^0) = a \ln T + b \times 10^{-3}T - d.$$
 (VI-20)

The values of a, b, c, and d for the respective phases are listed in Appendix IVA.

c. Approximated Values for Gaseous Phases

Europium dibromide is the only gaseous species for which heat capacity, enthalpy, and entropy data are not available. Therefore, in light of the previously discussed trends of metal dibromides (\underline{cf} . III, E, 4, a, (2)), only the molecular symmetry need be specified for approximation of these functions. In the molecular beam deflection experiments of Buechler, $\underline{et\ al.}_{,\,}^{8,9}$ gaseous dihalides of the alkaline earths were found to be both bent ($\underline{CaF_2}$ and $\underline{SrCl_2}$) and linear ($\underline{CaCl_2}$). On the assumption that a trend, which is apparently dependent upon the cation-anion ratio, continues, strontium and europium dibromides should exhibit linear structures. Therefore the experimental data for gaseous mercuric dibromide⁶⁹ were selected for the europium species.

2. Absolute Entropies

a. Approximated Values for Solids

In the absence of experimental values, the standard entropies of all the condensed phases were approximated using equations (III-31) and (III-32). Westrum's approximated entropy values¹⁷ for Eu₂O₃(s) (35.0 eu) and for the lattice contributions to the binary europium oxides (Eu, 14.1 eu; O in Eu₃O₄, -1 eu; O in EuO, -2 eu) were used, while Latimer's⁷¹ lattice values (Eu, 14.1 eu; O, 0.5 eu; Br, 10.9 eu) were employed in estimations for oxide bromide phases. The magnetic contributions used for Eu(III) (3.5 eu) and Eu(II)(4.2 eu) were those recommended by Westrum ¹⁷. The results of these entropy approximations also appear in Appendix IVA.

b. Entropy Values for Gaseous Species

Although entropy data are available for $\mathrm{Eu}(g)^{88}$ and $\mathrm{Br}(g)^{69}$, no value appears for $\mathrm{EuBr_2}(g)$. Therefore, the estimated free energy functions at $298^0\mathrm{K}$ for linear gaseous dibromides 70 were employed in an entropy approximation. Since S_{298}^0 is equal to $-\mathrm{fef}_{298}$ (cf. equation III-22), an estimated value for $\mathrm{EuBr_2}$ (74.2 eu) was obtained by graphical interpolation according to molecular weight between the fef values for $\mathrm{ZnBr_2}$ (-67.66 eu), $\mathrm{CdBr_2}$ (-73.56) and $\mathrm{HgBr_2}$ (-76.31 eu). Although the S_{298}^0 value was 2.2 eu lower than that for $\mathrm{HgBr_2}$, inclusion of a magnetic contribution for $\mathrm{Eu}(\mathrm{II})$ increased the final estimate to

approximately that of the mercury species. Therefore, the entropy value employed for $EuBr_2(g)$ (76.3 eu) is that given for $HgBr_2(g)$ ⁶⁹.

3. Free Energy Functions

Free energy functions are available for $\mathrm{Eu}(s,\ell,g)^{88}$ and $\mathrm{Br}(g)^{69}$, but the values for the remainder of the phases were calculated according to equation (III-22) from the experimental and approximated data described in sections (VI, G, 1) and (VI, G, 2). The $(\mathrm{H_T^0} - \mathrm{H_{298}^0})$, $(\mathrm{S_T^0} - \mathrm{S_{298}^0})$, and fef values in the temperature ranges of the measurements are listed in Appendix IVB for $\mathrm{Eu_2O_3}(s)$, $\mathrm{Eu_3O_4}(s)$, $\mathrm{EuO}(s)$, $\mathrm{EuBr_2}(s,\ell)$, $\mathrm{Eu_3O_4Br}(s)$, and $\mathrm{EuOBr}(s)$. For reasons which will be discussed (cf. VII, E, 2), the fef values for $\mathrm{EuO}(s)$ were calculated using $\mathrm{S_{298}^0} = 15.0$ eu instead of the estimated 16.3 eu. Since the estimated heat capacity and standard entropy data for $\mathrm{EuBr_2}(g)$ are identical to those of the mercury species, the published fef values for $\mathrm{HgBr_2}(g)^{69}$ were employed.

The free energy function changes for the various vaporization reactions, (VI-1 - VI-4) and (VI-13), were calculated from available 69 , 88 and estimated (Appendix VIB) functions employing relationship (III-23). These values for Δ fef of the reactions are listed for the temperature ranges of the measurements in Appendix IVC. Values for Δ fef at specific intermediate temperatures were obtained by graphical interpolation of these data.

4. Additional Thermochemical Values

The additional thermochemical data which were employed in the data reduction (ΔH_f^0 , ΔG_f^0 , S^0 , and D_0 values at 298°K) appear with their sources in Appendix IVD. However, the entropy and free energy of $\mathrm{Eu_2O_3}(s)$ were estimated as follows. Combination of the S_{298}^0 values of $\mathrm{Eu(s)^{88}}$ and $O_2(g)^{69}$ with the estimated entropy of $\mathrm{Eu_2O_3}(s)^{17}$ via relationship (III-28) yields $\Delta S_{f\ 298}^0$ of $\mathrm{Eu_2O_3}(s)$ of -77.1 eu. When this value is combined with $\Delta H_{f\ 298}^0$ of $\mathrm{Eu_2O_3}(s)$ (-393.9 kcal/gfw)¹², an approximated $\Delta G_{f\ 298}^0$ for $\mathrm{Eu_2O_3}(s)$ of -370.9 kcal/gfw results.

H. Thermodynamic Results

1. Treatment of Trieuropium Tetraoxide Data

The least squares pressure equation (VI-14) was employed with relationships (III-11) and (III-12) to give the enthalpy and entropy of vaporization of $\text{Eu}_3\text{O}_4(\text{s})$ as follows: $\Delta\text{H}_{1810}^0 = 86.2 \pm 1.4 \text{ kcal/gfw}$, and $\Delta\text{S}_{1810}^0 = 28.2_0 \pm 0.8_2 \text{ eu}$. Reduction of these values to 298^0K with the aid of $(\text{H}_{\text{T}}^0 - \text{H}_{298}^0)$ and $(\text{S}_{\text{T}}^0 - \text{S}_{298}^0)$ data $(\underline{\text{cf}}$. Reference 88 and Appendix IVB) and relationships (III-17) and (III-18) yielded $\Delta\text{H}_{298}^0 = 93.5 \pm 2.5 \text{ kcal/gfw}$ and $\Delta\text{S}_{298}^0 = 39.4 \pm 1.7 \text{ eu}$. A value of $\Delta\text{G}_{298}^0 = 81.7 \pm 2.5 \text{ kcal/gfw}$ was thereby obtained. From the temperature-pressure data $(\underline{\text{cf}}$. Appendix IIIA), the corresponding Δfef values $(\underline{\text{cf}}$. Appendix IVC), and equation (III-25), a third law value of $\Delta\text{H}_{298}^0 = 92.2_8 \pm 0.5_6 \text{ kcal/gfw}$ was obtained (cf. Appendix IIIA).

The energetics of formation of $\operatorname{Eu_3O_4}(s)$ were obtained from the second law results. The enthalpy change for reaction (VI-1) was combined with data listed in Appendix IVD according to relationship (III-27) to yield ΔH_{f}^0 298 $\operatorname{Eu_3O_4}(s)$ = -542.4 \pm 3.6 kcal/gfw. The error limit was obtained via equation (III-35) by combination of the estimated error in data reduction with the 2.6 kcal discrepancy in the measured enthalpies of formation of $\operatorname{Eu_2O_3}(s)^{12}$. Substitution of the free energy of vaporization and the necessary free energy of formation values from Appendix IVD into equation (III-27) gives ΔG_{f}^0 298 of $\operatorname{Eu_3O_4}(s) = -510.4 \pm 3.6$ kcal/gfw.

An S_{298}^0 Eu₃O₄(s) value of $48._6 \pm 2._6$ eu resulted from use of the entropy of vaporization and the entropies of Eu₂O₃(s) and Eu(g) (<u>cf</u>. Appendix IVD) in relationship (III-20). The quoted error includes a 2.0 eu uncertainty in the Eu₂O₃ value.

2. Treatment of Europium Monoxide Data

From equation (VI-15), which represents the pressure of europium for reaction (VI-2), the following enthalpy and entropy of vaporization at the median temperature (1546°K) were obtained: $\Delta H_{1546}^0 = 75.9_1 \pm 0.9_4$ kcal/gfw and $\Delta S_{1546}^0 = 28.6_6 \pm 0.6_1$ eu. By use of tabulated enthalpy and entropy data (<u>cf</u>. Reference 88 and Appendix IVB), these values were reduced (<u>cf</u>. equations (III-17) and (III-18)) to 298°K and yielded $\Delta H_{298}^0 = 80.3 \pm 2.0$ kcal/gfw, $\Delta S_{298}^0 = 33.9 \pm 1.3$ eu, and $\Delta G_{298}^0 = 70.2 \pm 2.0$ kcal/gfw. The measured

temperatures and pressures (<u>cf</u>. Appendix IIIB), the calculated \triangle fef values (<u>cf</u>. Appendix IVC), and equation (III-25) were employed to give the third law value of $\triangle H_{298}^0 = 80.0_0 \pm 0.4_2$ kcal/gfw. No noticeable temperature trend was observed in the results (<u>cf</u>. Appendix IIIB).

The energetics of formation and the standard entropy were calculated from the second law data with the aid of the Eu₃O₄(s) results (cf. VI, H, 1), the data listed in Appendix IVD, and relationships (III-27) and (III-20). These values are: $\triangle H_{f\ 298}^{0}$ EuO(s) = -145. $_{2}$ \pm 4. $_{1}$ kcal/gfw, $\triangle G_{f\ 298}^{0}$ EuO(s) = -136. $_{6}$ \pm 4. $_{1}$ kcal/gfw, and S_{298}^{0} EuO(s) = 15. $_{0}$ \pm 3. $_{0}$ eu. The second law result for Eu₃O₄(s) (48.6 eu) was employed in the calculation of the standard entropy value.

3. Treatment of Europium Dibromide Data

The results of the vaporization of liquid europium dibromide according to reaction (VI-3) were treated in the following way. From the pressure equation (VI-16) (median temperature, 1377° K), values of $\Delta H_{1377}^{\circ} = 58.2_{7} \pm 0.7_{6}$ kcal/gfw and $\Delta S_{1377}^{\circ} = 23.0_{3} \pm 0.5_{6}$ eu were obtained, and were reduced to 298° K with data for $EuBr_{2}(s, l)$ (cf. Appendix IVB), that of $HgBr_{2}(g)^{69}$ (cf. VI, G, 1, c), and relationships (III-17) and (III-18). For the vaporization of $EuBr_{2}(s)$ $\Delta H_{298}^{\circ} = 71._{4} \pm 2._{7}$ kcal/gfw and $\Delta S_{298}^{\circ} = 36._{8} \pm 2._{8}$ eu. The estimated errors were calculated by assuming an error of $\pm 20\%$ in the reduction to 298° K.

Combination of the measured data and the free energy changes (Appendices IIIC and IVC) yielded a third law $\Delta H_{298}^0 = 69.5_4 \pm 0.4_0$ kcal/gfw with no temperature trend in the values (cf. Appendix IIIC).

The energetics of formation were calculated as follows. Combination of the enthalpies of formation of $Eu(g)^{88}$ and $Br(g)^{69}$ and the dissociation energy estimated for $EuBr_2^{30}$, gives an estimated ΔH_{f}^{0} EuBr₂(g) of -106.₆ kcal/gfw. If this value is combined with the enthalpy of vaporization, $\Delta H_{f\ 298}^{0} \ \text{EuBr}_{2}(s) = -178._{0} \pm 3._{0} \ \text{kcal/gfw} \ \text{is obtained}.$ second law absolute entropy of the dibromide was obtained from the entropy of vaporization, the entropy of EuBr₂(g) (cf. Appendix IVA) and relationship (III-20). The resulting value, S_{298}^{0} EuBr₂(s) = 39.₅ ± 3.₀ eu, was subsequently combined with the entropies of Eu(s) and Br₂(ℓ) (cf. Appendix IVD) in relationship (III-28) to give $\Delta S_{f}^{0}_{298}$ EuBr₂(s) = -16.2 \pm 3.0 eu. From the enthalpy and entropy of formation, $\Delta G_{f\ 298}^{0}$ EuBr₂(s) = -173.₂ ± 3.₀ kcal/gfw was obtained. addition, ΔS_{f}^{0} 298 EuBr₂(g) = 20.6 eu was calculated from $\Delta S_{f~298}^{0}$ EuBr₂(s) and the entropy of vaporization. When this latter value was combined with the estimated enthalpy of formation an approximate value of $\Delta G_{f\ 298}^{0}$ EuBr₂(g) = -112.8 kcal/gfw was obtained.

By extrapolation of pressure equation (VI-16) to one atmosphere, the normal boiling point of ${\rm EuBr_2}(\ell)$ was calculated to be 2530 \pm 35°K. The (${\rm H_T^0}$ - ${\rm H_{298}^0}$) data for ${\rm EuBr_2}(\ell)^{31}$ were graphically extrapolated beyond 1500°K by utilizing

the trend established by BBr $_3(\ell)$ data 31 to obtain estimated enthalpy functions at 2000 0 and 2500 0 K (42 and 49 kcal/gfw, respectively). From these values, an enthalpy of vaporization at 2530 0 K (ΔH_V^0 EuBr $_2(\ell)$ = 52. $_0$ ± 3. $_0$ kcal/gfw) was calculated. Since at the boiling point ΔS_V^0 = $\Delta H_V^0/T_b$, an entropy of vaporization of ΔS_V^0 = 20. $_6$ ± 1. $_9$ eu was obtained.

4. Treatment of Trieuropium Tetraoxide Monobromide Data

Unlike the previously treated vaporization reactions in which only one gaseous species was observed, the vaporization of trieuropium tetraoxide monobromide according to reaction (VI-4) involves two vapor species (EuBr₂(g) and Br(g)). However, the equilibrium data described by equation (VI-17) (median temperature 1399°K) give only the dibromide pressure. The equilibrium pressure of Br(g) was calculated from the dibromide equation by relationship (VI-11) and substituted into the equilibrium constant for the vaporization reaction to give:

$$K(VI-4) = 0.50626(P_{EuBr_2})^2$$
, or (VI-21)

$$log K(VI-4) = 2log P_{EuBr_2} - 0.29557. (VI-22)$$

By substitution of equation (VI-17) into (VI-22) the temperature dependence (1198 6 < T < 1600 0 K) of the equilibrium constant was calculated as:

$$log K(VI-4) = -(2.8195 \pm 0.0243 \times 10^{4}/T) +11.101 \pm 0.177.$$
(VI-23)

For reaction (VI-4), $\triangle H_{1399}^0 = 129._0 \pm 1._1$ kcal/gfw and $\triangle S_{1399}^0 = 50.8_1 \pm 0.8_1$ eu were obtained. These results were reduced to 298^0 K with necessary data (<u>cf</u>. Appendix IVB, Reference 69, and relationships (III-17) and (III-18)), to give $\triangle H_{298}^0 = 137._6 \pm 2._0$ kcal/gfw, $\triangle S_{298}^0 = 64._7 \pm 2._9$ eu, and $\triangle G_{298}^0 = 118._3 \pm 2._0$ kcal/gfw. Point by point substitution of the log P_{EuBr_2} values (<u>cf</u>. Appendix IIID) into relation—ship (VI-22) and subsequent combination with $\triangle fef$ values for the reaction (<u>cf</u>. Appendix IVC) and relationship (III-25), yielded a third law $\triangle H_{298}^0 = 139.4_7 \pm 0.9_2$ kcal/gfw. Analysis of the third law values (Appendix IIID) revealed no apparent temperature trend.

Combination of the second law enthalpy change with the enthalpy of formation of $\operatorname{Eu_2O_3}(s)^{12}$, $\operatorname{Br}(g)^{69}$, and $\operatorname{EuBr_2}(g)$ (cf. VI, H, 3; Appendix IVD) and relationship (III-27) yielded $\operatorname{\Delta H_f^0}_{298}$ $\operatorname{Eu_3O_4Br}(s) = -597._7 \pm 5._1$ kcal/gfw. Again, the indicated error includes the 2.6 kcal discrepancy in the measured enthalpies of the sesquioxide¹²,¹³. Use of the free energy of vaporization and the free energies of formation of the products in equation (III-27) gave $\operatorname{\Delta G_f^0}_{298}$ $\operatorname{Eu_3O_4Br}(s) = -565._0 \pm 5._1$ kcal/gfw. The entropy of vaporization was combined with necessary data (cf. Appendix IVD and Reference 69) according to equation (III-20) to yield $\operatorname{S_{298}^0}$ $\operatorname{Eu_3O_4Br}(s) = 64._5 \pm 3._1$ eu.

5. <u>Estimation of Thermodynamic Data for Europium Monoxide</u> Monobromide

Although the vaporization reaction for europium monoxide monobromide (cf. equation (VI-13)) has been determined, no equilibrium pressure measurements have been made; however, combination of thermodynamic arguments and vaporization data from europium dibromide and trieuropium tetraoxide monobromide allows estimation of the equilibrium pressure equation for the vaporization, and hence, estimation of thermodynamic values for EuOBr(s). The activity of EuBr₂(g), i.e. its pressure, must be less than that in equilibrium with the condensed EuBr₂ phase, but greater than that in equilibrium with Eu₃O₄Br(s). Knowledge about the entropy of the vaporization reaction when combined with these pressure limits, allows estimation of a pressure equation. Since the vaporization reactions of both Eu₃O₄Br(s) and EuOBr(s) involve two solid phases and identical vapor species, ΔS_{m}^{0} EuOBr(s) should be approximately equal to $\Delta S_{\pi}^{0} Eu_{3}O_{4}Br(s)$. An alternate approach involves estimation of the entropy of vaporization at 2980K from approximated values of the standard entropies of reactants and products (cf. Appendix IVA) via relationship (III-19). If the $\triangle S_{298}^{0}$ value so obtained (65.92 eu) is corrected to the median temperature $(1400^{\circ}K)$ of the EuBr₂ and Eu₃O₄Br vaporization measurements with the aid of tabulated data (cf. Appendix IVB, and Reference 69), a $\Delta S_{1400}^{0} = 56.65$ eu is obtained. When this entropy change is converted into an intercept term, its value (5.89) agrees

with that observed for the Eu₃O₄Br vaporization (5.699).

If an intermediate pressure selected from equations (VI-16) and (VI-17) is combined with the estimated intercept, the following pressure equation is obtained.

$$log P_{EuBr_2}(IV-13) = -(1.403 \times 10^4/T) + 5.89.$$
 (VI-24)

When this equation is treated in a manner directly analogous to that employed for ${\rm Eu_3O_4Br(s)}$ (cf. VI, H, 4), the following values are obtained for the enthalpy of vaporization: $\Delta {\rm H_{1400}^0} = 128.5 \; {\rm kcal/gfw} \; {\rm and} \; \Delta {\rm H_{298}^0} = 135.5 \; {\rm kcal/gfw}.$

Substitution of the approximated enthalpy change at 2980K and the enthalpies of formation of the products of equation (VI-13) (cf. VI, H, 4) into relationship (III-27) gives $\triangle H_{f}^{0}$ EuOBr(s) = -203.3 ± 6.5 kcal/gfw. The error reflects the deviations in the enthalpies of formation of $Eu_3O_4Br(s)$ (± 5.1 kcal) and $EuBr_2(g)$ (± 3.1 kcal), and the difference in enthalpies of formation calculated for EuOBr(s) using the slopes of the $EuBr_2(\ell)$ and $Eu_3O_4Br(s)$ pressure equations (cf. equations (VI-16) and (VI-17)) as limiting values for obtaining the enthalpy of vaporization of EuOBr. For the EuBr₂(ℓ) limit, $\triangle H_{298}^0 = 123.5 \text{ kcal/gfw and } \triangle H_{f298}^0$ $EuOBr(s) = -200.2 \text{ kcal/gfw}, \text{ while for the } Eu_3O_4Br(s)$ boundary, $\Delta H_{298}^{0} = 136.0 \text{ kcal/gfw}$, and $\Delta H_{f\ 298}^{0} = -203.4$ kcal/gfw. The small difference in the enthalpies of formation (3.2 kcal/gfw) arises because of the large value of v_{i} (equation III-27). From the estimated ΔG_{298}^{0} of

vaporization and free energies of formation of the vaporization products, $\triangle G_{f\ 298}^{0}$ EuOBr(s) = -193.₄ ± 6.₅ kcal/gfw.

6. Compilation of Thermodynamic Results

The thermodynamic results obtained in the preceeding calculations are tabulated for median vaporization temperatures in Table III and for 2980K in Table IV. Estimated values appear in parentheses. In Table V, thermodynamic values at the boiling point of europium dibromide are presented.

Second law vaporization results at median measurement temperature. Table III.

Phase	Vaporization Reaction	Median T (⁰ K)	$^{\Delta extsf{H}_{ extsf{T}}^{oldsymbol{0}}}_{ extsf{T}_{ extsf{V}}^{oldsymbol{0}}}(extsf{kcal}/ extsf{gfw})$	$^{\Delta S}^{0}_{\mathrm{Tvap}}$ (eu)
Eu304(s)	(VI-1)	1810	86.2 ± 1.4	$28.2_0 \pm 0.8_2$
Euo(s)	(VI-2)	1546	$75.9_{1}^{\pm} 0.9_{4}$	$28.6_{6} \pm 0.6_{1}$
$\mathtt{EuBr_2}\left(\mathtt{s}\right)$	(VI-3)	1377	$58.2_{7}^{\pm} 0.7_{6}$	$23.0_3 \pm 0.5_6$
Eu304Br(s)	(VI-4)	1399	$129{0}\pm1{1}$	$50.8_1 \pm 0.8_1$
$\mathtt{EuOBr}\left(\mathtt{s}\right)$	(VI-13)	(1400)	(128.5)	(56.65)

Table IV. Thermodynamic results at 2980K.

Phase	$rac{2 ext{nd}}{ riangle H^{oldsymbol{0}}}$	$rac{3 ext{rd}}{\Delta ext{Ho}}$ law $\Delta ext{Ho}$ $(ext{kcal}/ ext{gfw})$	(ne)	(na)	$-\triangle H_{\hat{\mathbf{f}}}^{0}$ (kcal/gfw)	$-\triangle G_{ extbf{f}}^{ extbf{0}}$ (kcal/gfw)
Eu304(s)	93.5± 2.5	$92.2_{8}^{\pm} 0.5_{6} 39{4}^{\pm} 1{7}$		1	542.4± 3.6	510.4± 3.6
\mathbf{E} uo (\mathbf{s})	80.3 ± 2.0	$80.0_0 \pm 0.4_2$	$33.9^{\pm}1.3$	$15.0^{\pm} 3.0$	145.2 [±] 4.1	$136.6^{\pm} 4.1$
$\mathtt{EuBr_2}(\mathtt{s})$	$71.4^{\pm}2.7$	$69.5_{4}^{\pm} 0.4_{0}$	$36.8^{\pm}2.8$	$39.5^{\pm} 3.0$	178.0 ± 3.0	$173.2^{\pm}3.0$
$Eu_3O_4Br(s)$	$137.6^{\pm} 2.0$	$139.4_{7}^{\pm} 0.9_{2}$	$64.7^{\pm}2.9$	64.5 ± 3.1	$597.7^{\pm}5.1$	565.0 ± 5.1
$\mathtt{EuOBr}\left(\mathtt{s}\right)$	(135.5)	!!!	(65.92)	(29.0)	$(203.3^{\pm}6.5)$	(193.4 ± 6.5)
$\mathtt{EuBr}_{2}\left(\mathtt{g}\right)$!	!!!	!!!	(76.3)	(106.6)	(112.8)

Thermodynamic results for liquid europium dibromide at the boiling point. Table V.

2nd law $\triangle H_V^0$ (kcal/gfw) $\triangle S_V^0$ (eu)	52.0 ± 3.0 20.6 ± 1.9
law	2530 ± 35 52.

CHAPTER VII

DISCUSSION

A. The Phase Diagram

1. Phases in the Europium-Oxygen-Bromine System

A general formula was given (cf. III, A, 1) for all possible stoichiometric oxide, bromide, and oxide bromide phases of europium; however, few of these have been observed (cf. VI, A, 1 and Figure 3). Several interesting observations are evident in the preparative results. All the anticipated phases in the ternary system must fall on or between the lines connecting EuO with EuBr₂ and Eu₂O₃ with EuBr3. Of the eight phases observed, only one composition, Eu₃O₄, falls between the limiting lines, <u>i.e.</u>, contains both di- and trivalent europium. This observation is not meant to imply that mixed valent bromides and oxide bromides are nonexistent, but, instead, indicates that the mixedvalent region of the phase diagram has not been investigated. Only the europium-oxygen binary and the ternary section for trivalent europium, i.e., stoichiometries on the line connecting Eu₂O₃ and EuBr₃, have been investigated thoroughly. The present vaporization studies have transversed the Eu-O binary from EuO to Eu₂O₃ and most of the trivalent, ternary

line. The region from EuBr₃ to EuOBr has been investigated by combination of the 4:1 (tribromide to sesquioxide) stoichiometry, which yielded a mixture of EuOBr and EuBr₃. Therefore, the existence of a europium analog of the Ln₂OBr₄ phases which were observed thermogravimetrically for the heavy lanthanides (Gd-Lu)¹⁹ is doubtful. Compositions along the divalent line have been only partly investigated, and the results suggest that phases other than Eu₃OBr₄ exist. No attempt has been made to prepare mixed-valent oxide bromides, which could probably be attained by reacting EuBr₂-Eu₂O₃, EuBr₃-EuO, EuBr₂-Eu₃O₄, or EuBr₃-Eu₃O₄ mixtures.

2. <u>Discrepancies Between the Present Results and the</u> Literature

a. On the Crystal Structure of Europium Dibromide

One unsuccessful attempt²² (<u>cf</u>. II, B, 1, a) to characterize the crystal structure of europium dibromide appears in the literature. In addition, an incorrect crystal symmetry (orthorhombic) is listed for the phase in a recent review of the lanthanide halides⁹⁰. Obviously the measurement for strontium dibromide monohydrate is the source of this error, but propagation of this inaccuracy only complicates and hinders further investigation. The present powder and single crystal X-ray diffraction data indicate that the tetragonal structure recently described for strontium dibromide²⁵, which is isostructural with EuBr₂, is correct. The diffraction pattern reported by Doell and Klemm²² agrees

with that observed for the tetragonal phase and suggests that they indeed prepared the pure dibromide.

Since pure samples of europium dibromide monohydrate were not obtained, the X-ray diffraction results were employed for its identification. Sass et al.²⁵ analyzed a sample of strontium dibromide monohydrate and suggested that it was the phase examined by Kammermans²³. The structure reported for the barium dichloride and dibromide monohydrates⁸⁴ displays the same symmetry, space group, systematic extinctions, number of molecules per unit cell, and heavy atom (metal and halide) coordinates as the structure described by Kammermans. Since the X-ray data for the initial hydrolysis products of europium dibromide also exhibit the same symmetry and systematic extinctions as these alkaline earth dihalide monohydrates, the phase is obviously the dibromide monohydrate.

b. On the Preparation of Europium Tribromide and Triiodide

Although attainment of europium tribromide by direct dehydration of the tribromide hexahydrates^{19,20} would not be expected to be a useful preparative procedure, dehydration of an ammonium bromide-tribromide hexahydrate matrix¹⁸ would appear feasible. However, numerous attempts to repeat the latter technique were unsuccessful. In every case, the products exhibited the same physical characteristics (light grey color and clear water solution) described by Taylor

and Carter, but chemical analysis (cf. Table I) clearly indicated the dibromide composition. In addition, the products were all isostructural with strontium dibromide. Since the europium dibromide product obtained by vapor transport (vacuum reduction) was clear and white, the greyish color apparently arose from minor contamination by the incompletely reduced, chocolate-colored phase of unknown composition observed by Doell and Klemm²¹. Although the tribromide was successfully prepared at temperatures of 1100 and 12 atm of bromine, the product was not attained at 600 and 1 atm. Therefore, preparation of the phase by the matrix technique under vacuum at high temperatures (350°) is most unlikely. This observed thermal instability of the tribromide is entirely consistent with the estimated free energies of formation of the di- and trihalides³¹. Although the tribromide is more stable than the dibromide at room temperature, the free energy curves cross at approximately 110-1150. Above the crossover temperature, the dibromide becomes increasingly more stable than the tribromide, and in the absence of a high bromine pressure, preparative attempts have little chance of success.

The free energy estimates for the europium iodine system³¹ indicate that the diiodide is 17 kcal/gfw more stable than the triiodide at 25° . This approximation is also consistent with the results of Asprey et al.⁹¹ who were unable to prepare europium triiodide under rigorous conditions (Eu metal under 100 atm I₂ at 600°).

As with the crystallographic data, much of the reference material on the lanthanide halides is filled with sweeping generalities which do not apply to those elements, europium in particular, which exhibit divalent character. The implication is given that all LnX₃ phases are readily prepared. For example, the preparative method suggested by Cotton and Wilkinson²⁴ for EuBr₂ or EuI₂ is the thermal decomposition of the trihalide. Because of the stringent conditions necessary to attain even the tribromide, any previously reported preparation of the triiodide must be questioned.

c. On the Composition of the Hexagonal Oxide Bromide

Previous discussions of the structures of europium phases have indicated that the chemistry of europium is often very similar to that of the heavier alkaline earth elements (Ca, Sr, Ba). The hexagonal oxide bromide phase appears to be isostructural with a phase recently reported for the oxide halides of strontium and barium⁹², 93. The lattice constants for the europium phase (a = $9.825 \pm 0.001 \, \text{Å}$, c = $7.510 \pm 0.004 \, \text{Å}$) are almost identical to those reported for the strontium analog (a = $9.82 \pm 0.01 \, \text{Å}$, c = $7.51 \pm 0.01 \, \text{Å}$), for which a composition (M₄OX₆), apparently based on miscibility observations and X-ray data, is given. In the present investigation excess dibromide is found in the EuO: 3 EuBr₂ product. The analytical data are also consistent with the Eu₃OBr₄ composition.

3. The Stabilities of Phases

a. Elucidation of the Vaporization Process

Examination of the vaporization reactions observed in the europium-oxygen-bromine system suggests definite trends in the modes of vaporization for the different phases. Of the various factors determining the mode of vaporization, Gilles44 lists first the stability of the gaseous species and second that of the condensed phase. These factors are readily applicable to the present system, but possibly in reverse order of importance. The stability of the sesquioxide is apparently the overriding factor in the vaporization of all oxygen containing phases, while that of the dibromide appears to determine the vaporization mode of the europium-bromine binary system. Obviously the stabilities of gaseous europium and europium dibromide are also of importance, but to a lesser extent. For all the oxides or oxide bromides, the flow of reaction is successively toward a more oxygen-rich condensed phase, until the congruently vaporizing sesquioxide is obtained. Likewise, in the Eu-Br binary, the stoichiometry shifts to that of the congruently vaporizing dibromide. In each case, the stoichiometry of the vapor is fixed by the composition change of the solid phase. For the oxide bromides, the stability of gaseous dibromide determines that the dibromide and bromine vapor species are observed instead of the gaseous tribromide. Characterization of the vaporization mode of Eu₃OBr₄ would

be an interesting investigation, but again, little freedom is possible. Gaseous dibromide and a second condensed Eu(II) phase (oxide bromide or oxide) is anticipated. Since vaporization of either the purely divalent or trivalent oxide bromide places an oxidation-reduction restriction on the system, the vaporization behavior of a mixed-valent oxide bromide might be more informative.

The present investigation has established general guidelines for the elucidation of the vaporization process of ternary phases containing one metallic component, i.e., MXY. Unless the phases of the two metal-anion binary systems are of comparable volatility, the composition of a vaporizing ternary will shift toward the less volatile binary system and finally to a congruently vaporizing composition within that binary. The composition of the vapor will be determined by shifts in the composition of the solid, but the gaseous species will be determined by the vaporization behavior of the more volatile metal-anion binary. If the vaporization modes (temperatures, pressures, and species) of the binary systems are first determined, the vaporization behavior of any ternary involving these anions may be readily predicted. In the elucidation of the vaporization mode of a congruently vaporizing binary, the stability of the gaseous species does assume the determining role. Only if the metal binary systems are of comparable volatility does the possibility of a congruently vaporizing ternary exist.

b. Disproportionation of the Oxide Bromides

The cooling curve data of Baev and Novikov43 indicate that the monoxide monochlorides of lanthanum and neodymium melt with decomposition to form the sesquioxide and a melt of unspecified composition at 9340 and 7910, respectively, but the data given are insufficient to determine if decomposition is actually occurring. Since an oxide bromide is expected to be less stable than the corresponding oxide chloride phase, disproportionation would be anticipated. However, at temperatures approximately 100^{0} higher than the disproportionation point reported for LaOC1, EuOBr(s) was found to be in equilibrium with Eu₃O₄Br(s) according to reaction (VI-13). An argument might be presented that the oxide bromide does disproportionate (in this case into $EuBr_3 \cdot xEu_2O_3(\ell)$ and $Eu_3O_4Br(s)$) and on cooling forms the EuOBr(s)-Eu₃O₄Br(s) mixture observed by X-ray diffraction. However, if disproportionation did occur, the tribromide product would instantly decompose into dibromide and gaseous bromine which would escape from the effusion cell and change the composition such that EuBr₂ and Eu₃O₄Br would be present on cooling. It is therefore apparent that the Russian workers have either erroneously interpreted a phase change as a melting point, or misinterpreted their decomposition products.

Thermodynamic instability (disproportionation) of both EuOBr and Eu_3O_4Br is expected at temperatures higher than those attained in the present equilibrium studies. A

consideration of the equilibrium pressure equations (VI-16), (VI-17) and (VI-24) for the gaseous dibromide indicates that they must cross at some temperature above the range of measurements. For Eu₃O₄Br(s) and EuBr₂(ℓ) (Equations VI-17 and VI-16) the calculated crossing temperature is 2040°K, while for EuOBr(s) and EuBr₂(ℓ) (Equations VI-24 and VI-16) the estimated crossover point is 1512°K. At temperatures above these respective values, the activity of EuBr₂(g) in equilibrium with EuBr₂(ℓ) is lower than that in equilibrium with solid oxide bromide, and therefore, disproportionation according to equations (VII-1) and (VII-2) is anticipated.

$$3 \operatorname{Eu_3O_4Br}(s) \longrightarrow 4 \operatorname{Eu_2O_3}(s) + \operatorname{EuBr_2}(\ell) + \operatorname{Br}(g)$$
 (VII-1)

4 EuOBr(s)
$$\longrightarrow$$
 Eu₃O₄Br(s) + EuBr₂(ℓ) + Br(g). (VII-2)

By combining the appropriate enthalpies of formation, the estimated free energy functions at high temperatures (\underline{cf} . Appendix V), and relationship (III-24), third law calculations have been effected at various elevated temperatures. These calculations indicate positive free energy changes for the reactions at temperatures above the anticipated disproportionation points. For reaction (VII-1) at 2500° K, ΔG_{2500}° = 0.74 kcal/gfw. This positive value appears to negate the pressure boundary argument used in approximating equation (VI-24) (\underline{cf} . VI, H, 5), but the use of approximated free energy functions at such high temperatures is obviously not

an exact method. For example, if the calculation for reaction (VII-1) at 2500^{0} K is effected with S_{298}^{0} Eu₂O₃ = 36 eu (instead of 35 eu), ΔG_{2500}^{0} = -9.26 kcal/gfw. Thus, even though thermodynamic calculations are unable to verify the disproportionation of the oxide bromides at the calculated crossover temperatures, these higher temperatures are more accurate than those previously proposed for disproportionation of the oxide chlorides⁴³.

B. The X-Ray Fluorescence Technique

The X-ray fluorescence technique has proven satisfactory for target collection analysis. Its most obvious advantage is that the procedure provides a rapid, direct, microanalytical procedure. The problems associated with quantitative removal of the effusate for spectrophotometric or spectrographic analysis or with the availability of neutron sources for activation analysis are eliminated. scanning procedure removes the difficulties of accurate alignment on the spectral maximum and of shifts in the maximum arising from the chemical environment of the analyzed element or from temperature effects on the analyzing crys-The disadvantages of the technique are the low ratio of characteristic to background counts obtained in the scanning procedure and the difficulty of accurately reproducing the conditions necessary for external standardization. The availability of a precision spectrometer would eliminate the unfavorable statistics by allowing the use of a fixed

angle procedure, while the necessity for reproduction of conditions appears to have been adequately eliminated by the control procedure.

The phenomena of enhancement and suppression should be considered in the selection of X-ray tubes and of materials for collection targets. If an element being analyzed has an X-ray absorption edge at a slightly longer wave length than a characteristic energy of the primary beam, the fluorescence spectrum of the element will be enhanced. Likewise, if the target material has its characteristic radiation in the same relationship to the absorption edge, the same effect will be observed. The problem of suppression arises for the reverse situation in the case of matrix analysis and occurs because an absorption edge of a second element in the matrix absorbs the characteristic radiation of interest. In this latter case, increased concentration of the second element decreases the observed quantity of characteristic radiation. The selection of X-ray tubes is controlled primarily by monetary considerations, but the choice of target material allows for more possibilities. In the present investigation the Eu $L\alpha_1$, transition was found to be more intense than the $L\alpha_1$, because of selective enhancement of the β transition by the secondary α radiation of the copper target. Problems with suppression do not arise in the present technique because of the superficial nature of the sample.

Although the accuracy of this fluorescence procedure has not been confirmed by independent analysis, the measurement of the vapor pressure of gold (cf. Appendix IIB) and the simultaneous analysis for both europium and bromine provide a basis for evaluation of the technique. Since a complete set of free energy functions is not available for any of the reactions studied in this investigation, the usefulness of third law values is only in checking the consistency of the thermodynamic approximations. In the case of gold, agreement of second and third law enthalpies is a check on the accuracy of the analytical method. The agreement obtained between the second law (88.7 ± 1.4 kcal/gfw) and third law $(88.0_0 \pm 0.5_6 \text{ kcal/gfw})$ enthalpies is indicative of the accuracy of the technique. These values are in agreement with the 88.84 kcal/gfw Knudsen effusion result obtained by Ward⁹⁴, the 88.3 kcal/qfw torsion effusion value of Hildebrand and Hall⁹⁵ and the 87.3 kcal/gfw value recommended by Hultgren et al. 96. In addition, the collection of EuBr₂ effusate in both the Eu₃O₄Br and EuBr₂ vaporization experiments allowed an internal check from simultaneous analysis of the two components. The agreement of the two analytical results is evidenced by the data in Figures 9 and 10, in which the pressures calculated from Eu and Br analytical data are seen to agree within experimental error.

The standard deviations in the slopes of the various calibration curves (\underline{cf} . Appendix IIA) indicate that the sensitivity and precision of the technique vary from

measurement to measurement. These various values result primarily from the use of different X-ray generators and analyzing crystals during the course of the investigation. For the gold calibration, a representative case for the technique, the precision is found to be $\pm 0.1~\mu g$ at the 95% confidence level. This reproducibility suggests that second law enthalpy data could be obtained without calibration of the spectrometer for absolute pressure measurements.

C. The Target Collection Knudsen Effusion Technique

1. The Attainment of Knudsen Conditions

The attainment of Knudsen conditions (cf. III, B, 2) in the present experimental procedures is evidenced by consideration of the trends and limits discussed previously (cf. III, B, 3). The temperature-pressure data indicate that inconsistencies and trends in the pressures are not observed either upon six to eight-fold variations of orifice areas (cf. Figures 7-10) or with successively increasing and decreasing temperatures (cf. Appendices IIIA-IIID for data in chronological order of collection). The third law enthalpies also exhibit no trend with temperature. These observations suggest that difficulties stemming from sampling and non-equilibrium problems are insignificant. Even though the pressures and orifice sizes are within the region of validity of the cosine law determined by Mayer⁵⁷ (cf. III, B, 3, b), the ratio of mean free path to orifice

radius has been calculated for a representative system by use of the relationship given by Dushman⁵⁶; L = $1/(2)^{1/2}\pi n\delta^2$. The mean free path of the molecule, L, is a function of the number of molecules/cm³, n, and the molecular diameter, δ . Values for n were calculated from the measured pressures by invoking the ideal gas assumption. For the vaporization of Eu₃O₄(s), the highest pressure, 7.4×10^{-4} atm, was observed at 2016°K with an orifice of radius 0.015 cm, while the lowest value, 3.3×10^{-6} atm, was measured at 1605°K with an orifice of radius 0.042 cm. If δ Eu(g) = 4.0 Å⁹⁷, these data points, which correspond to L/R ratios of 3.5 and 42, respectively, are well within the region of molecular flow (L/R \geq 1) set by Dushman⁵⁶.

2. Temperature Gradients

The most troublesome difficulty encountered in the target collection experiments is the presence of a temperature gradient across the cell. Since asymmetric-type cells exhibit a much greater tendency for surface gradients than symmetric types, the problem appears to result from heating by induction. Although comparisons of sample and optical cavity temperatures for both cell designs indicate that the difference was never greater than $\pm 5^{\circ}$, samples of europium dibromide were consistently found on the crucible lid after vaporization measurements. The only explanation for this behavior is that it resulted from a temperature gradient within the sample cavity. The effect of this gradient on

the pressure measurements is unknown, but the results of Ward49 show that the cosine law is obeyed in the forward direction only when the sample is on the surface directly opposite the orifice. For a solid sample, the effect of a small gradient is therefore not expected to be great, but complete transport of the sample to the lid requires that most of the effusate in the forward direction comes from re-evaporation off the bottom and walls of the cell. The low vapor pressure of the dibromide in the temperature range investigated indicates that complete transport of the sample could not have occurred during the exposure time of the first target, or even of the first few targets. However, the lack of a noticeable trend in the pressure values with chronological order of exposure suggests that the presence of a temperature gradient has not greatly affected the pressure measurements for europium dibromide.

3. Crucible Materials

Any involvement of the crucible material in the equilibrium is also important. Weight loss measurements indicate the selected crucible materials are suitable. Since molybdenum was a noninteracting container material for growing single crystals of europium monoxide from the melt at temperatures 200-300° above the maximum temperature of the trieuropium tetraoxide measurements⁹⁸, no difficulties with either Eu₃O₄ or EuO are to be anticipated. Graphite, which has previously been employed in Knudsen effusion measurements

on SrCl₂⁹⁹, appears to be both inert and impervious to both gaseous and condensed europium dibromide. The normally refractory metals (Mo and W) cannot be used in the presence of gaseous bromine or the condensed oxide bromide because of the stability and volatility of the gaseous halides of these elements¹⁰⁰. The volatility of molybdenum dibromide in the temperature range studied easily accounts for weight losses of greater than 100% of theoretical. In studies of the oxide bromides, the condensed phase must be separated from the graphite crucible to prevent reduction of the oxide by carbon.

D. Evaluation of Thermodynamic Approximations

1. Heat Capacity Approximations

For all condensed phases other than europium sesquioxide and europium dibromide, relationships (III-29) and (III-30) have been employed in approximation of the heat capacity equations. Other than the second-third law enthalpy agreement (cf. Table IV), which serves as a check on the consistency of heat capacity and entropy approximations, little evidence for their accuracy exists. Equation (III-29) has been tested for systems in which measured sets of data are available 101. Use of the heat capacity equation for γ -Fe₂O₃(s) to calculate a value for β -Fe₃O₄(s) at 15000K yields 48.4 cal/deg gfw versus the reported 48.0 cal/deg gfw. At 15000K, the heat capacity of Cu₂O(s) (26.98 cal/deg gfw),

which is estimated from CuO(s) data, agrees with the experimental value (23.45 cal/deg gfw) within 15%; at 2980K, the estimated and experimental values agree within 7%. These results are well within the ±20% error limits assumed for second law data reduction. If the heat capacity approximations from either binary phase via equation (III-30) is valid (cf. III, E, 4, a), then the approximation from one binary to the second binary should also be valid. Since experimental data for $Eu_2O_3(s)^{14}$ and Brewer's enthalpy and entropy function approximations for $\operatorname{EuBr}_2(\ell)^{29}$ are available, a check on the internal consistency of the present approximations is possible. If the heat capacity data of $Eu_2O_3(s)$ is converted via equation (III-30) to an expression for that of EuOBr(s), the value should be the same as that which would be approximated for EuBr₂(s) since the cation to anion ratio is the same. In order to compare the results with Brewer's approximations, $(H_T^0 - H_{298}^0)$ and $(S_T^0 - S_{298}^0)$ were calculated for $EuBr_2(s)$ at 1400^0K (22,330 cal/gfw and 30.91 eu, respectively). Addition of the enthalpy (6,000 cal/gfw) and entropy of fusion (6.3 eu) for $EuBr_2(s)$ yields $(H_T^0 - H_{298}^0) =$ 28,330 cal/gfw and $(S_{\pi}^{0} - S_{298}^{0}) = 37.2$ eu for EuBr₂(ℓ). These results compare favorably with Brewer's values of 29,600 cal/gfw and 37.5 eu, and are well within his $\pm 20\%$ limits of accuracy. These results suggest that the method might be employed to estimate heat content functions for any metal-anion binary if data for a similar binary are available.

The theoretical basis for equations (III-29) and (III-30) is very simple. The method assumes that the metal in an ionic lattice is the major contributor to the heat capacity function, and that its contribution in a second lattice may be approximated by employing the known heat capacity of any similar phase of the metal. The anion contribution is assumed to obey Kopp's rule⁶⁵ which is employed to adjust the heat capacity to the correct metal-anion stoichiometry. Such an approach should give an internally consistent set of heat capacities, and, hence, should result in reasonably accurate second law reductions, especially for incongruent vaporizations, i.e. those having a solid as reactant and as product.

2. Entropy Approximations

Since several discussions of the theoretical basis for Latimer's method are available ^{17,71,72}, a comparison of the estimated and experimental (second law) entropy values obtained in this investigation is probably most instructive. The estimated values (cf. VI, G, 2, a) and the calculated second law results, which are based on experimental data and the independently approximated heat capacities, appear in Table VI. The agreement is indicative of the consistency of the heat capacity and entropy approximations and suggests that in the absence of necessary lattice or magnetic contributions to the entropy, the second law results may be employed for the calculation of free energy functions.

Table VI. Comparison of estimated and experimental S_{298}^0 .

Phase	Estimated S ₂₉₈ (eu)	Second Law S ₂₉₈ (eu)
Eu ₃ 0 ₄ (s)	49.0	48. ₆ ± 2. ₆
EuO(s)	16.3	15.0 ± 3.0
EuBr ₂ (s)	40.1	395 ± 30
Eu ₃ O ₄ Br(s)	63.8	64. ₅ ± 3. ₁

E. Evaluation of Vaporization and Thermodynamic Results

1. Trieuropium Tetraoxide Data

In light of the vaporization results for $\operatorname{Eu_2O_3}(s)^{15}$, the presence of gaseous europium monoxide should be anticipated for $\operatorname{Eu_3O_4}(s)$ at the higher temperatures. The sesquioxide vaporizes congruently by two competing modes to produce in one case $\operatorname{Eu}(g)$ and $\operatorname{O}(g)$ and in the other $\operatorname{EuO}(g)$ and $\operatorname{O}(g)$. These two equilibria and reaction (VI-1) are all subject to the gas phase equilibrium described by equation (VII-3).

$$EuO(g) = Eu(g) + O(g).$$
 (VII-3)

Use of pressures reported by Panish¹⁵ for Eu(g) and EuO(g) at 2000° K permits an approximation of the equilibrium constant for reaction (VII-3). If the congruent vaporization of Eu₂O₃ to Eu(g) and O(g) is assumed to be the dominant mode ($P_{Eu(g)} > P_{EuO(g)}$), the pressure of monatomic

oxygen can be calculated from the observed europium pressure by taking cognizance of their mass differences. A value for K(VII-3) = 2.6×10^{-7} atm is thereby obtained. If the oxygen pressure calculated at the extremum dictated by the two vaporization modes is combined with the experimental pressure of Eu(g) at 2000^{0} K, the anticipated upper and lower limits of Eu0(g) pressure can be set for the Eu₃O₄-Eu₂O₃ system to be $2 \times 10^{-6} \leq P_{EuO}$ atm $\leq 7 \times 10^{-5}$. The value observed mass spectrometrically is $\leq 3 \times 10^{-6}$. Thus, the contribution of europium monoxide to the target collection measurements is inconsequential, and the data have not been corrected for it.

Consistency of the enthalpy and entropy values with other thermochemical data is evident. The enthalpy of formation of ${\rm Eu_3O_4(s)}$ (-542.4 kcal/gfw) would be expected to be more negative than the sum of the enthalpies of formation of EuO and ${\rm Eu_2O_3}^{12}$ (-539.1 kcal/gfw). Likewise, the enthalpies of formation of the europium oxides should become increasingly negative with increasing oxygen content, as follows: ${\rm \Delta H_f^0}_{\rm 298}$ EuO(s) = -145.2 kcal/gfw, ${\rm \Delta H_f^0}_{\rm 298}$ EuO1.33(s) = -180.8 kcal/gfw, and ${\rm \Delta H_f^0}_{\rm 298}$ EuO1.50(s) = -196.9 kcal/gfw. The entropy of formation of Eu3O4(s) (-107.3 eu) is of the magnitude observed for other M3O4 phases 102: Fe3O4 (-82.5 eu), Mn3O4 (-85.2 eu), and Pb3O4 (-94.0 eu). Consideration of the formation reaction indicates that the more negative value arises for the europium phase because of the large entropy of elemental europium. Although the absolute entropy

is also difficult to evaluate because of the magnetic nature of europium, $S_{298}^0 = 48.6$ eu is consistent with values for Mn_3O_4 (35.5 eu), Fe_3O_4 (35.0 eu), and Pb_3O_4 (50.5 eu) in light of the mass differences of the metals¹⁰².

2. Europium Monoxide Data

Even though the similarities of the divalent lanthanides and the alkaline earths are numerous, an important difference between the two is the existence of the trivalent lanthanide oxidation state. The vaporization behavior of strontium or barium monoxide 103 , 104 indicates that EuO(s) should vaporize principally to the gaseous monoxide. However the stability of the Eu₃O₄(s) phase, which has gaseous europium as the principle species in the Eu₃O₄-Eu₂O₃ twophase region, forces europium to be the only gaseous product in the EuO-Eu₃O₄ composition range.

The argument is presented (cf. VI, H, 5) that a close correspondence should be observed between the ΔS_T^0 values for two vaporization processes which both involve a solid as product and reactant in equilibrium with the same vapor. The Eu₃O₄-Eu₂O₃ and EuO-Eu₃O₄ equilibria should provide a test for this reasoning. The entropy changes observed at the median measurement temperature of reactions (VI-1) and (VI-2) (28.2 eu and 28.7 eu respectively) substantiate the validity of the argument.

The third law enthalpy calculations for vaporization equation (VI-2) provide a critical test of the entropy value

of EuO(s). According to Westrum's estimate 17, the sum of lattice and magnetic contributions to the entropy of EuO is 16.3 eu, while the second law result is 15.0 ± 3.0 eu. These values agree within standard deviation, but the 3.0 eu uncertainty arises mainly from a large error (± 2.0 eu) assumed for the approximated entropy of Eu₂O₃ and may not reflect a true uncertainty. Although the discrepancy does not appear to be great, the coefficients of reaction (VI-2) are such that a 1.3 eu difference in S_{298}^{0} of EuO gives rise to a 8.0 kcal difference in the third law enthalpy. The third law result (72.64 ± 0.59 kcal/gfw) obtained by using free energy functions based on S_{298}^{0} EuO(s) = 16.3 eu is several kilocalories less than the second law value (75.9 kcal/gfw) at the median temperature (15460K). The value of 2980K must be larger than the value at the elevated temperature because of the lower heat capacity of the gaseous product. However, the third law enthalpy $(80.0_0 \pm 0.4_2 \text{ eu})$ obtained by using free energy functions calculated with $S_{298}^{0} = 15.0$ eu agrees within 0.3 kcal/gfw with second law value. This result suggests that, relative to the 35.0 eu entropy of Eu₂O₃(s), the entropy of EuO(s) should be 1 eu lower than approximated. Perhaps Westrum's 17 estimate of 4.2 eu for the magnetic contribution of divalent europium is too large since the use of this value to approximate the contribution of Eu(II) in $\mathrm{Eu_3O_4}$ again results in a S_{298}^0 value in excess of the second law result.

The consistency of the present thermodynamics data with previous measurement is evident. The enthalpy of formation agrees exactly with the calorimetric value of Burnett and Cunningham⁷ and fits well into a correlation of ionic radii of the divalent alkaline earths with their enthalpies of formation 102 presented in Table VII. The ionic radii are calculated from the experimental lattice parameters of the NaCl-type monoxides 78 using a 1.40 Å radius for the oxide ion 97 . The entropy of formation (-28.8 eu) is in agreement with the values reported for other MO phases 102; SrO (-24.5 eu), SnO (-23.2 eu), and PbO (-25.8 eu); however, the value again reflects the large entropy of elemental europium. Similarly, the S_{298}^{0} value for EuO is consistent with that of other monoxide phases 102 when their mass differences are considered: SrO (13.0 eu), SnO (13.5 eu), EuO (15.0 eu), and PbO (16.1 eu).

Table VII. Correlation of the divalent radii and enthalpies of formation of metal monoxides.

МО	M ⁺² Radius (A)	ΔH ⁰ _{f 298} (kcal/gfw)
CaO	1.00	-151.9
EuO	1.17	-145.2
SrO	1.17	-141.1
BaO	1.35	-133.5

3. Europium Dibromide Data

The vaporization and thermodynamic results for europium dibromide are consistent with the various estimated values. The equilibrium pressure equation is well within the limits set by Brewer²⁸. Although the observed vapor pressure is lower than the estimated median value, the boiling point is higher. The enthalpy of vaporization at 298° K (71.4 kcal/gfw) is in excellent agreement with the 72 kcal/gfw value estimated by Feber³⁰. Since the approximated dissociation energy recommended by Feber has been employed in the data reduction, the remaining thermodynamic values are also in agreement. The enthalpy of vaporization at the boiling point (52.0 kcal/gfw) agrees with Brewer's approximated value (50 kcal/gfw)²⁸; the entropy of vaporization at the boiling point (20.6 eu) is in good agreement with Trouton's rule.

4. <u>Trieuropium Tetraoxide Monobromide and Europium</u> Monoxide Monobromide Data

Since no previous vaporization or thermodynamic measurements have been made for any lanthanide oxide bromide, evaluation of the data is difficult. Although gaseous niobium monoxide tribromide (NbOBr $_3$) species are reported 105 and might be anticipated for transition group VB elements, none was observed for europium. The stabilities of europium sesquioxide and dibromide (<u>cf</u>. VII, A, 3, a) probably prevent the formation of these phases. The thermodynamic values

may be compared with those obtained for the LnOCl phases 43 . The estimated enthalpy of formation of EuOBr (-203. $_3$ kcal/gfw) is consistent with the more negative values (-230 to -245 kcal/gfw) observed for the monoxide monochlorides. The enthalpy of bromination of a divalent europium oxide phase should be essentially constant, and the difference between the enthalpies of formation of Eu $_3$ O $_4$ (s) and Eu $_3$ O $_4$ Br(s) and those of EuO(s) and EuOBr(s) are 55.1 kcal/gfw and 58.1 kcal/gfw, respectively.

F. On the Existence of Lower Oxides of Ytterbium

Although the lower oxides of europium are easily obtained, prepartive procedures for the corresponding phases of other lanthanides have been unsuccessful. Brauer et al. 106 indicate that attempts to prepare LnO and Ln₃O₄ (Ln = Nd, Sm, Yb) by the reduction of the oxide bromides with lithium hydride and by combination of the metals with their sesquioxides have been unsuccessful. The results of Felmlee and Eyring 107 and of Butherus and Eick 108 indicate that the previously reported monoxides are either oxide-nitride or oxide-carbide phases with NaCl-type lattices. The experimental results of the present investigation should be helpful in determining if, and in what temperature range, the existence of other lower lanthanide oxides is to be anticipated.

To effect third law calculations on the reactions of interest, certain thermodynamic data must be approximated.

Estimated entropies were obtained by using the schemes of Westrum¹⁷ and Latimer⁷¹ for oxide and oxide bromide phases, respectively, in conjunction with the measured entropy of $Yb_2O_3(s)$ (31.8 eu)¹⁷. Since Yb(II) is isoelectronic with Lu(III), for which no magnetic anomolies have been observed, a magnetic contribution was not included in the 11.1 eu value approximated for S_{298}^{0} of YbO(s). The entropies of Yb₃O₄(s) and Yb₃O₄Br(s) were estimated by summing the entropies of Yb₂O₃ and YbO and correcting the results for anionic lattice contributions. In a similar manner, the S_{298}^{0} value for YbOBr is obtained from the YbO entropy. The free energy functions for ytterbium oxide and oxide bromide phases were calculated at various temperatures from the fef of the corresponding europium phase by subtracting S_{298}^{0} of the europium compound and adding S_{298}^{0} of the ytterbium phase.

The enthalpies of formation of ytterbium oxides and oxide bromides may be estimated because of general trends in the lanthanide series. The enthalpies of formation of lanthanide monoxide monochlorides increase linearly (i.e., become more positive) across the series 43. The effect of this trend appears in the decreasing thermal decomposition temperatures 109,110 of the oxide chlorides with increasing molecular weight. Since an identical decomposition trend is observed for the oxide bromides 19, an enthalpy of formation of YbOBr (-195 kcal/gfw) may be estimated from that of EuOBr and the trend set by the measured oxide chloride

enthalpies. The enthalpy change for bromination of Eu(II) in EuO(s) (-58 kcal/gfw) must be corrected for the difference in bond strength of the Eu(III)-Br and Yb(III)-Br bonds. This difference may be obtained from the estimated enthalpies of formation of EuBr₃ and YbBr₃³⁰, which give values of -66 and -61 kcal/gfw per bromine bond, respectively. This 5 kcal difference implies that the enthalpy of bromination of YbO(s) should be -53 kcal/gfw. Use of this value gives ΔH_f^0 YbO(s) = -142 kcal/gfw.

The enthalpy of formation of the metal monoxides also may be calculated <u>via</u> a Born-Haber cycle. The enthalpy of formation of a monoxide phase is given by the following equation:

$$\Delta H_{f\ 298}^{0} = \Delta H_{V}^{0} + 1/2 D_{0} + IP - EA - U,$$
 (VII-4)

where ΔH_V^0 and IP represent the enthalpy of vaporization and the ionization potential of the metal, respectively, D_0 and EA the dissociation energy and electron affinity of oxygen, and U the lattice energy. For an isostructural series of compounds, the common steps in the cycle $(D_0$, EA, and U) may be expressed in terms of a constant and the variable r, the equilibrium separation of nearest-neighbor ions in the lattice. Therefore, the enthalpy of formation of EuO(s) may be used to calculate a general equation which is a function of ΔH_V^0 , IP, r, and constants. Values for the second ionization potentials 111 and enthalpies of vaporization 88 are available for europium and ytterbium. The value for

r (2.58 Å) is readily calculated from the lattice constant of EuO. Since no experimental data are available for YbO, the Yb(II) radius may be estimated from the radius of Eu(II) and Eu(III)¹¹² (1.17 Å/0.95 Å). Combination of this 1.25 ratio with the 0.85 Å radius of Yb(III)¹¹² gives a Yb(II) radius of 1.06 Å, which in turn yields r = 2.46 Å for YbO(s). Use of this distance in the Born-Haber equation gives $\Delta H_{f~298}^{0}$ of YbO(s) = -144 kcal/gfw. The average value (-143 kcal/gfw) between this result and the previous estimate has been selected for the thermodynamic calculations.

The enthalpy of formation of ytterbium tetraoxide may also be approximated by analogy to the europium data. The enthalpy of formation of $\mathrm{Eu_3O_4}$ is observed to be 3.3 kcal more negative than the sum of the enthalpies of EuO and $\mathrm{Eu_2O_3}$. Addition of this difference to the sum of the $\mathrm{Yb_2O_3}$ and YbO values gives $\Delta\mathrm{H^0_{f~298}}$ for $\mathrm{Yb_3O_4}$ of -580 kcal/gfw. Combination of this tetraoxide value with the difference in enthalpies of formation of $\mathrm{Eu_3O_4}$ and $\mathrm{Eu_3O_4Br}$ and inclusion of the 5 kcal/gfw correction for the Yb-Br bond yields a $\Delta\mathrm{H^0_{f~298}}$ of -630 kcal/gfw for $\mathrm{Yb_3O_4Br}$. These values are presented in Appendix V with other approximated data and values from the literature.

Third law calculations have been used to obtain the free energy changes for the lithium hydride reduction of the oxide bromides of europium and ytterbium (equations VII-5 - VII-8).

$$3 \text{LnOBr}(s) + 3 \text{LiH}(\ell) \longrightarrow 3 \text{LnO}(s) + 3 \text{LiBr}(\ell) + 3/2 \text{ H}_2(g)(\text{VII}-5)$$

$$3 \text{LnOBr}(s) + 3 \text{LiH}(\ell) \longrightarrow \text{Ln}_2O_3(s) + \text{Ln}(s) + 3 \text{LiBr}(\ell) + 3/2\text{H}_2(g).$$

$$(\text{VII}-6)$$

$$3 \text{Ln}_3O_4\text{Br} + 3 \text{LiH}(\ell) \longrightarrow 3 \text{Ln}_3O_4(s) + 3 \text{LiBr}(\ell) + 3/2\text{H}_2(g).(\text{VII}-7)$$

$$3 \text{Ln}_3O_4\text{Br}(s) + 3 \text{LiH}(\ell) \longrightarrow 4 \text{Ln}_2O_3(s) + \text{Ln}(s) + 3 \text{LiBr}(\ell) + 3/2\text{H}_2(g).$$

$$(\text{VII}-8)$$

Since the melting point of LiH (960°K) appears to mark the onset of rapid reduction, 1000°K has been selected for the calculations. The liquid state is assumed for LiBr because long heating is required to volatilize the phase after the reduction is apparently complete. The results listed in Table VIII clearly exhibit the differences observed experimentally; namely, that the lower oxides of europium are readily attained by hydride reduction, while those of ytterbium are not because sesquioxide formation is favored. Since ytterbium hydride is actually observed instead of the free metal¹⁰⁶, reactions (VII-6) and (VII-8) are even more favored than indicated.

Since attempts to prepare ytterbium monoxide by reduction of the sesquioxide with the metal according to reaction (VII-9) have also been unsuccessful¹⁰⁶, an examination of the energetics of this reaction for Ln = Eu and Yb is of interest.

$$Ln(s, \ell, g) + Ln_2O_3(s) \longrightarrow 3LnO(s).$$
 (VII-9)

The data given in Appendix V have again been employed in third law calculations of the free energy changes. The

Table VIII. Free energy changes calculated for the reduction of europium and ytterbium oxide bromides with lithium hydride.

Lanthanide	∆G ⁰ at 1000	⁰ K(kcal/gfw)
Reaction Products	Eu	Yb
3 LnO(s)	-54	-74
$Ln_2O_3(s) + Ln(s)$	-21	-91
3 Ln ₃ O ₄ (s)	-61	-71
$4 \ln_2 O_3(s) + \ln(s)$	-17	-81

Table IX. Free energy changes for the reaction of europium and ytterbium with their sesquioxides at various temperatures.

$\Delta G_{T}^{0} \text{ (kcal/gfw)}$ Ln 298^{0}K 100^{0}K 1400^{0}K 20						
Ln	298°K	100 ⁶ K	1400°K	2000°K		
Eu	-39	-33	-30			
Yb	8	16	21	114		

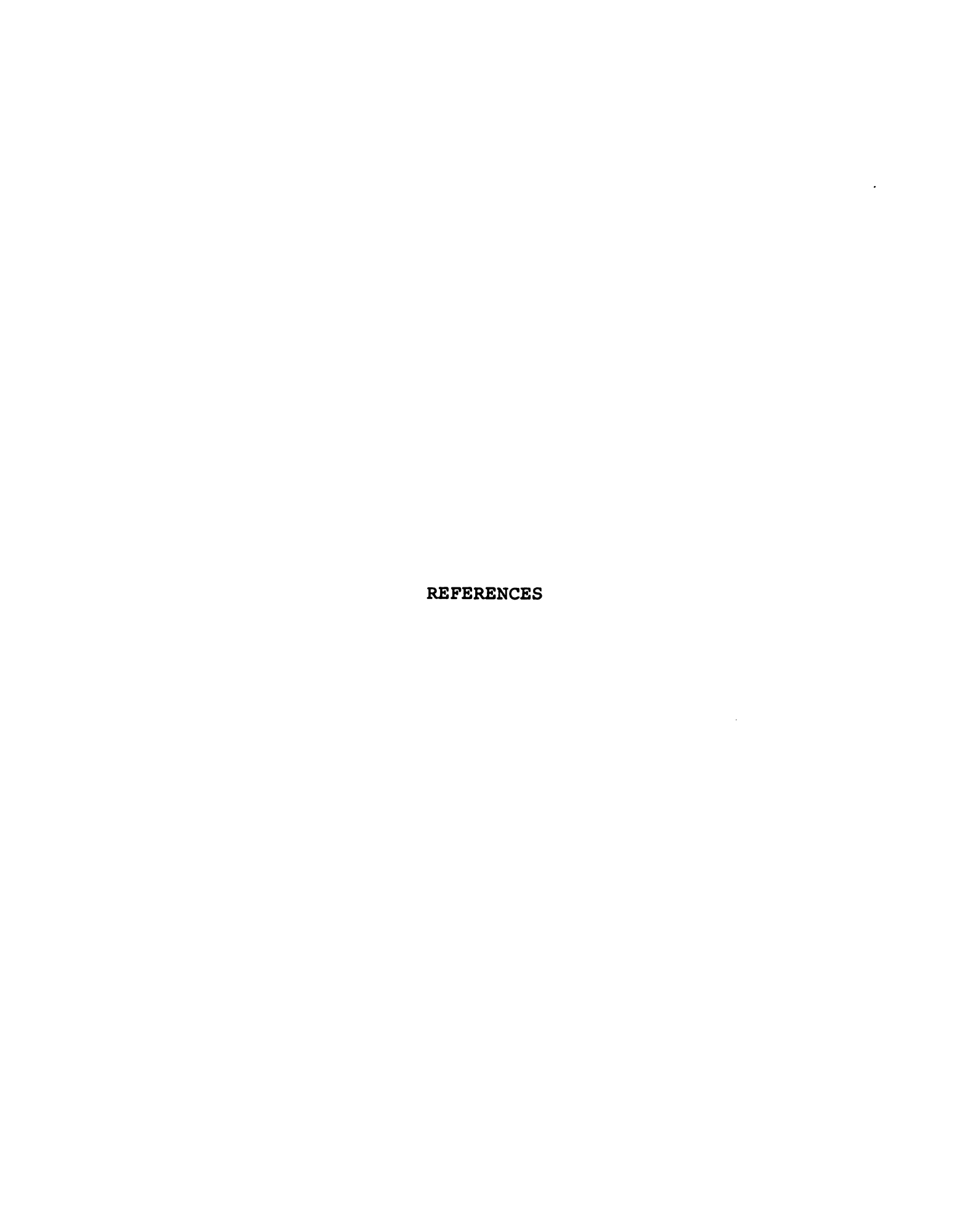
results listed in Table IX indicate that the preparation of YbO at elevated temperatures is impossible because of the disproportionation reaction to the metal and the sesquioxide. However, the trend in $\triangle G_T^0$ is such that the phase might be stabilized at low temperatures if it were prepared by condensation of the gaseous monoxide. In order for YbO to be thermodynamically stable, <u>i.e.</u>, $\triangle G_T^0 \leq 0$ for reaction VII-9, its $\triangle H_f^0$ ≥ -148.5 kcal/gfw.

Although the question of why no lower oxides other than those of europium appear to exist has not been answered directly, the free energy calculations for reactions (VII-5) -(VII-9) give an indication. With the exception of the europium and ytterbium sesquioxide values (-394 and -434 kcal/gfw, respectively), the enthalpies of formation of the lanthanide sesquioxides vary in a monotonically decreasing manner from lanthanum to lutetium (-428 to -449 kcal/gfw)¹⁷. The anomalously high enthalpy of formation of Eu₂O₃, which deviates from the trend by 40 kcal/qfw, allows its lower oxides to be stable. The stability of ytterbium sesquioxide, with a deviation of only 14 kcal/qfw, prevents the attainment of divalent oxides. Gschneidner 113 has recently explained the deviations of the enthalpies of formation of the europium and ytterbium sesquioxides in terms of the promotional energy required to overcome the divalent electronic configuration and form the trivalent configuration present in the sesquioxides. If this enthalpy deviation, which appears to measure divalent tendencies of the metals, is a valid indicator, the possibility of preparing the lower oxides of samarium and other lanthanides, which show no deviation, i.e. divalent tendency, is indeed unlikely.

CHAPTER VIII

SUGGESTIONS FOR FUTURE INVESTIGATIONS

The europium-oxygen-bromine ternary has proved to be an interesting chemical system, but numerous possibilities for continued investigation are apparent. The phase diagram in the region EuBr₂-EuBr₃ probably contains stoichiometric and nonstoichiometric phases, while the preparative possibilities of the oxide bromides have not yet been exhausted. Certainly the composition of the hexagonal oxide bromide should be determined. Absolute equilibrium pressures of bromine could be determined for the EuBr₂-EuBr₃ region by use of a controlled-temperature, visible-spectrometer cell with calibration of the instrument with bromine. This procedure could simultaneously provide thermodynamic and phase data for this composition range. The crystal structure investigations of EuBr₂ and Eu₃O₄Br, both of which appear to be new structure types, should be completed. As better values become available for the enthalpy and entropy of formation of $Eu_2O_3(s)$ and the entropy of Eu(s), the thermodynamic calculations for Eu₃O₄(s), EuO(s), Eu₃O₄Br(s), and EuOBr(s) should be reevaluated.



REFERENCES

- 1) K. A. Gschneidner, Jr., "Rare Earth Alloys", D. Van Nostrand Company, Inc., New York, 1961, pp 239-251.
- 2) R. C. Rau, "Rare Earth Research II, Proceedings of the Third Conference on Rare Earth Research", K. S. Vorres, Ed., Gordon and Breach, New York, N.Y., 1964, pp 117-134.
- 3) H. Baernighausen, J. Prakt. Chem., 34(4), 1 (1966).
- 4) H. A. Eick, N. Baenzinger, and L. Eyring, <u>J. Amer. Chem.</u> Soc., 78, 5147 (1956).
- 5) J. C. Achard, C. R. Acad. Sci. Paris, 245, 1064 (1957).
- 6) B. T. Mathais, R. M. Bozorth, and J. H. Van Vleck, Phys. Rev. Lett., 7, 160 (1961).
- 7) J. L. Burnett and B. B. Cunningham, AEC Report UCRL-11126, Berkeley, Calif., Feb. 1964.
- 8) J. C. Achard and M. G. Chaudron, <u>C. R. Acad. Sci. Paris</u>, 250, 3025 (1960).
- 9) H. Baernighausen and G. Brauer, Acta Crystallogr., 15, 1059 (1962).
- 10) R. C. Rau, ibid., 20, 716 (1966).
- 11) H. Baernighausen, Z. Anorg. Allg. Chem., 349, 280 (1967).
- 12) E. J. Huber, Jr., G. C. Fitzgibbon, and C. E. Holley, Jr., <u>J. Phys. Chem.</u>, 68, 2720 (1964).
- 13) J. M. Stuve, U.S. Bureau of Mines Report of Investigation 6640, Reno, Nev., Oct. 1964.
- 14) L. B. Pankratz, E. G. King, and K. K. Kelley, <u>ibid</u>., 6033, Washington, D.C., Jan. 1962.
- 15) M. B. Panish, <u>J. Chem. Phys.</u>, 34, 1079 (1961).

- 16) C. F. Guerci, and U. L. Moruzzi, <u>Bull. Amer. Phys. Soc.</u>, 9, 225 (1964).
- 17) E. F. Westrum, Jr., "Advances in Chemistry Series 71. Lanthanide/Actenide Chemistry", R. F. Gould, Ed., American Chemical Society, Washington, D.C., 1967, pp 25-50.
- 18) M. D. Taylor and C. P. Carter, <u>J. Inorg. Nucl. Chem.</u>, 24, 387 (1962).
- 19) I. Mayer and S. Zolotov, <u>ibid.</u>, 27, 1905 (1965).
- 20) D. Brown, S. Fletcher, and D. G. Holah, <u>J. Chem. Soc.</u>, A, 1968, 1889 (1968).
- 21) W. Klemm and W. Doell, Z. Anong. Allg. Chem., 241, 233 (1939).
- 22) W. Doell and W. Klemm, ibid., 241 239 (1939).
- 23) M. A. Kammermans, Z. Kristallogr., 101, 406 (1939).
- 24) F. A. Cotton and G. Wilkinson, "Advanced Inorganic Chemistry", 2nd ed, John Wiley and Sons, Inc., New York, N.Y., 1966, pp 1070-1071.
- 25) R. L. Sass, T. Brackett, and E. Brackett, <u>J. Phys. Chem.</u>, 67, 2862 (1963).
- 26) M. D. Taylor, Chem. Rev., 62, 503 (1962).
- 27) G. I. Novikov and O. G. Polyachenok, <u>Usp. Khim</u>., <u>33</u>, 732 (1964); <u>Russ. Chem. Rev</u>., <u>33</u>, 342 (1964).
- 28) L. Brewer, "Chemistry and Metallurgy of Miscellaneous Materials: Thermodynamics", L. L. Quill, Ed., McGraw-Hill Book Co., Inc., New York, N.Y., 1950, paper 7.
- 29) L. Brewer, L. A. Bromley, P. W. Gilles, and N. L. Lofgren, <u>ibid</u>., paper 6.
- 30) R. C. Feber, AEC Report LA-3164, Los Alamos, N.M., 1965.
- 31) C. E. Wicks and F. E. Block, "Thermodynamic Properties of 65 Elements--Their Oxides, Halides, Carbides, and Nitrides", U.S. Department of Interior, Bureau of Mines Bulletin 605, U.S. Government Printing Office, Washington, D.C., 1963.
- 32) A. Carrington and D. H. Leavy, <u>J. Chem. Phys.</u>, <u>44</u>, 1298 (1966).

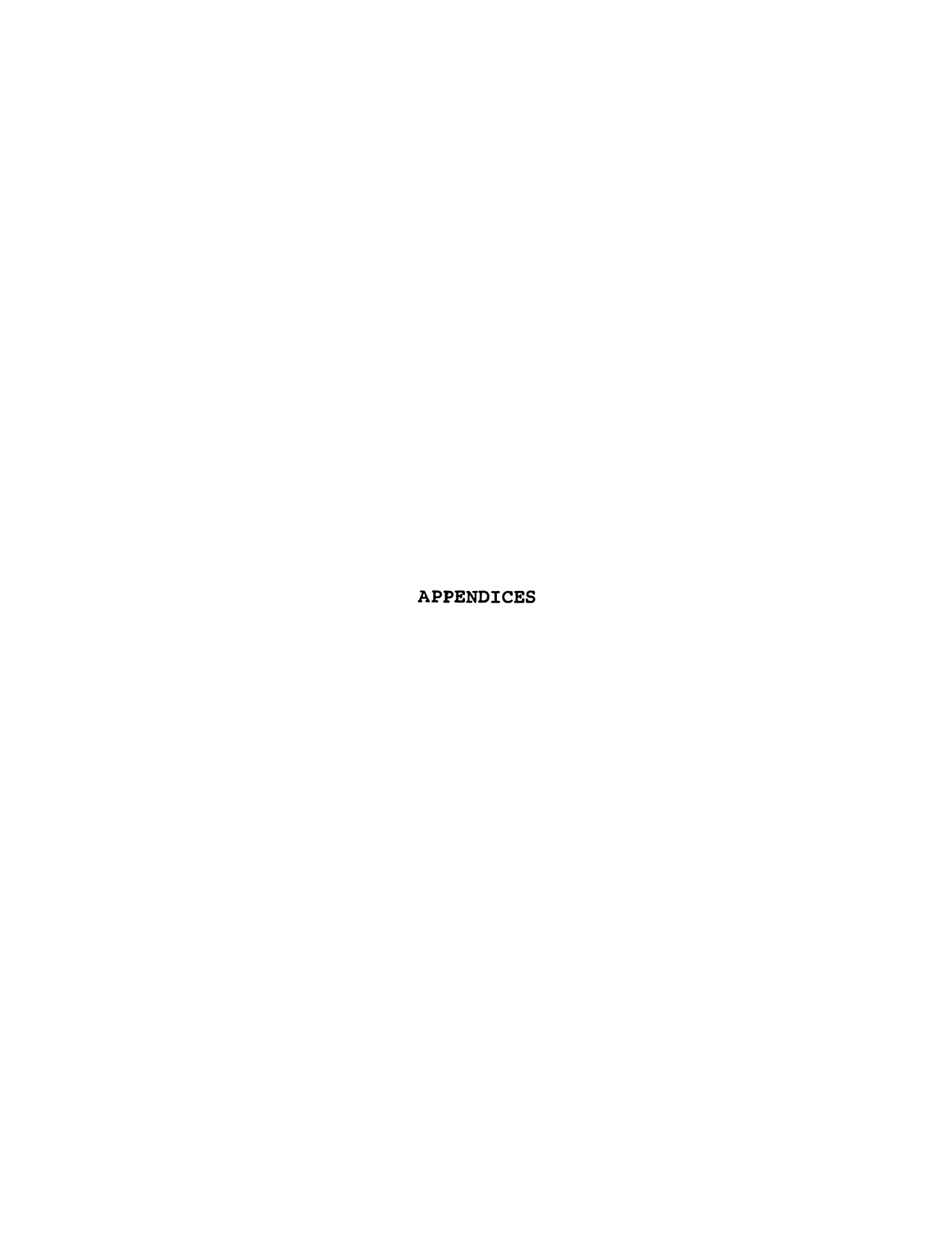
- 33) H. Grenbaut, G. Pannetier, and P. Goudmand, <u>Bull. Soc.</u> Chem. Fr., 1962, 80 (1962).
- 34) A. Pflugemacher, H. Rabben, and H. Dahmen, Z. Anorg. Allg. Chem., 279, 313 (1955).
- 35) A. J. Arivia, P. J. Aymonino, and H. J. Schumacher, ibid., 298, 1 (1959).
- 36) H. Baernighausen, G. Brauer, and N. Schultz, <u>ibid</u>., 338, 250 (1965).
- 37) W. H. Zachariasen, Acta Crystallogr., 2, 388 (1949).
- 38) N. Schultz and G. Reiter, <u>Naturwissenschaften</u>, 54, 469 (1967).
- 39) C. W. Koch, A. Broido, and B. B. Cunningham, <u>J. Amer. Chem. Soc.</u>, 74, 2349 (1952).
- 40) C. W. Koch and B. B. Cunningham, <u>ibid.</u>, 75, 796 (1953).
- 41) C. W. Koch and B. B. Cunningham, ibid., 76, 1471 (1954).
- 42) F. Weigel and H. Hang, Chem. Ber., 94, 1548 (1961).
- 43) A. K. Baev and G. I. Novikov, <u>Zh. Neorg. Khim.</u>, <u>10</u>, 2457 (1965); <u>Russ. J. Inorg. Chem.</u>, <u>10</u>, 1337 (1965).
- 44) P. W. Gilles, "The Application of Fundamental Thermodynamics to Metallurgical Processes", Gordon and Breach, New York, N.Y., 1967, pp 281-298.
- 45) J. L. Margrave, "Physiochemical Measurements at High Temperature", J. Bockris, J. White, and J. Mackenzie, Eds., Academic Press, Inc., New York, N.Y., 1959, Chapter 10.
- 46) M. Knudsen, Ann. Phys., 28, 75 (1909); English Translation by L. Venters, Argonne National Laboratory (1958).
- 47) M. Knudsen, <u>ibid.</u>, 28, 999 (1909); English Translation by K. D. Carlson and E. D. Cater, Argonne National Laboratory (1958).
- 48) R. J. Ackermann, AEC Report ANL-5482, Lemont, Ill., Sept. 1955.
- 49) J. W. Ward, AEC Report LA-3509, Los Alamos, N.M., Jan. 1966.
- 50) P. Clausing, Physica, 9, 65 (1929).

- 51) W. G. Pollard and R. D. Present, Phys. Rev., 73, 762 (1948).
- 52) A. R. Miller, J. Chem. Phys., 42, 3734 (1965).
- 53) A. R. Miller, "The Fraction of Effusing Molecules Striking a Collector Plate over a Circular Capillary", Aerojet-General Nucleonics Report AN-1328, San Ramon, Calif., Dec. 1964.
- R. P. Iczkowski, J. L. Margrave, and S. M. Robinson, J. Phys. Chem., 67, 229 (1963).
- 55) R. A. Kent, Ph.D. Thesis, Michigan State University, East Lansing, Mi., 1963.
- 56) S. Dushman, "Scientific Foundations of Vacuum Technique", John Wiley and Sons, Inc., New York, N.Y., 1949, Chapter 2.
- 57) H. Mayer, Z. Phys., 58, 373 (1929); English Translation by K. D. Carlson, Argonne National Laboratory (1958).
- 58) K. D. Carlson, P. W. Gilles, and R. T. Thorn, <u>J. Chem.</u> <u>Phys.</u>, 38, 2064 (1963).
- 59) R. J. Ackermann, R. J. Thorn, and G. H. Winslow, Abstracts, 135th National Meeting of the American Chemical Society, Boston, Mass., April 1959.
- 60) G. M. Rosenblatt, P. Lee, and M. B. Dowell, <u>J. Chem.</u> <u>Phys.</u>, <u>45</u>, 3454 (1966).
- 61) G. M. Rosenblatt, <u>J. Phys. Chem.</u>, <u>71</u>, 1327 (1967).
- 62) G. H. Stout and L. H. Jensen, "X-Ray Structure Determination--A Practical Guide", The Macmillan Co., New York, N.Y., 1968.
- 63) W. Parrish, "Advances in X-Ray Diffraction", Centurex Publishing Company, Eindhoven, 1962.
- 64) J. L. Margrave, "Physiochemical Measurements at High Temperature", J. Bockris, J. White, and J. Mackenzie, Eds., Academic Press, Inc., New York, N.Y., 1959, Chapter 2.
- 65) G. N. Lewis and M. Randall, "Thermodynamics", Revised by K. S. Pitzer and L. Brewer, McGraw-Hill Book Co., Inc., New York, N.Y., 1961.
- 66) D. Cubicciotti, <u>J. Phys. Chem.</u>, <u>70</u>, 2410 (1966).

- 67) P. A. Pilato, Ph.D. Thesis, Michigan State University, East Lansing, Mi., 1968.
- 68) J. M. Haschke and H. A. Eick, <u>J. Phys. Chem.</u>, 72, 1697 (1968).
- "JANAF Interim Thermochemical Tables", D. R. Stull, Project Director, Dow Chemical Co., Midland, Mi., 1960 and Supplements.
- 70) L. Brewer, G. R. Somayajulu, and E. Brackett, Chem. Rev., 63, 111 (1963).
- 71) W. M. Latimer, "Oxidation Potentials", 2nd ed, Prentice Hall, Englewood Cliffs, N. J., 1952, Appendix III.
- 72) F. Grønwold and E. F. Westrum, Jr., <u>Inorg. Chem.</u>, $\frac{1}{2}$, 36 (1962).
- 73) J. W. Youden, "Statistical Methods for Chemists", John Wiley and Sons, Inc., New York, N.Y., 1951.
- 74) W. Feller, "An Introduction to Probability Theory and Its Applications", 2nd ed, John Wiley and Sons, Inc., New York, N.Y., 1960, pp 115-116.
- 75) J. J. Stezowski, Ph.D. Thesis, Michigan State University, East Lansing, Mi., 1968.
- 76) H. Diehl and G. F. Smith, "Quantitative Analysis", John Wiley and Sons, Inc., New York, N.Y., 1955, p 113.
- 77) P. G. Hambling, Acta Crystallogr., 6, 98 (1953).
- 78) J. D. H. Donnay, Ed., "Crystal Data Determinative Tables", 2n ed, American Crystallographic Assn., Washington, D.C., 1963, p. 841.
- 79) O. Lindquist and F. Wengelin, Ark. Kemi, 28, 179 (1967).
- 80) M. J. Buerger, "X-Ray Crystallography", John Wiley and Sons, Inc., New York, N.Y., 1942.
- 81) M. C. Powers, "X-Ray Fluorescent Spectrometer Conversion Tables", Philips Electronic Instruments, Mt. Vernon, N.Y., 1960.
- 82) H. J. Neff, <u>Arch. Eisenhuettenw.</u>, 34, 903 (1963); Siemens Pamphlet Eg 4/10e, Aug. 1964.
- 83) M. Marezio, H. A. Plettinger and W. H. Zachariasen, Acta Crystallogr., 14, 234 (1961).

- 84) B. A. Vajnstejn and Z. G. Pinsker, Zh. Fiz. Khim., 24, 432 (1950); A. J. C. Wilson, Ed., "Structure Reports for 1950", Volume 13, International Union of Crystallography, Oosthoek's Uitgevers Mij, Utrecht, Netherland, 1954, pp 209-210.
- 85) N. F. M. Henry and K. Lonsdale, Eds., "International Tables for X-Ray Crystallography", Volume I, International Union of Crystallography, Kynoch Press, Birmingham, England, 1952.
- 86) R. W. Kiser, "Introduction to Mass Spectrometry and Its Applications", Prentice-Hall, Inc., Englewood Cliffs, N.J., 1965.
- 87) J. W. Hastie, P. Ficalora, and J. L. Margrave, <u>J. Less-Common Metals</u>, <u>14</u>, 83 (1968).
- 88) R. Hultgren, R. L. Orr, P. D. Anderson, and K. K. Kelley, "Supplement of Selected Values of Thermodynamic Properties of Metals and Alloys", private communication, R. Hultgren.
- 89) A. Buechler, J. Stauffer, and W. Klemperer, <u>J. Chem.</u>
 Phys., 40, 3471 (1964).
- 90) R. E. Thoma, "Progress and Science and Technology of the Rare Earths", Volume 2, L. Eyring, Ed., Pergamon Press, New York, N.Y., 1962, pp 90-122.
- 91) L. B. Asprey, T. K. Keenan, and F. H. Kruse, <u>Inorg.</u> Chem., 3, 1137 (1964).
- 92) B. Frit, B. Tanguy, and P. Hagenmuller, <u>Bull. Soc.</u> Chem. Fr., 1966, 2190 (1966).
- 93) B. Frit, M. M. Chbany, and P. Hagenmuller, <u>ibid.</u>, 1968, 127 (1968).
- 94) J. W. Ward, <u>J. Chem. Phys.</u>, $\underbrace{47}_{}$, 4030 (1967).
- 95) D. L. Hildebrand and W. F. Hall, <u>J. Phys. Chem.</u>, 66, 754 (1962).
- 96) R. Hultgren, R. L. Orr, P. D. Anderson, and K. K. Kelley, "Selected Values of Thermodynamic Properties of Metals and Alloys", John Wiley and Sons, Inc., New York, N.Y., 1963.
- 97) L. Pauling, "The Nature of the Chemical Bond", 3rd ed, Cornell University Press, 1960.
- 98) C. F. Guerci and M. W. Shafer, <u>J. Appl. Phys.</u>, <u>37</u>, 1406 (1966).

- 99) R. E. Loehman, R. A. Kent, and J. L. Margrave, <u>J. Chem.</u> Eng. Data, 10, 296 (1965).
- 100) L. Brewer, L. A. Bromley, P. W. Gilles, and N. L. Lofgren, "The Chemistry and Metallurgy of Miscellaneous Materials: Thermodynamics", L. L. Quill, Ed., Mc-Graw-Hill Book Co., Inc., New York, N.Y., 1950, paper 8.
- 101) K. K. Kelley, U.S. Bureau of Mines Bulletin 584, U.S. Government Printing Office, Washington, D.C., 1960.
- 102) F. D. Rossini, D. D. Wagman, W. H. Evans, S. Levine, and I. Jaffe, Circular 500, National Bureau of Standards U.S. Government Printing Office, Washington, D.C., 1952.
- 103) R. F. Porter, W. A. Chupka, and M. G. Inghram, <u>J. Chem.</u>
 Phys., 23, 1347 (1955).
- 104) M. G. Inghram, W. A. Chupka, and R. F. Porter, <u>ibid</u>., 23, 2159 (1955).
- 105) C. O. Schulz and F. E. Stafford, <u>J. Phys. Chem.</u>, <u>72</u>, 4686 (1968).
- 106) G. Brauer, H. Baernighausen, and N. Schultz, Z. Anorg. Allg. Chem., 356, 46 (1967).
- 107) T. L. Felmlee and L. Eyring, <u>Inorg. Chem.</u>, <u>7</u>, 660 (1968).
- 108) A. D. Butherus and H. A. Eick, <u>J. Amer. Chem. Soc.</u>, 90, 1715 (1968).
- 109) W. W. Wendlandt, <u>J. Inorg. Nucl. Chem.</u>, <u>5</u>, 118 (1957).
- 110) W. W. Wendlandt, <u>ibid</u>., 9, 136 (1959).
- 111) A. Eucken, Ed., Landolt-Boernstein, Vol. I(1), Springer Verlag, Berlin, Germany, 1950, pp 211-212.
- 112) D. H. Templeton and C. H. Dauben, <u>J. Amer. Chem. Soc.</u>, <u>76</u>, 5237 (1954).
- 113) K. A. Gschneidner, Jr., <u>J. Less-Common Metals</u>, <u>17</u>, 13 (1969).



APPENDIX I: Observed $\sin^2\theta$ (λ = 1.54051 Å) and Interplanar d-Values

Appendix IA: Tetragonal EuBr₂

Rela- tive Inten- sity	hkl	$\sin^2 heta$	d value	Rela- tive Inten- sity	hkl	sin²θ	d value
VW	110	.00891	8.160	S	321	.06953	2.921
w	001	.01184	7.079	w-m	330	.07986	2.726
w-m	101	.01630	6.033	S	302	.08716	2.609
w	111	.02078	5.343	m-s	420	.08876	2.585
vw	201	.02974	4.466	m-s	312	.09159	2.545
s	211	.03412	4.170	m	421	.10067	2.528
vw	220	.03570	4.077	w-m	322	.10469	2.381
w	310	.04451	3.651	w-m	402	.11792	2.243
w	002	.04723	3.544	w-m	501	.12268	2.199
w-m	102	.05166	3.389	m	520	.12841	2.149
m-s	311	.05624	3.248	m	521	.14045	2.055
m	202	.06501	3.021	w	313	.15051	1.985

Appendix IB: Orthorhombic EuBr₂·H₂O

W	110	.01186	7.073	s	230	.06902	2.932
m	020	.01810	5.725	m	040	.07242	2.862
w-m	210	.03259	4.267	W	301	.09545	2.493
w-m	101	.03966	3.868	s	231	.10104	2.423
w	111	.04379	3.681	m-s	041	.10485	2.379
w	130	.04721	3.545	m	400	.11236	2.298
w	021	.05042	3.430	m-s	002	.12891	2.145
vs	211	.06498	3.022				

		1
		Í

140
Appendix IC: Orthorhombic EuBr₃

Rela- tive Inten- sity	hkl	$ extst{sin}^{oldsymbol{2}} heta$	d value $(\overset{\Omega}{\mathtt{A}})$	Rela- tive Inten- sity	hkl	$ extstyle{sin}^{ extstyle{2}} heta$	d value (X)
s	020	.01466	6.362	s	320	.07881	2.744
m	200	.02872	4.561	m-s	240	.08727	2.607
vw	001	.03629	4.043	m	231	.09819	2.458
vw	011	.04035	3.835	s	311	.10450	2.383
w	220	.04313	3.709	w	400	.11411	2.280
w	111	.04768	3.527	w	420	.12866	2.147
w	121	.05865	3.181	m	060	.13369	2.107
w	201	.06573	3.004	m	151	.13557	2.092
s	211	.06892	2.934	m-s	002	.14708	2.008
m-s	031	.06978	2.916	vw	102	.15456	1.959
							1 00 1
vs Append	131	.07676	2.780	m •6HaO	341	.16035	1.924
vs Appendw			2.780 inic EuBr ₃ 6.745		341	.16035	3.493
Append ———w	ix ID:	Monocl	inic EuBr ₃	·6H ₂ O			
Append	010	Monocl	inic EuBr ₃	·6H ₂ O	012	.04862	3.493
Append w m	010 101	Monocl .01304 .01397	inic EuBr ₃ 6.745 6.515	•6H ₂ O w vw	012 020	.04862	3.493 3.377
Append w m	010 101 101	.01304 .01397 .01575	6.745 6.515 6.138	*6H ₂ O w vw w	012 020 I20	.04862 .05202 .05798	3.493 3.377 3.199
Append w m m w	010 101 101 110	.01304 .01397 .01575 .01895	6.745 6.515 6.138 5.595	•6H ₂ O w vw w	012 020 120 301	.04862 .05202 .05798 .06480	3.493 3.377 3.199 3.026
Append w m w m	010 101 101 110 011	.01304 .01397 .01575 .01895 .02196	6.745 6.515 6.138 5.595 5.198	·6H ₂ O w vw w w	012 020 120 301 310	.04862 .05202 .05798 .06480 .06635	3.493 3.377 3.199 3.026 2.990
Append w m m w m	010 101 101 110 011 200	.01304 .01397 .01575 .01895 .02196	6.745 6.515 6.138 5.595 5.198 4.998	·6H ₂ O w vw w w w	012 020 120 301 310 212	.04862 .05202 .05798 .06480 .06635 .06892	3.493 3.377 3.199 3.026 2.990 2.934
Append w m w m m m	010 101 101 110 011 200 111	.01304 .01397 .01575 .01895 .02196 .02375 .02696	6.745 6.515 6.138 5.595 5.198 4.998 4.691	*6H ₂ O w vw w w w vw	012 020 120 301 310 212 212	.04862 .05202 .05798 .06480 .06635 .06892 .07603	3.493 3.377 3.199 3.026 2.990 2.934 2.793
Append w m m m m m m	010 101 101 110 011 200 111 111	.01304 .01397 .01575 .01895 .02196 .02375 .02696 .02871	6.745 6.515 6.138 5.595 5.198 4.998 4.691 4.546	·6H ₂ O w vw w w vw w vw	012 020 120 301 310 212 212 311	.04862 .05202 .05798 .06480 .06635 .06892 .07603	3.493 3.377 3.199 3.026 2.990 2.934 2.793 2.756
Append w m m m m m m	010 101 101 110 011 200 111 111	.01304 .01397 .01575 .01895 .02196 .02375 .02696 .02871	6.745 6.515 6.138 5.595 5.198 4.998 4.691 4.546 4.073	·6H ₂ O w vw w w vw w vw w	012 020 120 301 310 212 212 311 221	.04862 .05202 .05798 .06480 .06635 .06892 .07603 .07813	3.493 3.377 3.199 3.026 2.990 2.934 2.793 2.756 2.677

		; (

APPENDIX II: X-Ray Fluorescence

Appendix IIA: Linear calibration curves for X-ray fluorescence

Vaporizing Substance	Element	(Counts/µg 4 min)	b
Eu ₃ 0 ₄ (s)	Eu	87 ± 23	54
EuO(s)	Eu	113 ± 13	18
EuBr $_{f 2}$ ($m\ell$) $_{ackslash}$	Eu	540 ± 24	42
$\mathtt{EuBr}_{2}\left(\ell ight)$	Br	858 ± 22	-38
$\mathtt{Au}(\ell)$	Au	202 ± 11	8

Appendix IIB: The Vapor Pressure of Gold

Introduction

In cooperation with the National Bureau of Standards in an attempt to establish vapor pressure standards, the vapor pressure of gold has been measured by the target collection Knudsen effusion technique. The results of such an investigation should also be useful for evaluation of the X-ray fluorescence technique.

Experimental

The gold sample employed in this investigation (99.999%) purity, NBS Standard Reference Material #685, 60 mil wire from spool #13-1-60) was provided by the National Bureau of

Standards. The 0.15-0.50 g portions employed in the measurements were prepared by metal fatigue and placed in molybdenum cells of the assymmetric design (cf.IV, K). Three orifice sizes (58.5 \times 10⁻⁴, 21.6 \times 10⁻⁴, and 7.0 \times 10⁻⁴ cm²) were used in the target collection experiments (cf. V, H) which extended over the temperature range 1598-1925°K. The quantity of effusate collected was analyzed by the X-ray fluorescence technique (cf. V, G). The linear calibration curve (Appendix IIA) was obtained for the La₁ line of gold by weighing onto copper targets 0.02-0.10 g quantities of standard solutions which were prepared by dissolving weighed samples of 24k gold (Engelhard Industries, Inc., Newark, N.J.) and HAuCl₄·3H₂O (49.1% assay, J. T. Baker Chemical Co.) in 3 ml of aqua regia and in water, respectively, and diluting.

Results

The following calculations were made under the assumption that monatomic gold is the only vapor species. A linear least squares equation describing the 30 data points (cf. Appendix IIC) obtained in 5 independent vaporization experiments is:

log P = -(1.8176 \pm 0.0304 \times 10⁴/T) + 5.937 \pm 0.176. From this equation, the following thermodynamic data have been obtained for the vaporization of gold at the median temperature: $\Delta H_{1762}^0 = 83._2 \pm 1._4 \text{ kcal/gfw}$ and $\Delta S_{1762}^0 = 27.1_7 \pm 0.8_1$ eu. These values have been reduced to 298^0K

with published enthalpy and entropy functions of to give $\Delta H_{298}^0 = 88._7 \pm 1._4 \text{ kcal/gfw}$ and $\Delta S_{298}^0 = 32.4_6 \pm 0.8_1 \text{ eu}$. A third law value of $\Delta H_{298}^0 = 88.0_0 \pm 0.4_2 \text{ kcal/gfw}$ (cf. Appendix IIC) was obtained through use of published free energy functions of these values are in excellent agreement with the second law value of $88.8_4 \pm 0.5_5 \text{ kcal/gfw}$ obtained by Ward of the heat of formation value of 88.3 kcal/gfw given by Hildebrand and Hall of the value of Hultgren et al. of 87.3 kcal/gfw.

Appendix IIC: Equilibrium pressures and third law enthalpies for Au

T (0K)	-log P _T	$^{ riangle H^{f 0}}_{298}$ (kcal/gfw)	T (0K)	-log P _T	$\triangle H_{298}^{0}$ (kcal/gfw)
1676	4.956	88.411	1925	3.451	87.421
1722	4.706	88.678	1843	3.847	87.277
1778	4.309	88.154	1772	4.411	88.701
1819	4.134	88.602	1672	4.896	87.724
1869	3.850	88.459	1640	5.128	87.885
1898	3.706	88.486	1853	3.842	87.690
1858	3.904	88.435	1910	3.562	87.767
1791	4.250	88.279	1688	4.839	88.056
1745	4.486	88.036	1725	4.552	87.617
1701	4.748	87.991	1674	4.899	87.759
1687	4.825	87.912	1650	5.03 6	87.693
1737	4.429	87.196	1613	5.316	87.907
1802	4.108	87.761	1598	5.462	88.205
1863	3.734	87.205	1710	4.686	87.955
1898	3.606	87.617	1774	4.332	88.160

APPENDIX III: Equilibrium Pressures and Third Law Enthalpies

Appendix IIIA: Trieuropium tetraoxide vaporization

T (0K)	-log P (atm) (ΔH_{298}^0 kcal/gfw)	T (0K)	<pre>-log P (atm)</pre>	$^{ riangle H_{f 298}^{f 0}}$ (kcal/gfw)
1700	4.847	91.79	1939	3.545	92.13
1765	4.464	91.99	1916	3.772	93.12
1854	3.997	92.28	1888	3.911	93.08
1824	4.141	92.10	1736	4.669	92.18
1793	4.357	92.43	1799	4.276	92.05
1736	4.698	92.43	1826	4.234	92.97
1722	4.663	91.46	1769	4.581	93.09
1754	4.527	91.91	1726	4.846	93.08
1805	4.301	92.53	1700	4.932	92.45
1867	3.941	92.39	1662	5.529	93.02
1927	3.491	91.14	1604	5.480	91.59
1899	3.781	92.45	1665	5.090	91.88
1842	4.043	92.11	1661	5.166	92.26
1788	4.463	93.06	1715	4.822	92.35
1738	4.784	93.20	1715	4.751	91.79
1664	5.087	91.80	1743	4.680	92.63
1888	3.748	91.67	1743	4.714	92.89
1950	3.459	91.86	1691	5.060	92.98
2016	3.131	91.63	1694	5.025	92.86
1972	3.348	92.11	1639	5.218	91.49
2014	3.105	91.32	1639	5.313	92.20

Appendix IIIB: Europium monoxide vaporization

1510	4.702	80.47	1661	3.697	80.39
1565	4.459	81.48	1713	3.384	80.27
1602	4.207	81.45	1758	3.116	80.08
1639	3.896	80.88	1756	3.118	80.00
1395	5.544	80.02	1728	3.312	80.36
1430	5.279	80.19	1687	3.508	80.11
1453	5.110	80.30	1636	3.859	80.48
1495	4.831	80.59	1452	5.122	80.33
1545	4.541	81.08	1500	4.774	80.46
1598	4.175	81.03	1534	4.643	81.25
1633	3.940	80.93	1473	5.035	80.84
1581	4.267	80.89	1474	5.072	81.10
1519	4.702	80.92	1423	5.403	80.62
1485	4.922	80.84	1421	5.406	80.54
1499	4.732	80.05	1392	5.654	80.58
1547	4.437	80.45	1369	5.854	80.54
1597	4.069	80.20	1334	6.141	80.32

	!
	İ
	:
	1
	i
	,
	i
)
	1

145
Appendix IIIC: Europium dibromide vaporization

T (K0)	-log P (atm)	$^{ riangle H^{f 0}_{f 298}}$ (kcal/gfw)	т (°к)	-log P (atm)	$^{ riangle H_{298}^0}$ (kcal/gfw)
1237	5.326	69.77	1412	3.951	69.33
1278	4.978	69.65	1367	4.260	69.31
1304	4.655	68.92	1318	4.633	69.40
1331	4.465	68.99	1345	4.481	69.71
1352	4.285	68.80	1383	4.193	69.61
1237	5.328	69.78	1439	3.9 3 0	70.38
1278	4.905	69.23	1511	3.411	70.05
1304	4.739	69.42	1568	3.119	70.47
1331	4.548	69.50	1476	3.598	69.82
1352	4.301	68.90	1445	3.790	69.71
1318	4.628	69.36	1412	4.006	69.69
1345	4.504	69.85	1367	4.352	69.89
1383	4.145	69.30	1185	5.654	69.15
1439	3.868	69.98	1228	5.324	69.33
1511	3.384	69.86	1246	5.128	69.05
1568	3.034	69.86	1185	5.674	69.26
1476	3.587	69.75	1228	5.403	69.77
1445	3.676	69.96	1246	5.234	69.66

Appendix IIID: Trieuropium tetraoxide monobromide vaporization

1219	5.860	139.11	1275	5.403	139.85
1261	5.462	139.07	1226	5.842	139.67
1331	4.846	138.87	1198	6.091	138.31
1331	4.890	139.42	1240	5.645	138.96
1367	4.582	139.11	1303	5.112	139.27
1219	6.000	140.67	1341	4.838	139.76
1261	5.514	139.63	1275	5.308	138.74
1331	4.809	138.44	1389	4.521	140.44
1331	4.816	138.52	1441	4.232	141.56
1367	4.504	138.13	1520	3.592	138.97
1407	4.313	139.47	1537	3.551	140.81
1352	4.611	138.03	1600	3.064	139.04
1423	4.170	139.10	1565	3.403	141.07
1505	3.602	138.78	1485	3.702	138.41
1455	4.068	140.68	1414	4.394	141.23
1407	4.366	140.16	1389	4.398	138.89
1352	4.611	138.03	1441	4.136	140.29
1423	4.244	140.06	1520	3.564	139.53
1505	3.682	139.88	1537	3.413	138.85
1455	4.101	141.12	1600	3.071	139.14
1198	6.100	139.45	1565	3.427	141.41
1240	5.685	139.40	1485	3.753	139.11
1303	5.072	138.79	1414	4.206	138.74
1341	4.861	140.05	1466	3.821	138.36

APPENDIX IV: Thermodynamic Values for Data Reduction

Appendix IVA: Approximated heat capacity, enthalpy and entropy values

Phase	a	b	С	đ	Estimated S ₂₉₈ eu
Eu ₃ O ₄ (s)	43.61	6.24	13,270	250.31	49.0
EuO(s)	12.54	2.08	3,830	72.60	16.3
$Eu_3O_4Br(s)$	49.57	6.24	15,050	284.26	63.8
EuOBr(s)	18.50	2.08	5,610	106.02	29.0
$\mathtt{EuBr}_{2}(\mathtt{s})$					40.1
$\mathtt{EuBr}_{2}(\mathtt{g})$					76.3

Appendix IVB: Enthalpy, entropy and free energy functions

 $\mathrm{Eu_{2}O_{3}}$ (s, monoclinic)($\mathrm{H_{T}^{0}-H_{298}^{0}}$),($\mathrm{S_{T}^{0}-S_{298}^{0}}$) values from reference 14.

T (0K)	$({\tt H_T^0-H_{298}^0})$ cal/gfw	$(S_{T}^{0}-S_{298}^{0})$ eu	$-(G_{f T}^{f 0}-H_{f 298}^{f 0})/{f T}$ eu
1100	26,840	42.75	53.35
1200	30,430	45.88	55.52
1300	34,070	48.79	57.58
1400	37,750	51.52	59.55
1500 1600	41,470 45,220	54.08 56.50	61.43 6 3 .24
1700	48,990	58.79	64.97
1800	52,780	60.96	66.64
1900	56,590	63.02	68.24
2000	60,140	64.98	69.78

Continued on next page

Appendix IVB: (Continued)

T (OK)	$(H_{\mathrm{T}}^{0}-H_{298}^{0})$ cal/gfw	$(S_{T}^{0}-S_{298}^{0})$ eu	$-(G_{\mathbf{T}}^{0}-H_{298}^{0})/\mathbf{T}$ e
Eu ₃ 0 ₄ (s)			
1300	48,700	70.49	82.30
1400	53,900	74.35	84.85
1500	59,170	77.98	87.53
1600	64,490	81.42	90.11
1700	69,880	84.69	92.58
1800	75,340	87.80	94.94
1900	80,850	90.78	97.22
2000	86,430	93.65	99.44
2uO(s)			The second s
1300	14,230	20.56	24.61
1400	15,760	21.69	25.43
1500	17,320	22.78	26.23
1600	18,900	23.79	26.98
1700	20,490	24.75	27.70
1800	22,110	25.69	28.41
EuBr ₂ (s,	ℓ) ($H_{\mathbf{T}}^{0}$ - H_{298}^{0}) and ($S_{\mathbf{T}}^{0}$ -	S ₂₉₈) values from the state of the state o	
SuBr ₂ (s,	<u> </u>		
	29 and 30 20,000	by graphical into	erpolation
1000	29 and 30 20,000 22,400	by graphical into	erpolation 49.10
1000 1100	29 and 30 20,000	29.00 31.50	49.10 51.20
1000 1100 1200	29 and 30 20,000 22,400 24,800	29.00 31.50 34.00	49.10 51.20 53.40
1000 1100 1200 1300	29 and 30 20,000 22,400 24,800 27,200	29.00 31.50 34.00 36.00	49.10 51.20 53.40 55.20
1000 1100 1200 1300 1400	29 and 30 20,000 22,400 24,800 27,200 29,600	29.00 31.50 34.00 36.00 37.50	49.10 51.20 53.40 55.20 56.50
1000 1100 1200 1300 1400 1500	29 and 30 20,000 22,400 24,800 27,200 29,600 32,000 34,400	29.00 31.50 34.00 36.00 37.50 39.00	49.10 51.20 53.40 55.20 56.50 57.80
1000 1100 1200 1300 1400 1500 1600	29 and 30 20,000 22,400 24,800 27,200 29,600 32,000 34,400	29.00 31.50 34.00 36.00 37.50 39.00	49.10 51.20 53.40 55.20 56.50 57.80
1000 1100 1200 1300 1400 1500 1600	29 and 30 20,000 22,400 24,800 27,200 29,600 32,000 34,400	29.00 31.50 34.00 36.00 37.50 39.00 40.00	49.10 51.20 53.40 55.20 56.50 57.80 58.60
1000 1100 1200 1300 1400 1500 1600	29 and 30 20,000 22,400 24,800 27,200 29,600 32,000 34,400	29.00 31.50 34.00 36.00 37.50 39.00 40.00	49.10 51.20 53.40 55.20 56.50 57.80 58.60
1000 1100 1200 1300 1400 1500 1600 Su ₃ O ₄ Br(29 and 30 20,000 22,400 24,800 27,200 29,600 32,000 34,400 s) 43,250 48,930	29.00 31.50 34.00 36.00 37.50 39.00 40.00	49.10 51.20 53.40 55.20 56.50 57.80 58.60
1000 1100 1200 1300 1400 1500 1600 Su ₃ O ₄ Br(1100 1200 1300	29 and 30 20,000 22,400 24,800 27,200 29,600 32,000 34,400 s) 43,250 48,930 54,660 60,460	29.00 31.50 34.00 36.00 37.50 39.00 40.00	49.10 51.20 53.40 55.20 56.50 57.80 58.60 94.43 97.91 101.22
1000 1100 1200 1300 1400 1500 1600 Eu ₃ O ₄ Br(1100 1200 1300 1400	29 and 30 20,000 22,400 24,800 27,200 29,600 32,000 34,400 s) 43,250 48,930 54,660	29.00 31.50 34.00 36.00 37.50 39.00 40.00	94.43 97.91 101.22 104.38
1000 1100 1200 1300 1400 1500 1600 2u ₃ O ₄ Br(1100 1200 1300 1400 1500	29 and 30 20,000 22,400 24,800 27,200 29,600 32,000 34,400 s) 43,250 48,930 54,660 60,460 66,330	29.00 31.50 34.00 36.00 37.50 39.00 40.00 69.75 74.68 79.27 83.57 87.62	94.43 97.91 101.22 104.38 107.40

Appendix IVC: Free energy function changes for the vaporization reactions

Phase	Eu ₃ 0 ₄ (s)	EuO(s)	$\mathtt{EuBr}_{2}(\ell)$	$Eu_3O_4Br(s)$
TOK	-∆fef (VI-1)	-∆fef(VI-2)	-∆fef(VI-3)	-∆fef(VI-4)
1000			34.86	
1100			33.77	59.76
1200			32.55	59.21
1300		31.77	31.52	58.79
1400		31.60	31.17	58.32
1500		31.35	30.68	57.88
1600	32.03	31.19	30.56	57.52
1700	31.79	31.03		
1800	31.62	30.78		
1900	31.41			
2000	31.14			

Appendix IVD: Thermodynamic functions from the literature

Phase	Thermodynamic Function at 298°K	Value	Reference 88	
<u> </u>	ΔH_f^0 kcal/gfw	41.9 ± 0.2		
$\mathtt{Eu_2O_3}(\mathtt{s})$	ıı ıı	-393.9 ± 0.9	12	
Br(g)	II	26.740	69	
Eu(g)	△G cal/gfw	34.212	88	
$\mathtt{Eu_2O_3}(\mathtt{s})$	11	(-370.9)	(est)	
Br(g)	11	19.700	69	
Eu(g)	S ⁰ eu	45.097	88	
$\mathtt{Eu_2O_3}(\mathtt{s})$	II .	(35.0)	17	
Br(g)	11	41.850	69	
E u (s)	11	19.31	88	
$\mathtt{Br}_{2}(\ell)$	п	36.38	69	
EuBr ₂ (g)	D ₀ kcal/gfw	(202)	30	

APPENDIX V: Data for Thermodynamic Calculations

	-∆H ₀	S298		$(G_{T}^{0}/H_{298}^{0}$)/T (eu)	
Phase	$-\Delta H^0$ (kca $1/298$)	(eu)	1000°K	1400°K	2000°K	2500°K
LiH(ℓ)	15.10 ^a		16.37 ^a			
LiBr(ℓ)	80.97 ^a		26.28 ^a			
$\mathbf{H_2}(g)$	0	_	34.76 ^a			
$\mathtt{Eu_2O_3}(\mathtt{s})$	393.9 ^b	35.0 ^b	51.08	59.55	69.8	77.9
$Eu_3O_4(s)$	542.6	49.0	72.72			
$Eu_3O_4Br(s)$	597.7	63.7	90.56		120.4	131.5
E uO (s)	145.2	15.0	21.89	25.43	29.72	
EuOBr(s)	203.3	29.0	38.92		50.0	54.1
Eu(s)	0	19.31 ^C	22.85 ^C	25.29 ^C		
$\mathtt{Yb_2O_3(s)}$	433.68 ^b	31.8 ^b	47.88	56.25	66.58	
$Yb_3O_4(s)$	580	40.9	64.72			
$Yb_3O_4Br(s)$	630	57.3	84.16			
YbO(s)	143	11.1	17.99	21.53	25.82	
YbOBr(s)	195	24.4	34.42			
${\tt Yb}({\tt s},\ell)$	0	14.30 ^C	17.82 ^C	20.17 ^C		
Yb(g)	-36.35 ^C				47.40 ^C	
$EuBr_2(s, l)$	178.0	40.1	49.1	56.50	58.3	61.0
Br(g)	-26.74 ^a	41.81 ^a	44.34 ^a		47.10 ^a	48.11 ^a
a _{Reference}	69 ^b Re	ference	17	^C Refere	nce 88	

		ł
		<u>!</u>

MICHIGAN STATE UNIVERSITY LIBRARIES
3 1293 03084 9941